Materials Science & Engineering R 166 (2025) 101073

Contents lists available at ScienceDirect

Materials Science & Engineering R

journal homepage: www.elsevier.com/locate/mser

Liquid metal alchemy: Unlocking self-healing gallium-based materials for next-generation electronics

Minghan Yu [a,b], Changming Cao [a], Zicheng Sa [a,b], Chen Zhang [c], Jiayun Feng [a,b,*], Qing Sun [a,b], Xinyang Ma [a], Jianchao Liang [a,b], Yuxin Sun [a], Rui Yin [c], Youyou Chen [c], Yaming Liu [e], Kaizheng Gao [f], Chao Yang [d,**], Xiaoqin Zeng [d,**], Paul K. Chu [g], Yanhong Tian [a,b,*]

[a] State Key Laboratory of Precision Welding & Joining of Materials and Structures, Harbin Institute of Technology, Harbin 150001, China
[b] Zhengzhou Research Institute, Harbin Institute of Technology, Zhengzhou 450041, China
[c] Sauvage Laboratory for Smart Materials, The School of Integrated Circuit, Harbin Institute of Technology, Shenzhen 518055, China
[d] National Engineering Research Center of Light Alloy Net Forming, School of Materials Science and Engineering, Shanghai Jiao Tong University, Shanghai 200240, China
[e] Macau University of Science and Technology Zhuhai MUST Science and Technology Research Institute, Zhuhai 519031, China
[f] State Key Laboratory of New Ceramics and Fine Processing, School of Materials Science and Engineering, Tsinghua University, Beijing 100084, China
[g] Department of Physics, Department of Materials Science & Engineering, and Department of Biomedical Engineering, City University of Hong Kong, Tat Chee Avenue, Kowloon 999077, Hong Kong, China

ARTICLE INFO

Keywords:
Liquid metal
Self-healing
Flexible electronics
Battery

ABSTRACT

Liquid metals, a novel functional material, show significant potential for diverse self-healing applications due to their remarkable physical and chemical properties. Their low melting points enable rapid flow in low-temperature environments, greatly enhancing material responsiveness during damage repair. The high electrical conductivity provides distinct advantages for restoring broken circuits or conductive pathways, while their fluidity offers a reliable foundation for filling cracks and reconstructing both mechanical structures and electrical functions. These unique characteristics allow liquid metals to demonstrate excellent stability and reliability in various complex environments, satisfying demands for high-performance materials under challenging conditions. Critically, these properties enable applications spanning stretchable electronics, biomedical devices, and energy systems. In the specific context of self-healing batteries, the high chemical reactivity of liquid metals facilitates alloying and de-alloying reactions, significantly improving cycle efficiency and lifespan. This paper provides a systematic review of the fundamental properties, application forms, and self-healing mechanisms of liquid metals. The healing process of electrical properties in the field of flexible materials and the key characteristics of mechanically reversible repair in a damaged environment are discussed. Meanwhile, the mechanism of liquid metals in the self-healing batteries is analyzed, including the effect of alloying and de-alloying on the optimization of battery performance. Finally, the challenges associated with liquid metals and self-healing materials are thoroughly examined, and potential solutions are proposed to address these issues, offering valuable theoretical and practical insights for future research and applications of liquid metal-based materials.

1. Introduction

In recent years, the rapid development of electronic information technology has driven significant transformations and innovations across various industries and disciplines [1]. Electronic devices have become indispensable components of modern life and industrial production. As the functional and performance requirements of electronic equipment continue to rise, traditional rigid, low-integration electronic devices are increasingly unable to meet the needs of people. Consequently, there has been a shift from rigid, low-integration devices to flexible, high-integration devices [2]. Flexible electronic devices are capable of operating in complex environments and exhibit a high degree of adaptability. These devices can bend and fold while maintaining functional integrity under external forces, making them a promising

* Corresponding authors at: State Key Laboratory of Precision Welding & Joining of Materials and Structures, Harbin Institute of Technology, Harbin 150001, China.
** Corresponding authors.
E-mail addresses: fengjy@hit.edu.cn (J. Feng), chaoyang0315@163.com (C. Yang), xqzeng@sjtu.edu.cn (X. Zeng), tianyh@hit.edu.cn (Y. Tian).

https://doi.org/10.1016/j.mser.2025.101073
Received 29 April 2025; Received in revised form 9 July 2025; Accepted 20 July 2025

candidate material for applications in wearable electronics [3], biomedical devices [4], and the energy field [5]. The development of flexible electronics heavily relies on breakthroughs in novel materials. Among these, metallic materials play a critical role in various applications due to their excellent thermal and electrical conductivity, as well as their mechanical properties [6]. However, the application of traditional rigid metals in flexible electronics is limited, especially in scenarios requiring high flexibility and durability. The emergence of liquid metals has accelerated developments in materials science and related fields. To date, the primary single-element liquid metals at room temperature are mercury (Hg), gallium (Ga), rubidium (Rb), cesium (Cs), and francium (Fr) [7]. While Hg has been widely used across various fields, its high toxicity and environmental hazards restrict its use in modern technology [8]. Rb and Cs, as alkali metals, exhibit high chemical reactivity, making them unstable for most applications, particularly due to their tendency to react with air [9]. Fr is a radioactive element, and its application is limited due to safety concerns and the complexity of handling [10,11]. In contrast, Ga and Ga-based liquid metal alloys stand out due to their unique advantages. They exhibit high electrical and thermal conductivity, good fluidity, low melting point, low viscosity, and relatively low toxicity. Additionally, the preparation of Ga-based liquid metal alloys is relatively straightforward, and they demonstrate excellent recyclability and performance in applications [12]. Their ability to remain in a liquid state at room temperature offers substantial potential for flexible electronics. (For the remainder of this article, unless otherwise specified, "liquid metal, LM" will refer to Ga and Ga-based liquid metal alloys.)

The liquid metal also possesses a unique characteristic: when it comes into contact with oxygen in the air, Ga rapidly oxidizes to form a thin oxide layer, typically composed of Ga_2O_3 or Ga_2O, with a thickness generally ranging from 1 to 3 nm [13]. This oxide layer significantly reduces the surface tension of the liquid metal and can limit its deformation under external forces or other fields, thereby helping to preserve its inherent physical properties and functions [14,15]. Importantly, this naturally formed oxide layer enables surface modification of the liquid metal. Surface engineering can further enhance the compatibility or wettability of LM with various substrate materials [16]. This characteristic allows liquid metal to exhibit excellent electrical properties and good mechanical response when integrated with flexible substrate materials [17]. When the oxide layer is disrupted by external forces, the liquid metal possesses a self-healing ability, allowing it to regroup and form a new oxide layer, thus maintaining its liquid state and functional characteristics [18]. This reconstruction closely aligns with the concept of self-healing materials in materials science. Self-healing materials are those that can restore their properties after damage, drawing inspiration from the natural self-healing mechanisms observed in biological systems [19]. Compared to traditional materials, self-healing materials exhibit superior performance in terms of service life and reliability. Research in self-healing materials typically categorizes them into two types based on their healing mechanisms: one relies on the reversibility of bonding within the material, utilizing intermolecular interactions or reversible chemical bonds to achieve self-healing; the other promotes self-healing through the application of external fields/solutions or the designing of specific structures [20]. Liquid metals, with their unique properties, have long been representative materials for self-healing systems based on microencapsulated structures [21]. When materials fracture or break under external forces, liquid metals can quickly flow and fill the damaged regions, thereby restoring electrical conductivity. Additionally, the high fluidity of liquid metals, along with the presence of the oxide layer, enables rapid reconstruction after damage, which can also alter the mechanical properties of the materials [22]. In the field of energy batteries, liquid metal also demonstrates its self-healing capabilities. However, its mechanism differs from both external and internal self-healing approaches. Instead, liquid metal achieves self-repair through its inherent fluidity and extremely high reactivity.

In summary, due to their unique properties, liquid metals present broad application prospects in materials science and related fields. They not only provide new approaches for the development of self-healing materials but also drive innovative designs in flexible electronic devices and energy equipment. This review summarizes recent advances in the research of liquid metals in self-healing materials, with a focus on their performance characteristics, self-healing mechanisms, and application prospects across various self-healing domains, as shown in Fig. 1. It is hoped that this review will provide valuable insights and inspiration for future research directions.

2. Development of gallium-based liquid metals and self-healing materials

The development roadmap of Ga-based liquid metals and self-healing materials is shown in Fig. 2.

The development trajectory of Ga-based liquid metals (green line) reveals that the discoveries of indium and gallium marked the beginning of a new era in liquid metal materials science. In 1863, German chemists Ferdinand Reich and Hieronymous Richter first discovered indium through spectral analysis of sphalerite at the Freiberg School of Mines in Germany, thereby supplementing element 49 in the periodic table [37]. Twelve years later, in 1875, the French chemist Paul-Émile Lecoq de Boisbaudran successfully identified gallium, confirming the existence of the element previously described as "eka-aluminum" [38]. Notably, its strikingly low melting point of just 29.76°C became a focal point of scientific interest. With the advent of the 20th century, the semiconductor revolution reignited interest in these metals. In 1950, scientists successfully synthesized the eutectic indium-gallium alloy (EGaIn), which remains in a liquid state at room temperature and exhibits exceptional conductivity. This breakthrough was followed in 1954 by the development of gallium-indium-tin (GaInSn) ternary alloy through tin incorporation, laying the technological foundation for modern flexible electronics. These milestones collectively underscore the transformative, cross-era significance of multiple liquid metal materials. From 2000–2010, research on Ga-based liquid metals continued to deepen. During this time, scientific teams worldwide focus on addressing gaps in their fundamental properties, including electrical, magnetic, and thermodynamic properties.

In 2002, Yamanaka et al. achieved a significant breakthrough in the controlled deposition of liquid metals on silicon substrates using surfactant-mediated epitaxy (SME). Their work demonstrated that SME could effectively modify the inherent morphological behavior of liquid metals during growth on semiconductor surfaces, enabling a transition from droplet formation to the development of ordered planar films. A key factor in this process was the use of indium as a surfactant, which segregated to the surface layer and promoted the formation of exceptionally flat liquid metal films. These findings highlighted the potential of SME for advancing the fabrication of high-quality thin films and quantum structures based on liquid metal systems [55]. In 2005, Pavel and colleagues achieved nanoscale temperature control by filling carbon nanotubes with gallium. The device consisted of a low-resistance region formed by Ga-filled carbon nanotubes and a high-resistance area formed by hollow ones. As the temperature rises, the Ga column within the channel expands, resulting in a linear decrease in the nanotube's resistance. Precise pre-adjustment of the Ga column's position using the pressure of an atomic force microscope (AFM) promotes this behavior. Thanks to the system's structural features, an electrically controlled thermal sensor switch based on the gap length of Ga-filled carbon nanotubes was successfully developed [39]. In 2007, Jason and Lyon summarized the development of liquid metal ion source (LMIS) and field-emission electric propulsion (FEEP) devices. By quenching the formation of the Taylor cone at the LMIS tip under discharge current, stable and reliable electron and ion emissions were achieved. The ability to regenerate the tip effectively addressed the issues of wear and limited lifespan associated with traditional probes. These advancements laid an important foundation for the future development of liquid metal

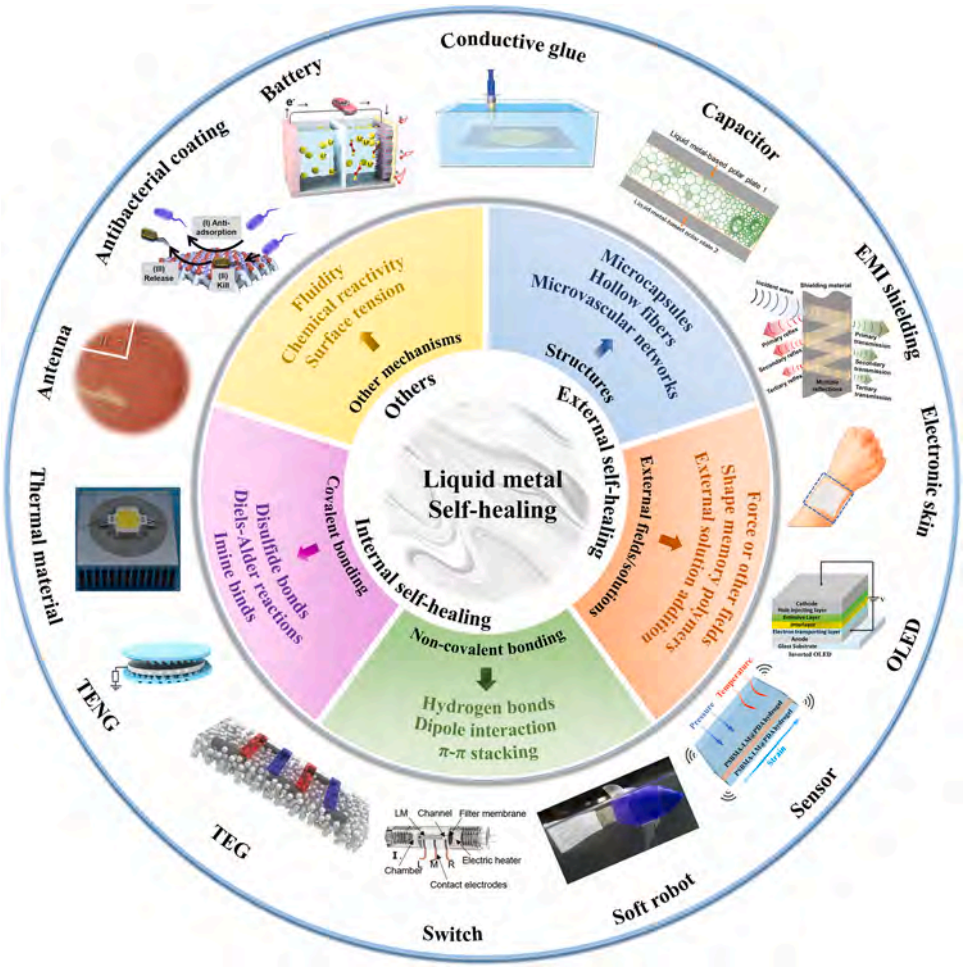

Fig. 1. Summary of the liquid metal, self-healing mechanism, and application of liquid metal in self-healing materials in this review. Antenna [23], Copyright 2021, MDPI. Antibacterial coating [24], Copyright 2021, Elsevier. Battery [25], Copyright 2021, Springer Nature. Conductive glue [26], Copyright 2022, Wiley-VCH. Capacitor [27], Copyright 2023, MDPI. Electromagnetic (EMI) shielding [28], Copyright 2021, Springer Nature. Electronic skin [29], Copyright 2023, Wiley-VCH. Organic light-emitting diode (OLED) [30], Copyright 2020, Wiley-VCH. Sensor [31], Copyright 2023, The Royal Society of Chemistry. Soft robot [32], Copyright 2017, PNAS. Switch [33], Copyright 2024, Wiley-VCH. Thermoelectric generator (TEG) [34], Copyright 2023, Wiley-VCH. Tribo-electric Nanogenerator (TENG) [35], Copyright 2022, Elsevier. Thermal material [36], Copyright 2021, The Royal Society of Chemistry.

technology in self-healing applications [56].

Compared with liquid metals, the development trajectory of self-healing materials (blue line) has evolved in parallel, with research into self-healing mechanisms spanning over a century of scientific exploration. This development vividly reflects the interdisciplinary integration from bio-inspiration to engineering applications. In 1899, Macmillon systematically described the phenomenon of tree bark healing through resin secretion after being cut, marking a new understanding of self-healing mechanisms in nature. In 1903, inspired by anatomical and pathological studies of ivory, Miller discovered that dental pulp undergoes a self-repair process similar to that observed in plants and other biological soft tissues, extending the concept of self-healing to higher biological systems [57]. During the 1950s, self-healing behaviors were successively observed in non-living systems, such as aluminum alloys and polymers [58]. After 1970, self-healing properties became closely linked to fuse systems, directly driving the large-scale application of self-healing materials in industrial protection systems [59]. Building on this foundation, in 1997, Jung et al. proposed the first structural self-healing material—a microcapsule system. They encapsulated styrene and polystyrene within polyoxymethylene urea (PMU) and found that when cracks damaged the microcapsules, the internal substances effectively repaired the cracks while maintaining the composite's stiffness [60]. This microcapsule-based self-healing system laid the theoretical groundwork for the development of advanced composite materials and more sophisticated self-healing structures. From 2000–2010, researchers focused on the self-healing mechanisms based on chemical bond reformation, marking a critical period of transition from molecular design to engineering applications. Through chemical bond reconstruction and structural innovation, the field achieved a leap from microscopic mechanisms to macroscopic performance. In 2002, Chen et al. developed a transparent organic polymer material with mechanical properties similar to epoxy resin at room temperature. At temperatures above 120°C, 30 % of the monomer bonds broke and reformed upon cooling, driven by the formation of a dynamic covalent network within the polymer [40]. This study, which demonstrated crack repair without additional components, sparked a wave of research into intrinsic self-healing mechanisms in polymers. In 2003, Aramaki fabricated a highly self-healing and corrosion-resistant protective film on zinc electrodes, maintaining over 95 % protection efficiency after hundreds of hours of testing [61]. This work provided new insights for anti-corrosion strategies in battery systems. In 2006, Trask and Bond et al. successfully developed a hollow fiber-based extrinsic self-healing structure based on the microcapsule mechanism and applied it to laminated composites. The healed laminates exhibited up to 87 % recovery in mechanical strength [41], showcasing the application of bio-inspired healing mechanisms in advanced composite systems. In

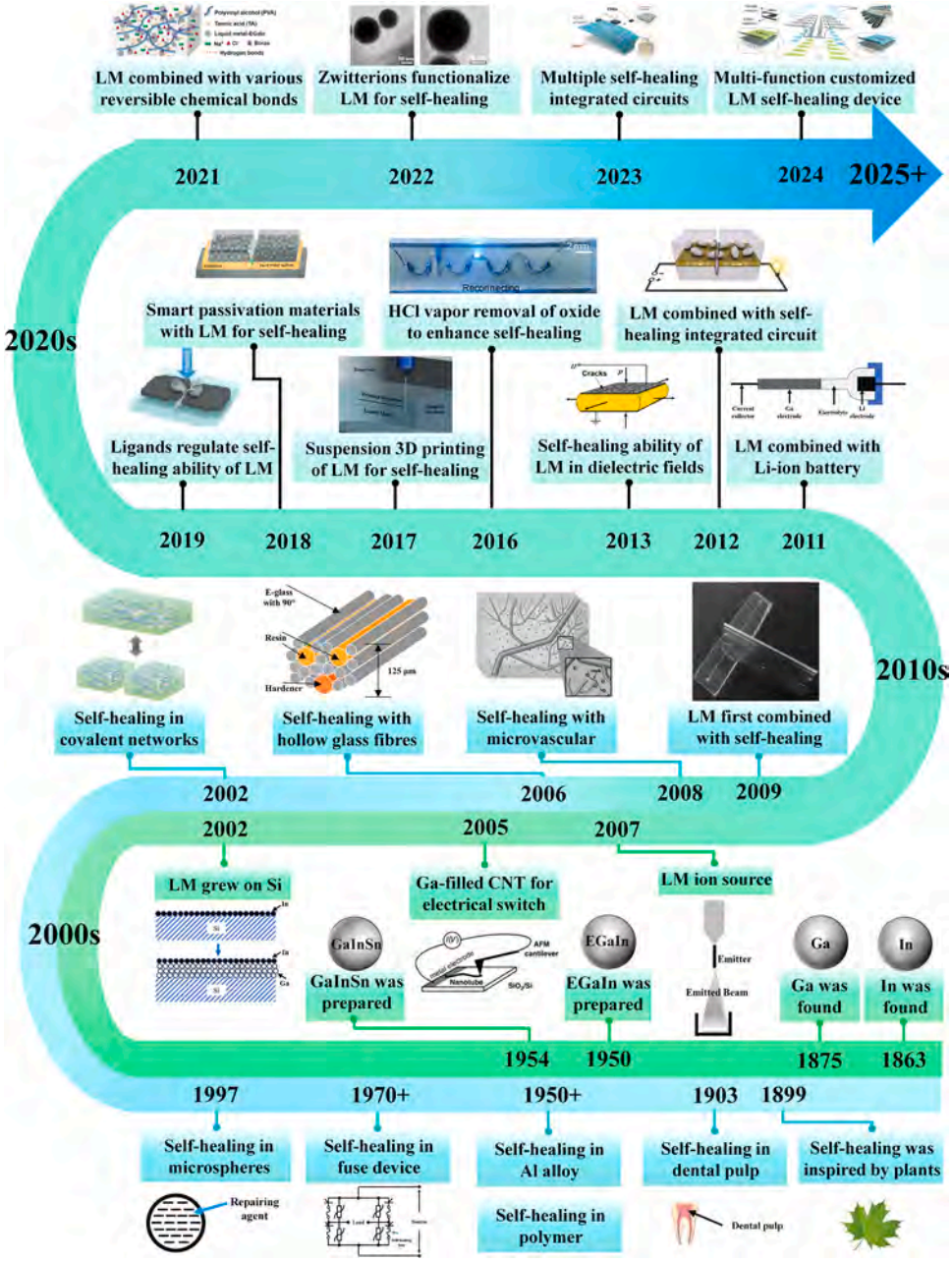

Fig. 2. The development roadmap of gallium-based liquid metals and self-healing materials. Ga-filled CNT for electrical switch [39], Copyright 2005, Wiley-VCH. Self-healing with hollow glass fibres [41], Copyright 2006, IOP Publishing. Self-healing with microvascular [42], Copyright 2008, Springer Nature. LM first combined with self-healing [43], Copyright 2009, Wiley-VCH. LM combined with self-healing integrated circuit [45], Copyright 2012, Wiley-VCH. Self-healing ability of LM in dielectric fields [46], Copyright 2013, AIP Publishing. HCI vapor removal of oxide to enhance self-healing [47], Copyright 2016, The Royal Society of Chemistry. Suspension 3D printing of LM for self-healing [48], Copyright 2017, Wiley-VCH. Smart passivation materials with LM for self-healing [49], Copyright 2018, Wiley-VCH. Ligands regulate the self-healing ability of LM [50], Copyright 2019, Wiley-VCH. LM combined with various reversible chemical bonds [51], Copyright 2021, Elsevier. Zwitterions functionalize LM for self-healing [52], Copyright 2022, Elsevier. Multiple self-healing integrated circuits [53], Copyright 2023, Wiley-VCH. Multi-function customized LM self-healing device [54], Copyright 2024, Wiley-VCH.

2008, Toohey et al. arranged hollow fibers in multiple directions to create a three-dimensional microvascular structure [42]. This innovation overcame the anisotropic limitations of hollow fibers, enabling the transport of healing agents to damaged areas via capillary action. This study integrated self-healing systems with multi-scale structures, further advancing the field.

Research into the fusion of liquid metals and self-healing mechanisms spans nearly a century, with a pivotal advancement occurring in 2009. Michael D. Dickey's team pioneered the integration of a liquid metal alloy (eutectic gallium-indium, EGaIn) with a PDMS elastomer, creating a reversibly deformable and mechanically tunable fluidic antenna [43]. This antenna exhibited high-efficiency radiation, reversible shape reconfiguration, mechanical tuning capability, and self-healing properties. This seminal work represented the first successful integration of liquid metal with an elastomer to achieve reversible antenna shape reconstruction. This approach overcame the inherent deformation limitations of traditional solid metal antennas by leveraging the fluidity of liquid metal to ensure electrical continuity during shape changes. It thereby offered a novel solution for flexible electronics, wireless sensing, and reconfigurable devices. This report formally inaugurated a new era

for liquid metal self-healing applications. In 2011, Deshpande et al. investigated the interaction between lithium electrodes and Ga-based liquid metals, providing fundamental insights into the behavior of gallium during battery cycling [44]. This groundbreaking work opened the door for liquid metal applications in battery systems, marking a transition from fundamental material research towards practical implementation and providing crucial theoretical and technical guidance for developing high-performance liquid metal batteries. The exceptional electrical properties of liquid metals spurred the development of combining conductive and dielectric materials with elastomers. In 2012, Scott R. White's team introduced an autonomous conductivity restoration technique based on microencapsulated liquid metal, aimed at addressing breaks in conductive pathways caused by thermomechanical failure in highly integrated circuits [45]. Unlike conventional methods reliant on external intervention (e.g., heating or manual repair), this approach embedded microcapsules within a dielectric layer. During crack propagation, the capsules rupture, releasing liquid metal that automatically fills the damaged region, enabling rapid reconstruction of the conductive path. This study constituted the first systematic validation of microencapsulated liquid metal for circuit self-healing. Experimental results demonstrated the system's ability to autonomously repair cracks in conductive paths caused by mechanical damage, achieving conductivity restoration within sub-millisecond timescales. This repair speed significantly surpassed all previous self-healing technologies and met practical real-time operational requirements. Furthermore, the restored electrical performance approached the original level. This fundamentally addressed a critical limitation of traditional systems, which typically restored only a single function. Building upon their earlier work, Michael D. Dickey's team proposed a self-healing, stretchable electrical conductor in 2013 [62]. The core design involved injecting liquid metal into microchannels formed within a self-healing polymer matrix, creating conductive wires possessing both mechanical and electrical self-healing capabilities. Following complete severance, conductivity could be restored immediately by manually realigning the cut ends, while the polymer substrate autonomously healed within minutes, significantly enhancing the durability of stretchable electronics. This work achieved the first demonstration of synchronous bidirectional self-healing, restoring both mechanical integrity and electrical functionality after complete material fracture. This breakthrough addressed a key constraint of traditional self-healing materials, which typically restored only one function. Crucially, unlike previous repair methods dependent on external support structures, the material could freely realign and heal after complete separation. This capability resolved a significant gap in the stretchable electronics field concerning dynamic self-repair and reconfiguration. It perfectly embodied the combination of internal and external self-healing mechanisms, lowered technical barriers to creating reconfigurable electronic devices, and laid the foundation for developing dynamic adaptive electronic systems. In the same year, Liu Jing's team applied liquid metal to dielectric elastomer actuators (DEAs), overcoming the strain limitations inherent in traditional rigid electrodes [46]. Moreover, the team discovered for the first time that liquid metal electrodes could achieve two-dimensional in-plane self-healing through the actuator's own motion. This process repaired electrode fractures and restored electrical conductivity. Their work experimentally revealed the mechanism behind this two-dimensional self-healing in liquid metal electrodes, establishing a new paradigm for the reliability design of flexible electronic devices. By quantitatively comparing the performance differences between liquid metal and traditional electrodes, the team demonstrated its clear advantages in low-voltage, high-strain scenarios. This research not only provides a core technical pathway for developing high-performance DEAs but also opens up new directions for enhancing the durability design of flexible electronics. In 2016, Li et al. extended the use of GaInSn to stretchable electronics using an inkjet printing system [47]. Departing from prior studies, they utilized HCl vapor permeating through the poly(dimethylsiloxane) (PDMS) channel walls to continuously remove the oxide layer on the liquid metal, enabling an "all-liquid channel" design. The subsequent year saw liquid metal combined with advanced suspension three-dimensional (3D) printing technology to fabricate self-healing materials, further improving precision [48]. In 2018, Chu et al. synthesized core-shell structured liquid metal microcapsules by in situ polymerization of urea-formaldehyde on a liquid metal colloid [49]. Utilizing phase separation between the capsules and a liquid prepolymer, they produced a passivating film containing liquid metal. The integration of the passivation layer with the self-healing system broadened the application scope of liquid metal-based self-healing materials. In 2019, Park et al. modulated the redox behavior of EGaIn within carboxylated polyurethane using bis (trifluoromethanesulfonyl)imide ligands. This strategy enhanced the reversible Faradaic reaction of gallium, improving the material's electrical healing efficiency [50]. Michael D. Dickey's team introduced a method for fabricating flexible and stretchable microwires by dielectrophoretic (DEP) assembly and sintering of EGaIn microdroplets within an elastic PDMS matrix in 2020 [63]. The key innovation lay in DEP's ability to assemble EGaIn microdroplets into conductive microfilaments with significantly reduced filler loading. This approach eliminated the need for post-processing steps, yielding EGaIn microwires with low resistance. Furthermore, the use of liquid metal circumvented the inherent compatibility mismatch issues in soft polymer composites containing solid fillers. During deformation, the inherent fluidity of EGaIn maintained metallic conductivity while preventing electrical failure upon elastomer fracture. The microwires maintained stable resistance when stretched to 100 % strain and under cyclic bending, a performance attributed to their serpentine structure. Notably, the microwires could be reshaped in situ to electrically reconnect severed conductors, restoring up to 74 % of the original conductivity after severe mechanical damage. This work constituted the first demonstration of DEP-directed alignment of EGaIn microdroplets in a polymer matrix, enabling on-demand circuit fabrication on soft substrates. The method successfully produced 5-mm-long conductive microwires that maintained excellent electrical performance under tensile and bending strain. Collectively, this study established a new manufacturing paradigm for flexible and stretchable electronics with significant application potential.

Post-2020, research combining liquid metals with self-healing materials has surged, as illustrated in Fig. 3, reflecting the growing emphasis on their integration. Recent research has primarily focused on: (1) Designing complex self-healing systems integrating liquid metals with multiple self-healing mechanisms to reduce healing time [51]; (2) Engineering the surface chemistry of liquid metals to enhance compatibility with substrates [52]; (3) Developing multi-scale and cross-scale integrated, multi-gradient liquid metal self-healing devices [53]; and (4) Tailoring liquid metal self-healing materials for specific application

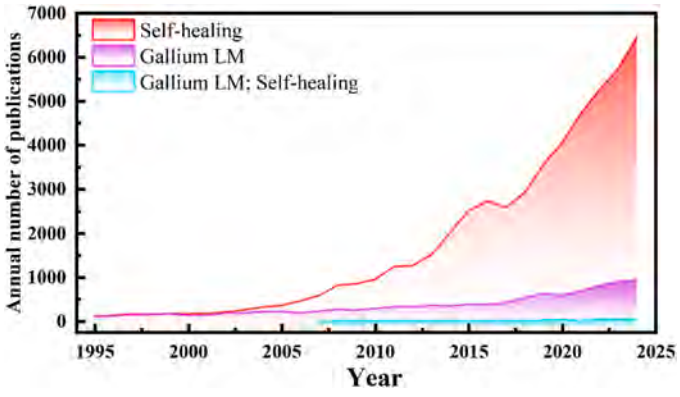

Fig. 3. Number of papers published in the past 30 years under different keywords (self-healing; Gallium-based liquid metal; double) Source: Web of Science.

scenarios [54].

As the majority of current self-healing mechanisms involve synergistic actions of multiple processes, this work comprehensively summarizes the developmental mechanisms of self-healing reported in recent years. Self-healing mechanisms are broadly classified into two categories: external self-healing and internal self-healing. External self-healing refers to mechanisms where the healing capability relies on externally supplied, pre-encapsulated, or embedded healing agents, or on the application of specific external energy fields (e.g., light, heat, electrical current) to drive the repair process. The core substances essential for healing (such as monomers, catalysts, or solvents) or the core energy input are not inherently available or triggerable by the material matrix itself following damage; they must be externally supplied or pre-embedded. Internal self-healing denotes mechanisms where the healing capability is entirely intrinsic to the material's inherent chemical structure and physical properties. The repair process relies solely on internally available reversible chemical bonds/interactions or phase transition behaviors. Crucially, under normal environmental conditions (or under the specific triggering conditions for which they are designed, such as heating or ambient humidity), these mechanisms initiate and complete repair without the need for external intervention to introduce specific healing agents or apply specific forms of external energy fields. The key characteristics of these mechanisms are detailed in Table 1.

Beyond the mechanisms cataloged in Table R1, electrostatic interactions warrant specific mention. As inherent non-covalent interactions within materials (e.g., ionic bonds, ion-dipole interactions), electrostatic forces represent an intrinsic material property. The healing process relies on the spontaneous reorganization of charged groups/ions near the damaged site (e.g., electrostatic attraction in polyelectrolyte complexes or ionogels) [133]. Furthermore, internal self-healing mechanisms involving reversible chemical bonds, such as Thiol-Michael reactions [134], Thioether bonds (R-S-R′) [135,136] represent an area promising more in-depth research in the future.

The synergistic evolution of liquid metals and self-healing materials has given rise to interdisciplinary innovations and emerging industries across materials science, electronic engineering, and biomedicine. The combination of liquid metal and self-healing mechanisms not only extends the life cycle of materials but also initiates a new research era. With continued advancements in fundamental research and engineering technologies, smart materials are poised to serve human civilization in increasingly intelligent and adaptive ways.

3. The properties of liquid metals and their application forms

Liquid metals have emerged as a research hotspot in materials science and engineering, primarily due to the simplicity of the preparation process. Among the various methods, the most widely used method involves heating pure gallium until it melts, followed by the addition of other metallic elements (such as In, Se) to induce alloying reactions, thereby producing the desired eutectic liquid metals [16]. This approach is favored for its straightforward steps, simple operation, and strong controllability over alloy composition. However, as research has progressed, the demand for liquid metal materials with specific properties has become increasingly prominent, particularly in controlling the droplet size of liquid metal, leading to the development of more refined preparation techniques.

Currently, techniques for controlling the droplet size of liquid metals are mainly divided into two categories: bottom-up synthesis methods and top-down synthesis methods [16]. Bottom-up synthesis methods primarily include techniques such as vapor deposition, high-temperature pyrolysis, and electrochemical processes. These methods achieve effective control over droplet size by regulating reactions involving Ga precursors, combined with precise manipulation of the oxide layer on the liquid metal surface. In contrast, top-down synthesis methods rely more heavily on microfluidic technology. By designing the microchannel structure and adjusting the flow rates of fluids, researchers can selectively produce and separate monodisperse liquid metal droplets of different sizes [137].

Apart from the diversity of preparation methods, liquid metals have many other outstanding physical and chemical properties. For a more specific overview of these properties, refer to Table 2 and the descriptions provided below. With continued in-depth research and a deeper understanding of these properties, liquid metals are expected to play an increasingly significant role in future technological innovations.

3.1. Basic characteristics

Compared to Hg, Ga and Ga-based liquid metals exhibit promising applications across various advanced technology fields, owing to their unique physical properties. Ga has a melting point of 29.8°C, which is significantly higher than that of Hg, causing it to remain in a solid state at room temperature (approximately 25°C). This characteristic offers distinct advantages in certain applications. For instance, in lubricants or batteries involving temperature fluctuations, Ga can effectively manage and regulate heat through solid-liquid phase transitions [141].

However, when Ga forms alloys with other metals, the resulting materials often have lower melting and boiling points. This behavior is largely attributed to Ga's internal structure. Ga exists in several metastable phases [14], each with relatively low melting points. In the solid state, Ga's structure is characterized by a coexistence of covalent and metallic bonds [142]. Upon alloying with other elements, the arrangement of Ga atoms changes, increasing interatomic distances. This anisotropic structural feature makes the crystal structure of Ga-based alloys more prone to fracture at lower temperatures, leading to reduced melting and boiling points [143]. For example, in the well-studied Galinstan, although many sources cite its melting point as −19°C, this actually refers to its freezing point. Due to supercooling, the actual melting point of Galinstan alloy is around 13.2°C [144]. This distinction makes EGaIn widely used for its excellent performance at room temperature, while Galinstan finds broader applications in low-temperature environments, particularly for its superconducting properties at cryogenic temperatures [145].

Another noteworthy property of liquid metals is their exceptionally high surface tension, approximately 10 times that of deionized water, which causes liquid metals to spontaneously form spherical shapes to minimize surface free energy [137]. Simultaneously, liquid metals have relatively low viscosity, at most 2.4 times that of deionized water. This combination of low viscosity and high surface tension allows liquid metals to quickly reassemble after being disrupted by external forces, forming self-healing systems. This characteristic has significant applications in self-healing materials and flexible electronic devices [146]. Furthermore, the high surface tension of liquid metals can be externally modulated. For instance, voltage-driven control methods [147] can alter the shape and flow properties of liquid metals by manipulating the electric double layer between the liquid metal and the substrate material. However, high surface tension also has challenges, such as poor adhesion to most substrates. In the field of printing, surface tension can impact the quality of printed patterns, leading to unstable electrical connections [139].

3.2. Chemical reactivity

Ga, as a typical post-transition metal, exhibits significant chemical reactivity, particularly in its sensitivity to oxygen when exposed to air. Liquid metals readily react with atmospheric oxygen, forming a self-passivating oxide layer of Ga_2O_3. This oxide layer not only reduces the surface tension of the liquid metal but also significantly alters its rheological properties, allowing the liquid metal to exist in non-spherical shapes. The process begins when electrons from the gallium atoms migrate to the adsorbed oxygen layer air exposure. This electron transfer ionizes the oxygen layer, leading to oxide formation. The electrostatic

Table 1
Summary of different self-healing mechanisms.

Classification of Self-healing Mechanisms	Refined Classification	Specific Mechanism	Schematic Diagram	Characteristics	Advantages	Disadvantages	Representative Materials/ Methods	Ref.
External self-healing	Structures	Microcapsules		Wrap the liquid repair agent in the solid shell.	Rapid response ·Simple preparation ·Trigger passively	·Uneven dispersion/size ·Repair stability (before/after self-healing)	Liquid metal; Wax/epoxy resin	[64–70]
		Hollow fibers	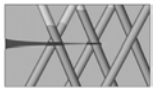	The hollow fiber structure contains the repair agent inside, which is dispersed in the matrix material in a specific arrangement.	·More repair agent ·Specific orientation ·Repair multiple times	·Complex process ·Size influence ·Prone to clogging	Glass pipette tube/ epoxy adhesive	[71–78]
		Microvascular networks	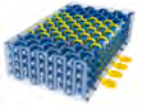	The three-dimensional microvascular network structure containing healing agents runs through the entire material matrix	·More repair agent ·Multi-directional repair ·Repair multiple times	·Complex process ·Performance limitation ·Leakage risk	Nylon wire/ epoxy resin	[42] [79–84]
	External Fields and Solutions	Applied fields	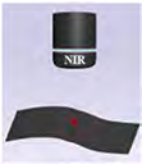	The self-healing method is achieved by relying on the external field to drive the internal specific materials.	·Local repair ·Controllable repair rate ·Contactless repair	·Require equipment ·Operational limitation ·Materials limitation	Thermal field; infrared rays	[85–87]

Classification of Self-healing Mechanisms	Refined Classification	Specific Mechanism	Schematic Diagram	Characteristics	Advantages	Disadvantages	Representative Materials/Methods	Ref.
External self-healing	External Fields and Solutions	Shape-memory	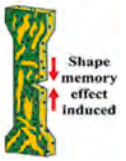	The shape-memory structure is stimulated to return to its original state, driving the internal repair substances to fill the damaged area.	·Repeatable trigger ·Major deformation repair	·External stimulation ·Unstable mechanical properties(after damage)	Thiol-acrylate-epoxy sequential dual-curing system	[88–92]
		Additive solutions		The micropores or microchannels inside the material interact with the external solution. After the solution penetrates, the repair is achieved through reaction or diffusion.	·Add solvent easily ·Flexible customization ·Wide application range	·High permeability ·Poor repair stability ·Prone to pollution	Water; Artificial sweat	[93]
Internal self-healing	Non-covalent Bonding	Hydrogen bonds	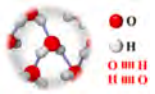	A kind of electrostatic attraction between hydrogen atoms and electronegative atoms (such as O, N, F), which is directional and saturated.	·Dynamic reversibility ·Biocompatibility	·Low strength ·Dissociation at high temperature	Polyvinyl alcohol (PVA)	[94–98]
		Dipole interaction	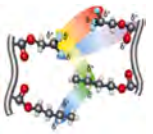	Dipole interaction is caused by the permanent dipole moments between polar molecules attracting each other ($\delta^{+}\rightarrow\delta^{-}$).	·Fast response ·No chemical residue	·Anisotropy ·Specific material system ·Sensitive to temperature	Fluorine-containing copolymers	[99, 100]

Classification of Self-healing Mechanisms	Refined Classification	Specific Mechanism	Schematic Diagram	Characteristics	Advantages	Disadvantages	Representative Materials/Methods	Ref.
Internal self-healing	Non-covalent Bonding	Host-guest interaction	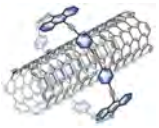	The non-covalent interactions between large cavity molecules (the host) and smaller molecules (the guest).	·Molecular recognizability ·Customized cavity size	·Complex structural design ·Large steric hindrance	Crown ether (CE); Cyclodextrin (CD)	[101–107]
		π-π stacking	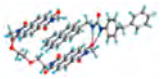	This interaction occurs between aromatic groups containing delocalized π-electron systems. Stacking method: (1) edge-to-face stacking; (2) offset stacking; and (3) face-to-face stacking.	·Improve electron transfer ·Regulate the material properties by the stacking mode	·Specific structure ·Weak binding force	Graphene-based nanomaterials (GNs)	[108–110]
		Metal-ligand coordination		The interaction between metal ions or complexes and electron-donating ligands forms complexes with specific geometric configurations.	·High designability ·Dynamic reversibility	·Environmental sensitivity ·Poor long-term stability ·Heavy metal ion toxicity	Fe^{3+}-Hydroxyethyl cellulose /Polyacrylic acid (Fe^{3+}-HEC/PAA)	[111–114]
		Hydrophobic associations	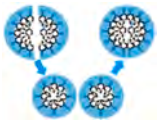	This bonding is unique to amphiphilic molecules carrying both hydrophilic and hydrophobic fragments.	·Underwater self-healing ·Good thermal stability	·Slow healing speed ·Failure in a dry environment	Acrylamide (hydrophilic); Stearyl methacrylate (hydrophobic)	[115–117]
Internal self-healing	Covalent Bonding	Disulfide bonds		A disulfide bond is a dynamic covalent bond formed between two sulfur atoms and is REDOX reversible.	·Rapid healing response ·High biocompatibility	·Low bonding energy ·REDOX reactions	Thiol/disulfide	[118, 119]
		Diels-Alder reactions	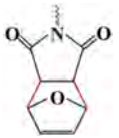	The Diels-Alder (DA) reaction is a reversible cycloaddition reaction between a conjugated diene (with 4 π electrons) and a diene (with 2 π electrons).	·Dynamic reversibility ·High bonding energy	·High healing temperature ·Long healing time	Ethene (dienophile); 1,3-butadiene (diene)	[120, 121]
		Imine bonds	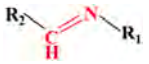	Imine bonds are mainly formed through the dehydration condensation of amines and aldehydes.	·Dynamic reversibility ·Environmentally friendly	·Environmental sensitivity ·Poor repair stability	Ethylenediamine/ acetylacetone	[122, 123]
		Borate ester bonds	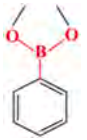	Boric acid ester bonds are formed by the dehydration condensation of boric acid and diols.	·Rapid healing response ·pH sensitivity	·Unstable in water ·Specific reaction conditions	Boronic acid/ 1,2-diol	[124, 125]

Classification of Self-healing Mechanisms	Refined Classification	Specific Mechanism	Schematic Diagram	Characteristics	Advantages	Disadvantages	Representative Materials/Methods	Ref.

(*continued on next page*)

Table 1 (*continued*)

Internal self-healing	Covalent Bonding	Transesterification reactions	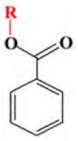	This bonding depends on the exchange of alkoxy groups between esters and alcohols under the action of heating or a catalyst, forming new esters and new alcohols.	·Extensive raw materials ·Environmentally friendly ·Strong controllability	·Slow reaction rate ·Side reaction products ·Limitations of reversible reactions	Triglyceride/ methanol	[126–128]
		Acylhydrazone bonds	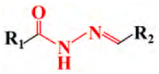	The acylhydrazone bond is composed of a functional group formed by the condensation of hydrazine with an aldehyde or ketone.	·Mild reaction conditions ·Dynamic reversibility ·pH/chemical dual response	·Slow reaction rate ·Poor mechanical performance	4,4'-biphenyldicarbox-aldehyde/ 1,3,5-benzenetri-carbohydrazide	[129–131]

Microcapsules [64], Copyright 2023, American Chemical Society. Hollow fibers [72], Copyright 2024, Elsevier. Microvascular networks [80], Copyright 2011, Wiley-VCH. Applied fields [132], Copyright 2025, Wiley-VCH. Shape-memory [133], Copyright 2025, Wiley-VCH. Additive solutions [93], Copyright 2018, Wiley-VCH. Hydrogen bonds [94], Copyright 2024, Springer Nature. (b) Dipole interaction [99], Copyright 2021, Wiley-VCH. (c) Host-guest interaction [101]. Copyright 2023, Wiley-VCH; (d) π-π stacking [108], Copyright 2010, American Chemical Society. (e) Metal-ligand coordination [111], Copyright 2024, The Royal Society of Chemistry. (f) Hydrophobic associations [115], Copyright 2021, Springer Nature.

Table 2
Comparison of properties of liquid metals, deionized water, and some conductive metals [7,13,138–140].

	Hg	Ga	EGaIn	GaInSn	DI H_2O	Au	Ag	Cu
Phase (25℃)	Liquid	Solid	Liquid	Liquid	Liquid	Solid	Solid	Solid
Melting point (°C)	−38.8	29.8	15.5	−19	0	1064.2	961.8	1084.6
Boiling point (°C)	356.6	2205	2000	> 1300	100	2807	2212	2567
Density (g/cm^3)	13.6	6.1	6.3	6.4	1	19.3	10.5	8.9
Viscosity (×10^{-3} Pa·s)	1.6	1.4	2	2.4	1	N/A	N/A	N/A
Surface tension (× 10^{-3} N/m)	487	707	624	718	72	N/A	N/A	N/A
Toxicity	High	Low	Low	Non	Non	Non	Low	Low
Specific heat (J/kgK)	140	409.9	403.5	366.5	4183	125.6	238.6	376.8
Thermal conductivity (W/mK)	8.5	29.3	26.6	16.5	0.6	317	429	401
Electrical conductivity (×10^6 S/m)	1.04	6.73	3.4	3.46	N/A	45	62	57
Remark		Surface tension and viscosity in liq.	Ga:75.5 % In:24.5 %	Ga:67 %; In:20.5 %; Sn:12.5 %		The viscosity and surface tension of high melting point metals after melting are not specified here.		

potential between the oxide-environment and oxide-metal interface (known as the Mott potential) lowers the energy barrier for ionic diffusion within the liquid metal, thereby accelerating the growth of the oxide layer [144]. The instantaneous growth of the oxide layer on liquid metals can be described by the Cabrera-Mott model, as shown in Eq. (1) [148]:

$$\frac{1}{x} = A - B\ln t \tag{1}$$

where x represents the oxide layer thickness, t is the oxidation time, and A and B are constants.

Despite the continuous increase in oxide layer thickness over time, gallium, like its Group III counterpart Al, exhibits a self-limiting oxidation behavior. This means that once the oxide layer reaches a certain threshold, the oxidation rate slows significantly, thereby preserving the internal flowability of the liquid metal. This self-limiting behavior stands in shark contrast to the porous and loosely bonded oxide layers typically formed during the oxidation of materials such as tin (Sn), bismuth (Bi), indium (In), and gadolinium (Gd) [148]. In aqueous environments, the Ga_2O_3 oxide layer on liquid gallium can further transform into gallium oxyhydroxide (GaO(OH)). Compared to Ga_2O_3, GaO(OH) exhibits lower passivation and is easier to process and remove [148]. This characteristic simplifies the practical handling of liquid metal and expands its possibilities for use in diverse environments. Further, the presence of an oxide layer enhances the versatility of liquid metal applications; for instance, introducing hydrogen bonds on the surface of liquid metals enables high compatibility with hydrogels [140,149].

Additionally, the low electrochemical potential of liquid metals offers unique advantages in redox reactions, making them particularly suitable for electrochemical processes. For example, in the Galinstan alloy, Ga can exist in multiple oxidation states, including Ga(0), Ga(I), and Ga(III); indium (In) can be found as In(0), In(I), and In(III); while Sn exists as Sn(0), Sn(II), and Sn(IV) [148]. This diversity of oxidation states allows liquid metals to adapt to various environmental conditions during electrochemical reactions, greatly expanding their potential applications in new energy technologies and electrochemical storage devices.

3.3. Biological adaptability

Liquid metals hold significant potential for biomedical applications, but concerns about their toxicity have drawn attention. Notably, compared to the previous generation of liquid metals, mercury, gallium-based liquid metals exhibit superior biocompatibility. Mercury has a saturated vapor pressure of 1 Pa at 42°C, indicating its high volatility at room temperature. Inhalation of mercury vapor can cause severe and often irreversible damage to the nervous system and kidneys. As a result, the use of mercury in biomedical applications is tightly regulated. In contrast, gallium has a saturated vapor pressure of only 10^{-35} Pa at 29.9°C, which is far lower than that of mercury [138]. This lower volatility means gallium poses a much-reduced inhalation risk to researchers and patients at room temperature. Also, liquid metals possess antibacterial properties, and studies have already demonstrated their application on fabric surfaces [150]. Consequently, gallium and its alloys have increasingly replaced mercury in biomedical research and applications.

Extensive studies have been conducted on the biocompatibility of gallium-based liquid metals. For instance, Kim et al. placed liquid metal in water to investigate its toxicity and compatibility with human cells. The study found that when the liquid metal remained undisturbed, only a small amount of Ga^{3+} was released into the growth medium, and the survival rate of human cells remained high, suggesting that the liquid metal is relatively safe in this state. However, when the liquid metal was subjected to ultrasonic waves or agitation, the release of indium from within the liquid metal increased significantly, along with a corresponding rise in cytotoxicity [151]. This finding shows the low toxicity of liquid metal in static environments, while highlighting the need for caution in dynamic conditions. Other studies have explored the toxicity of gallium compounds introduced into the body via various routes, including intravenous injection, intraperitoneal injection, subcutaneous injection, and oral administration [152]. The results indicate that toxicity is significantly higher for injection routes compared to oral ingestion. Nevertheless, gallium compounds overall exhibit relatively low toxicity, providing strong support for continued exploration of liquid metals in biomedical applications.

Research on the application of liquid metals in medical fields has already gained traction, particularly in utilizing light or magnetic fields to realize specific functions within the human body. For example, Lu et al. mixed EGaIn with graphene quantum dots (GQDs), significantly enhancing the photothermal conversion efficiency of the liquid metal. Upon light exposure, spherical nanoparticles first dispersed into nanoscale fragments, which then transformed into hollow nanorods composed primarily of GaO(OH), with indium atoms forming nanospheres [153]. This transformation not only demonstrates the morphological changes of liquid metal under light stimulation but also highlights its potential for biomedical applications. In another study, Svetlana et al. fabricated well-dispersed, modified EGaIn nanoparticles. Under near-infrared laser irradiation, these nanoparticles were disrupted, accompanied by a rise in surface temperature. This temperature increase was further amplified by eddy currents in the magnetic field, providing possibilities for targeted therapy within the body [154]. By directing the liquid metal with external magnetic fields or light sources, it can accumulate at diseased sites and release drugs. Alternatively, its elevated temperature can be used to destroy cancer cells. This approach not only enables precise drug delivery but also facilitates direct elimination of tumor cells through localized heating.

The photothermal and magnetothermal properties of liquid metals provide two effective mechanisms for biomedical applications, including sterilization and anti-tumor treatments. The first mechanism involves liquid metal shape changes that directly disrupt cell membranes or walls, interfere with membrane potentials, and generate free radicals. This method avoids the issue of antibiotic resistance associated with prolonged drug use and can be broadly applied to various microbial killing processes, directly and effectively damaging or eliminating cells. The second mechanism involves energy conversion, where light or magnetic energy is transformed into heat, for sterilization [155]. This technique can target deep tissues that are difficult to reach with traditional therapies, allowing light to be applied to otherwise inaccessible areas inside the body. As a result, it reduces the need for chemical agents and minimizes the side effects of drugs.

3.4. Application performance

Liquid metals, with their unique combination of fluidity and metallic properties, have demonstrated immense potential in various emerging fields. While their electrical and thermal conductivity may not match excellent conductive materials such as gold, silver, or copper, liquid metals still outperform most polymers and other nearly insulating materials in these aspects. However, the application of liquid metals often requires solving the problem of their high surface tension. In most cases, liquid metals must be dissolved in solvents or encapsulated for practical application [138]. Particularly in flexible and wearable devices, liquid metals offer excellent conductivity and thermal performance while retaining fluidity. This provides a new approach to designing flexible electronic devices with excellent performance.

In earlier studies, Ag and Cu were commonly used in hydrogels as conductive phases due to their superior conductivity. However, these rigid metals require a high solid content to achieve the percolation threshold in hydrogels, which degrades their mechanical properties. To lower the percolation threshold and enhance the mechanical

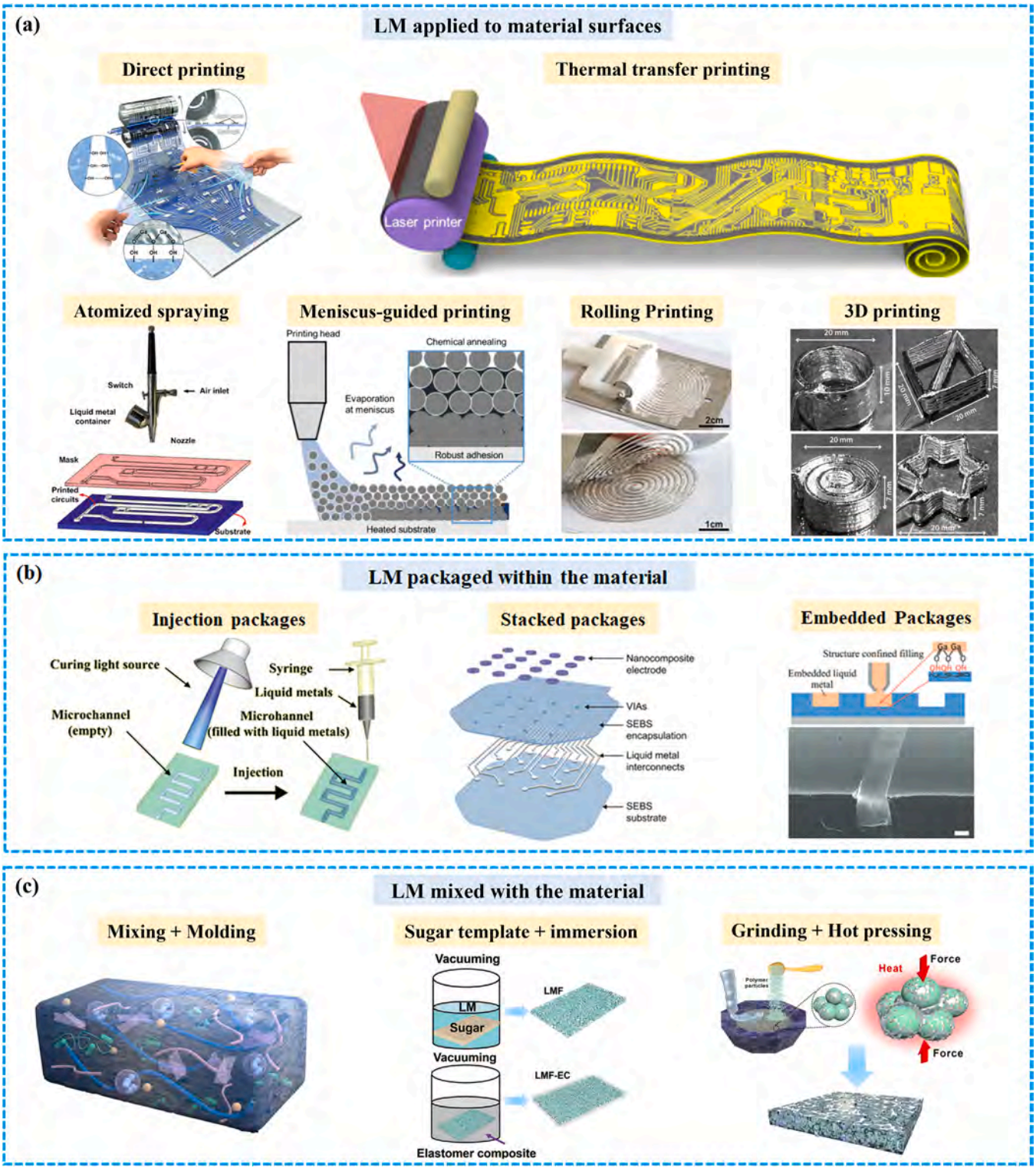

Fig. 4. Different forms of liquid metal in materials. (a) Liquid metal is molded on the surface of the substrate by printing and spraying. Direct printing [178], Copyright 2020, Wiley-VCH. Thermal transformer printing [168], Copyright 2022, American Chemical Society. Atomized spraying [169], Copyright 2014, Springer Nature. Meniscus-guided printing [170], Copyright 2022, Springer Nature. Rolling printing [172], Copyright 2018, Wiley-VCH. 3D printing [173], Copyright 2018, Wiley-VCH. (b) Liquid metal is encapsulated inside the substrate by injecting, laminating. Injection packages [174], Copyright 2022, The Royal Society of Chemistry. Stacked packages [175], Copyright 2022, AAAS. Embedded packages [179], Copyright 2022, The Royal Society of Chemistry. (c) Liquid metal is dispersed throughout the three-dimensional structure of the substrate via mold casting,sugar-template immersion, and grinding hot-press methods. Mixing + molding [180], Copyright 2024, Elsevier. Sugar template + immersion [176], Copyright 2020, Wiley-VCH. Grinding + hot pressing [177], Copyright 2022, Elsevier.

performance of hydrogels, researchers have turned to amorphous conductive fillers such as ionic liquids and liquid metals [138]. Ionic liquids conduct electricity through the movement of internal anions and cations under an electric field, but ion enrichment may occur during application, affecting signal stability at high current densities [156]. In contrast, liquid metals, due to their metallic nature, allow electrons to move rapidly under an electric field. The collision between electrons and metal atoms is also one of the reasons for their excellent thermal conductivity.

As an alternative to mercury, gallium-based liquid metals exhibit a unique property of volumetric expansion with temperature, making them ideal candidates for use in thermometers and thermocouples as temperature indicators. These discoveries further broaden the potential for liquid metals in temperature-related applications. Moreover, liquid metals are often temperature-sensitive in practical applications, and their low melting points give rise to a distinctive behavior of negative thermal expansion during the liquid-to-solid transition [157]. Leveraging this property, Wang et al. designed an insulator-conductor reversible hydrogel. Liquid metal droplets solidify upon freezing and are encapsulated in elastomer to form conductive pathways. As the temperature rises, the droplets re-melt and disperse, breaking the conductive paths and rendering the material insulating [158]. This semiconductor-like behavior at variable temperatures expands the application range of liquid metals.

In studies of electrical properties, researchers have combined liquid metals with hydrogels to develop a novel material known as liquid metal embedded elastomer (LMEE). Experiments revealed that at low liquid metal content, the internal conductive pathways of the material were incomplete, requiring external pressure to force the liquid metal to rupture and form conductive connections [159]. Hydroxyl groups (-OH) in the hydrogel exhibit a strong affinity with the Ga_2O_3 on the surface of the liquid metal, enhancing the binding of the liquid metal inside the hydrogel. This improves overall conductivity while preserving the hydrogel's mechanical properties, enabling the material to respond quickly to external stimulation [160]. To further enhance the electrical performance, researchers began combining traditional rigid conductive metals with liquid metals. Wang et al. developed a composite conductive polymer by integrating Ag and EGaIn into an the organic elastomer. During tensile testing, the rupture of liquid metal particles maintained electrical connections between silver flakes and particles, significantly improving the elastomer's tensile performance and electrical stability. The EGaIn particles act as electrical anchors for silver, a critical factor in maintaining both the mechanical and electrical properties of the composite materials [161].

In addition to electrical properties, liquid metals also exhibit notable dielectric properties. Bartlett et al. studied EGaIn-silicone elastomer composites and found that as the liquid metal content increased, the effective relative dielectric constant of the composite material rose significantly. When the liquid metal content reached 50 %, the effective relative dielectric constant was more than 400 % higher than that of the pure elastomer, while the dissipation factor remained low. Furthermore, reducing the liquid metal particle size also helped increase the effective dielectric constant, offering new possibilities for developing high-performance dielectric materials [162].

Despite their advantages in thermodynamic and electrical properties, liquid metals have weak inherent magnetism, requiring specific treatment to transform them into magnetically responsive materials. Magnetic processing of liquid metals typically involves stirring, grinding, or ultrasonication of magnetic particles with the liquid metal in a strong alkaline environment. Removing the oxide layer of liquid metal accelerates the mixing or reaction between the highly reactive internal metal of liquid metal and the magnetic material [163]. Cao et al. prepared a ferromagnetic liquid metal putty-like material (FM-LMP) by pouring EGaIn into NdFeB and stirring under a strong magnetic field. Although this material was prone to demagnetization, it exhibited superior electrical performance compared to unmixed magnetic materials [164]. Additionally, the magnetized liquid metal displayed strong plasticity similar to putty, and when the NdFeB content reached 20 wt%, the storage modulus of FM-LMP increased to 2.8×10^6 Pa. Another method for preparing magnetically responsive liquid metals involves forming core-shell structures with liquid metal as the core and magnetic material as the shell. Kim et al. used electroplating to coat low-residual-stress permanent magnets (CoNiMnP) on the surface of Galinstan particles. However, the external magnetic field caused the surface coating to break, due to the non-uniformity of the coating, resulting in the coated liquid metal droplets that were no longer spherical, which negatively affected their movement on paper [165]. Zhang et al. prepared the Ni/Al/EGaIn motor by plating a nickel (Ni) cap on the surface of EGaIn and then adding aluminum foil to a NaOH solution. By coating the surface of liquid metal with magnetic metals, liquid metal gains magnetic responsiveness, greatly expanding its potential application in the field of magnetics [166].

3.5. Forms of liquid metals in applications

As discussed above, due to their intrinsic high surface tension, liquid metals are rarely applied directly in scientific research or industrial production. Instead, they are predominantly used by being encapsulated or mixed within matrix materials or solvents. In this section, we summarize the action forms in which liquid metals are utilized in applications, as illustrated in Fig. 4. Specifically, these applications can be categorized into three main forms:

(1) Liquid metal applied to the material surface

This approach involves patterning polymers containing liquid metal on flexible substrates through printing or coating techniques, as shown in Fig. 4(a). Various methods, such as direct writing, thermal transfer, atomized spraying, meniscus-guided printing, rolling printing, and 3D printing, are employed, each with its own advantages and fields of application. Direct writing allows precise patterning of micron- to nanoscale inks, commonly used in electronic circuit boards and sensors in the field of information technology [167]. Thermal transfer, a well-established modern industrial printing technique, is widely used for printing on surfaces like automobiles and textiles [168]. Atomized spraying efficiently deposits materials onto both flexible and rigid surfaces, ensuring high material utilization and uniform coating, making it suitable for functional coating applications [169]. Meniscus-guided printing is a novel technology that uses solvent evaporation to form a meniscal-like liquid-gas interface during the printing process. This enables precise control of droplet flow and evaporation, making it ideal for high-precision printing [170,171]. Rolling printing, with its scalability and high efficiency, is a proven technique for industrial applications and is extensively used in the mass production of components like RFID tags [172]. While 3D printing is slower compared to other methods, its ability to design and print additively makes it suitable for high-precision and complex geometric shapes, commonly used for custom prosthetics and organs in the biomedical field [173].

(2) Liquid metal packaged within the material

When liquid metal is not mixed with polymers or solvents, it is typically encapsulated within substrate materials, as shown in Fig. 4(b). Liquid metal is imported into internal channels of the substrate, forming conductive pathways through direct contact. Injection packages involve preparing a substrate with internal channels, which are then filled with liquid metal using pressure devices like syringes, followed by sealing [174]. Stacked packages build on injection packages by adding vertical designs, enhancing the mechanical strength and integration of the overall structure [175]. In contrast, embedded packages position liquid metal in surface grooves rather than internal channels, making it more suitable for heat dissipation applications. These methods preserve the

excellent electrical and thermal conductivity of liquid metals while effectively controlling their flow areas, facilitating easy recycling and reuse.

(3) Liquid metal mixed with the material

Mixing liquid metal with substrate material is one of the most common methods used in laboratory preparation because it is simple and does not require complex equipment, as shown in Fig. 4(c). The mixing-molding method enables the combination of materials in various states and morphologies, which are then cast into custom molds for curing under specific conditions [31]. This method is frequently employed in the preparation of flexible electronic hydrogels. In contrast, the sugar template-immersion method reverses this process by first forming a porous structure from a sugar template, which is then immersed in liquid metal to create a sugar/liquid metal composite [176]. After dissolving the sugar in water or another solvent, the porous liquid metal structure is placed into an elastomer solution for curing. Owing to its unique structural properties, this method is often used for fabricating scaffolds in bioengineering. The grinding-hot pressing method is commonly applied in electronic packaging materials [177]. Grinding ensures thorough mixing of liquid metal with electronic and thermal conductive phases, followed by hot pressing to interconnect substrates while eliminating voids in the liquid metal paste. This results in a higher density after curing compared to previous methods.

The versatility and adaptability of liquid metal applications allow for customization to meet diverse needs, ranging from surface coating to encapsulation and mixing. Each form offers distinct advantages and serves specific fields, showcasing the vast potential of liquid metals in both scientific research and industrial applications. As research on liquid metals advances and technologies evolve, these application methods are expected to further expand their potential, driving innovation in new materials and technologies.

4. Application and healing mechanism of liquid metal self-healing materials

As materials science continues to advance, materials with a wide range of excellent physical and chemical properties are being increasingly applied across various fields. In recent years, wearable flexible electronic materials have attracted significant research interest due to their potential in human motion detection and physiological signal monitoring. These materials are typically composites of elastomers and conductive fillers, designed to retain excellent conductivity even under substantial bending and stretching. Additionally, they need to quickly self-repair after damage from external mechanical stress to restore their original properties. While the traditional internal self-healing materials have certain self-healing ability, they often have poor conductivity or are even insulating, which limits their suitability for signal transmission.

Researchers often enhance conductivity by incorporating conductive elements, such as silver nanoparticles and graphene. However, when these materials fracture, the conductive particles may prevent surface healing. Moreover, the interface compatibility between these solid particles and elastomers is often limited, potentially shortening the material's lifespan. Liquid metals, with their excellent fluidity and self-healing properties, are considered ideal candidates for addressing these challenges. Especially, liquid metals form an oxide layer on their surface, enhancing compatibility with elastomeric substrates and enabling highly integrated composite materials. Their fluidity, coupled with the use of microencapsulation, allows liquid metals to adjust their form flexibly during stretching or deformation, thereby enhancing the material's adaptability.

Beyond the inherent fluidity of liquid metals, their high surface tension is an indispensable property in self-healing processes [181]. It serves as a critical factor in maintaining the structural stability of microencapsulated LM self-healing systems. While the native oxide layer on LM surfaces can impede droplet coalescence, the high surface tension enables LM droplets to overcome atomic-scale separation distances, effectively breaching the oxide layer's barrier [182–184]. This facilitates droplet merging, enlarges the liquid bridge, and ultimately establishes conductive pathways. Furthermore, driven by surface tension, the coalesced LM forms a stable liquid bridge. This configuration significantly resists re-separation under external disturbances (e.g., mechanical vibration), ensuring the durability and efficacy of the healed structure. The efficiency of self-healing is also profoundly influenced by LM droplet size [185]. Higher surface tension combined with smaller droplet size accelerates coalescence kinetics [186,187]. Nanoscale LM droplets rapidly aggregate under the influence of surface tension, thereby enhancing self-healing efficiency. This capability ensures robust aggregation even within complex environments.

Additionally, during phase transitions, the volumetric expansion of LM requires surface tension to counterbalance disruptive forces and maintain droplet integrity [188]. In chemical cross-linking processes, surface tension promotes intimate contact between the LM and functional groups (e.g., -OH, -NH_2) within the polymer matrix [189]. This facilitates the formation of dynamic chemical bonds, strengthening the self-healing capacity of the composite material. These fundamental aspects of surface tension governing LM self-healing will be systematically explored in the subsequent sections.

In the event of mechanical damage or cracking, the liquid metal can quickly flow to the damaged area, filling the cracks and restoring the conductive path, thus achieving the self-healing function of the material. This fast recovery mechanism not only significantly improves the durability of flexible electronic materials but also broadens their potential in various applications.

In addition to applications in flexible electronics, the high chemical reactivity of liquid metals enables alloying and de-alloying processes with active metal electrodes. This mechanism partially addresses battery failure issues, thereby enhancing battery performance and extending service life.

Since this paper focuses on liquid metal's self-healing applications, its applied mechanisms inherently involve external self-healing. Thus, classification based solely on internal versus external self-healing methods is impractical. In subsequent sections, we first categorize applications by domain: flexible electronics and energy applications. For flexible electronics, we further classify external self-healing mechanisms based on whether they require external fields or solutions, distinguishing autonomous self-healing (no external intervention) from assisted self-healing (requiring external resources) [190,191]. In energy applications, self-healing primarily leverages liquid metals' chemical properties- especially their high reactivity- to achieve self-repair. This mechanism is most prominent in batteries with metal electrodes.

4.1. Self-healing liquid metal materials without external resources supporting

In the study of self-healing materials, liquid metal is typically embedded in polymer matrices as microdroplets. These small droplets form a thin oxide layer on their surfaces, which has a significant effect on electrical conductivity. Additionally, the gap between droplets contributes to high resistance. To address this, Markvicka et al. developed a method where liquid metal is mixed with a flexible silicone elastomer and then cured [159]. When the cured elastomer is subjected to external force, the internal liquid metal droplets are broken and redistributed to form a larger area of conductive path, thereby reducing the increase in resistance caused by the oxidation layer on the particle surface, as shown in Fig. 5(a). Such pressure-induced formation of low-resistance conductive paths is a feature that traditional solid conductive phases cannot achieve.

Further experiments revealed that when these newly formed conductive paths are damaged, the liquid metal can regenerate new circuits in situ. This behavior is enabled by the fluidity of liquid metal,

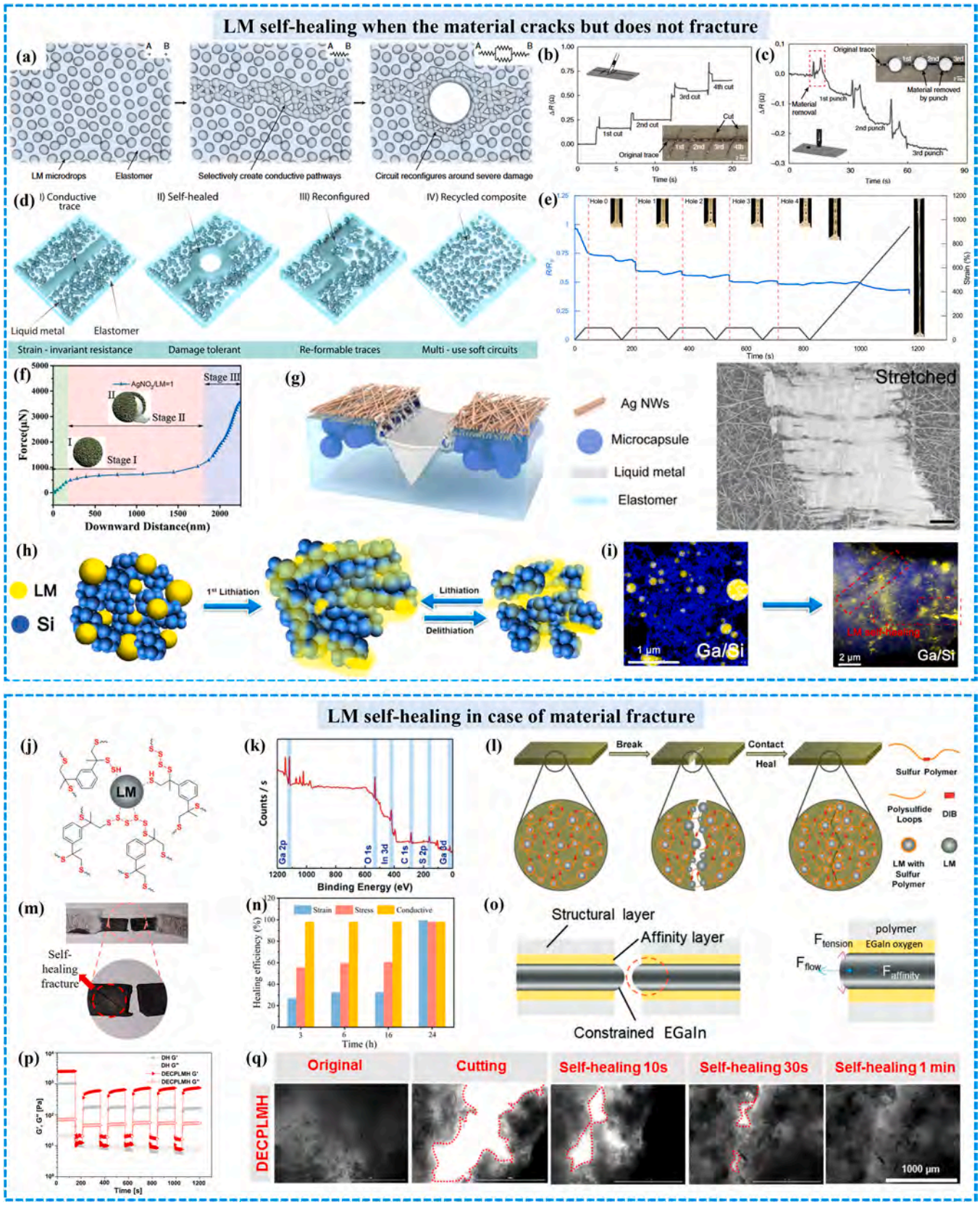

(caption on next page)

Fig. 5. Self-healing mechanisms of LM without the assistance of external conditions and applications. (a) Schematic of the internal self-healing mechanism of LM after damage to the substrate, where the liquid metal reconfigures to generate new circuits; (b) Changes in overall resistance of LM after self-healing after cutting the substrate; (c) Changes in overall resistance of liquid metal after self-healing after perforator piercing the substrate [159], Copyright 2018, Springer Nature. (d) Stabilized conductive paths inside the substrate using embossing; (e) Resistance and strain curves of complexe after multiple perforations and stretching [192], Copyright 2021, Springer Nature. (f) Typical force–distance curve for Ag@LMPs [193], Copyright 2020, Wiley-VCH. (g) Schematic of LM self-healing during stretching and SEM image at crack, scale: 2 μm [194], Copyright 2023, American Chemical Society. (h) Schematic diagram of LM self-healing during Li/Si anode charging and discharging process. (i) STEM plots of Li/Si anode before and after charging and discharging [195], Copyright 2018, Elsevier. (j) Schematic diagram of LM interaction with surfaces, polysulfide loops, and thiol terminal groups; (k) XPS spectrum for LM obtained from LMESP; (l) Illustration of self-healing process of LMESP materials [196], Copyright 2019, Wiley-VCH. (m) Self-healed hydrogel did not break at the original fracture after secondary stretching; (n) Histogram of self-healing efficiency represented by different indicators at different times [197], Copyright 2023, The Royal Society of Chemistry. (o) Schematic diagram of the treatment of the substrate to change the wettability of LM in the material [198], Copyright 2022, Wiley-VCH. (p) Elastic modulus change curve of hydrogel when strain is switched from 1 % to 1000 % in alternating steps. (q) Bright field image during hydrogel self-healing process [199], Copyright 2021, Springer Nature.

allowing droplets to quickly reconnect and re-establish conductive paths in the damaged areas, thus preserving conductivity after damage. Figs. 5 (b) and 5(c) illustrate changes in resistance when the elastomer is subjected to cutting and puncturing damage, respectively. The effects of different damage types on resistance vary: when the elastomer is cut with a blade, the position of the conductive path remains relatively unchanged, and the liquid metal in the original path flows towards the surrounding damaged areas, reducing the amount of liquid metal in the conductive path, which is the primary cause of increased resistance in the elastomer.

In contrast, when the material is damaged by a punch, the external force causes liquid metal droplets around the puncture to rupture and disperse, allowing the conductive path to reconfigure with reduced resistance [192]. This self-reconfiguration characteristic of conductive paths is widely utilized in imprinting processes, allowing the conductive circuits to be customized into various shapes, as illustrated in Fig. 5(d). Fig. 5(e) shows the resistance changes in an elastomer treated with imprinting after being punctured. Compared to the unstamped material in Fig. 5(c), which shows a slight resistance fluctuation when punching, the resistance curve of the imprinted material is more stable, demonstrating enhanced damage resistance. This liquid metal-based self-healing conductive network not only exhibits excellent electrical stability and damage recovery capabilities but also provides new design strategies for applications in flexible electronic materials, especially in smart sensing and wearable devices.

In liquid metal research, the limited resistance to external pressure due to a thin surface oxide layer is a challenge. To enhance its compressive strength, Zheng et al. applied a silver coating to the surface of EGaIn using a chemical reduction method, forming Ag@LM core-shell particles [193]. They also studied the maximum load under mechanical stress. Nanoindentation tests revealed that the mechanical behavior of the Ag@LM particles could be divided into three different stages, as shown in Fig. 5(f). In the first stage, as the indenter came into contact with the particle surface, the pressure increased with displacement. In the second stage, while displacement continued to increase, the applied force remained almost constant, indicating gradual compression of the liquid metal structure. At 1500 nm, cracks began to form within the liquid metal, leading to leakage. By 1750 nm, the indenter came into contact with other particles, showing a trend similar to that observed in the first stage. This study demonstrated that the critical force for maintaining the integrity of the Ag@LM structure is around 500 μN, observed at the early part of the second stage (approximately 150 nm). These findings provide new insights into achieving self-healing of liquid metal under minimal external stress.

The binding of silver and liquid metal is not limited to Ag@LM core-shell structures. Lin et al. developed a stretchable conductive composite made of silver nanowires and liquid metal (Ag NW/LM) [194], exhibiting remarkable electrical stability under high strain, as shown in Fig. 5 (g). In tensile tests, the top silver nanowire layer fractured first, which in turn facilitated the release of the underlying liquid metal to fill the cracks and maintain a smooth surface, ensuring stable electrical output under high strain. Experiments showed that the conductive layer made of a single Ag layer failed at around 80 % strain, while the dual-layer Ag NW/LM design continued to function at 1000 % strain, greatly expanding the composite's potential applications.

The self-healing capabilities of liquid metal also present unique advantages in battery applications. Han et al. mixed nanosilicon with GaInSn liquid metal to prepare anodes for lithium-ion batteries [195]. During the initial lithiation process, the silicon nanoparticles expanded significantly. Due to external stress, the liquid metal fractured and dispersed uniformly throughout the electrode, providing a wetting effect, as shown in Fig. 5(h) and (i). STEM imaging revealed that the liquid metal could sufficiently fill the cracks formed by silicon expansion, reducing electrode volume changes and minimizing the contact area between the electrode and electrolyte, ultimately extending the battery's lifespan.

However, one major challenge in the practical applications of liquid metal is its incompatibility with non-metallic materials, which limits its performance optimization. To address this problem, Xin et al. developed a liquid-metal-embedded sulfur polymer composite (LMESP) material by mixing liquid metal with 1,3-diisopropylbenzene (DIB) and adding elemental sulfur [196], which undergoes ring-opening polymerization, as shown in Fig. 5(j). This reaction resulted in interactions between the liquid metal and polysulfide loops/thiol groups, further evidenced by XPS spectra showing peaks for Ga 2d, Ga 3d, In 3d, O 1 s, C 1 s, and S 2p in Fig. 5(k). When the fractured surfaces of the material came into contact, the fluidity of the liquid metal, along with interactions between polysulfide loops/thiol ligands and polymer chains, enabled self-healing, as shown in Fig. 5(l). The LMESP composite achieved self-healing at room temperature within 24 h, and the resistance was restored to 1.86 Ω, close to the original 1.1 Ω. In contrast, conventional pure sulfur polymers typically require high temperatures for self-healing. The integration of liquid metal with sulfur compounds overcame this limitation: the liquid metal showed excellent compatibility with the polymer matrix, while sulfur bonds with a low glass transition temperature enabled effective self-healing at room temperature. Thus, the combination of internal and external self-healing mechanisms in LMESP produced a synergistic effect, achieving a "$1 + 1 > 2$" outcome.

The fluidity of liquid metals is a distinguishing feature that sets them apart from other conductive metal materials, and this characteristic is particularly prominent in the self-healing processes of elastomers. During fracture and the subsequent healing process, the position of the liquid metal tends to shift, resulting in structural differences between the healed section and the corresponding area of the original elastomer. This behavior causes questions about whether repeated stretching could lead to a fracture at the same location.

Li and colleagues employed EGaIn as an initiator in a one-pot synthesis to create a composite hydrogel consisting of liquid metal, PVA, and P (acrylamide-co-octadecyl methacrylate (P(AAm-co-SMA)), referred to as LM/PVA/P(AAm-co-SMA) hydrogel [197]. Within this material system, self-healing is primarily driven by the hydrophobic association network of P(AAm-co-SMA), hydrogen bonding between the PVA and P(AAm-co-SMA) networks, and physical crosslinking involving the liquid metal and these networks. These various physical crosslinking interactions enable the hydrogel to dissipate large energy, resulting in a

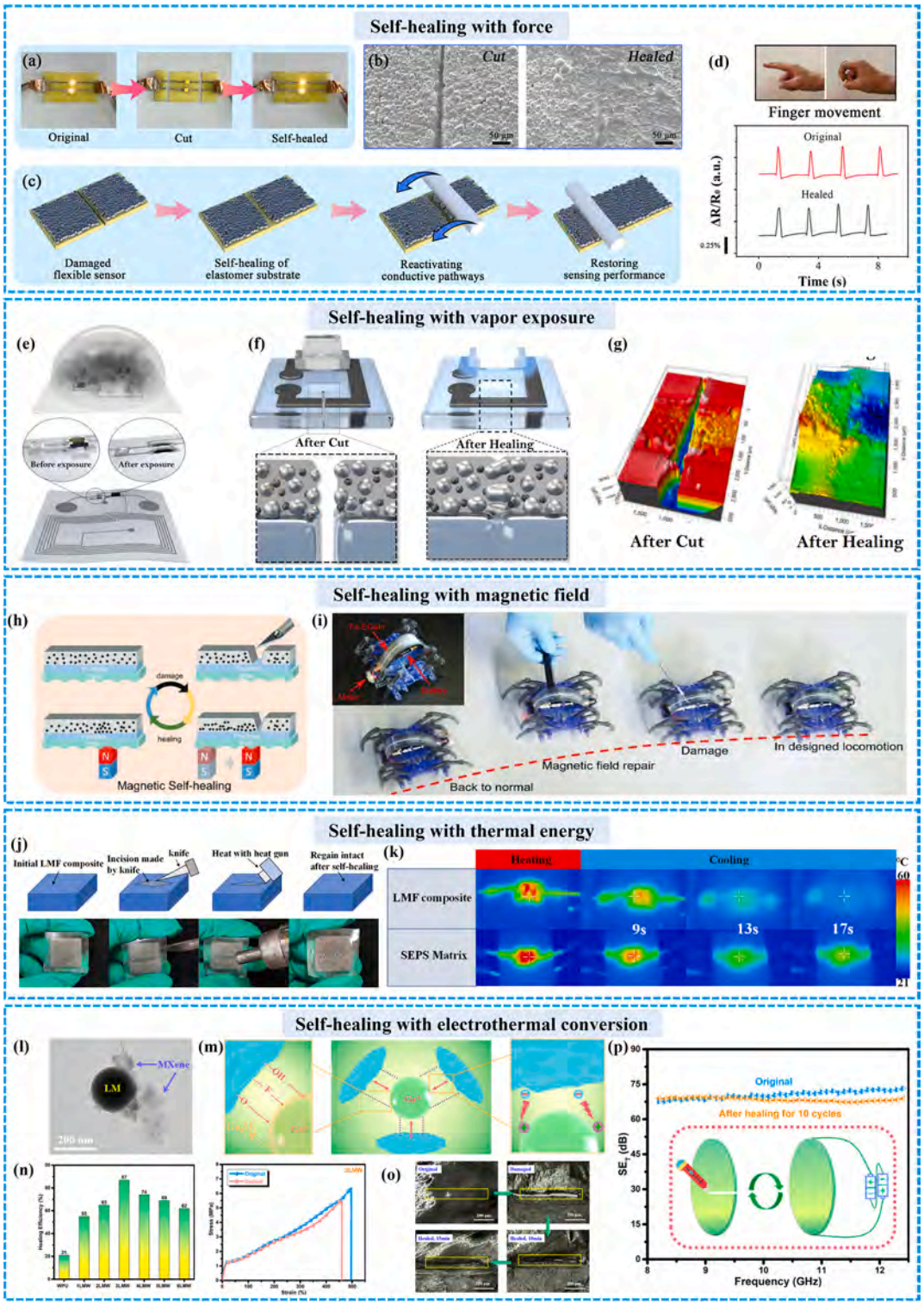

Fig. 6. Schematic diagrams of self-healing that require the use of external fields or additional substances, and applications.Self-healing with force: (a) Photographs of electrical properties that can be reproduced in contact with a cross-section. (b) SEM images before and after section repair. (c) Schematic diagram of the overall sensing performance with the help of the Teflon stick repair. (d) Schematic of the change in finger movement resistance measured by the original and repaired sensors [200], Copyright 2023, American Chemical Society. Self-healing with vapor exposure: (e) Schematic representation of the polymer-solvent transition before and after vapor exposure. (f) Schematic of vapor exposure-assisted self-healing. (g) Optical profilometer images before and after fracture healing [201], Copyright 2021, Springer Nature. Self-healing with magnetic field: (h) Schematic diagram of Fe-EGaIn self-healing under the action of a magnetic field. (i) Picture of a robot working again after a magnet-guided repair of a damaged conductive line [202], Copyright 2019, Wiley-VCH. Self-healing with thermal energy: (j) Schematic as well as photograph of LMF composite thermal self-healing process. (k) Comparison of heat dissipation results between matrix and LMF composites by infrared thermography [203], Copyright 2022, Elsevier. Self-healing with electrothermal conversion: (l) TEM images of LM@MXene nanocomposites; (m) Schematic diagram of two interfacial interactions between LM and MXene. (n) Self-healing efficiency with different LM contents and stress-strain curves of 3LMW films before and after healing. (o) Optical images of the self-healing process of damaged 3LMW films under a 5 V voltage at different time intervals. (p) EMI SE changes of 6LMW films before and after 10 healing cycles [204], Copyright 2022, Elsevier.

fracture elongation of up to 2000 %. At room temperature, after 24 h of healing treatment, the healing efficiency of the material can reach more than 99 %. The study further examined the fracture behavior of the healed hydrogel under subsequent stretching. As shown in Fig. 5(m), the location of the second fracture did not coincide with that of the first, indicating that the presence of liquid metal does not significantly impact the tensile performance of the hydrogel despite structural differences in the healed regions. Fig. 5(n) illustrates self-healing efficiencies across different healing times, showing that electrical properties recover almost instantly upon contact between fractured surfaces, while mechanical properties, such as stress and strain, require prolonged cross-linking of covalent and non-covalent bonds for complete restoration.

In hydrogels with low liquid metal content, the fluidity of the liquid metal is mostly limited to the area around the fracture. However, for materials where liquid metal is encapsulated within the matrix, a fracture could result in leakage of liquid metal, leading to potential short circuits or even device failure. To address this issue, Fang and colleagues used 3D printing to encapsulate EGaIn within microchannels, creating an elastic, self-healing circuit layer that was then integrated with other components to form a device called “iMethy” [198]. To prevent liquid metal leakage at the fracture surface, they applied a rolling-printing technique to add an oxide layer as an affinity layer on the PDMS mechanical skeleton. On the PDMS surface, EGaIn exhibited a high “non-equilibrium” contact angle, and the affinity layer changed the wettability between EGaIn and PDMS, as shown in Fig. 5(o). Even after multiple healing cycles, the electrical functionality of the conductive pathways was maintained at a basic level of stability. This work not only reveals the self-healing capabilities and mechanisms of liquid metal hydrogels but also explores their fracture behavior and electrical stability under repeated stretching, providing valuable insights for the design of future flexible and self-healing electronic devices.

Based on the excellent self-healing and other beneficial properties of various materials, Xu et al. have thoroughly examined the potential of biomimetic self-healing materials with liquid metal in clinically relevant applications [199]. They highlight that energy dissipation during chemical bond rupture is closely associated with diverse interactions and complex physical processes within the material. This makes the presence of reversible chemical bonds within the crosslinked network of hydrogels critical for enhancing overall material performance. By increasing the diversity and complexity of reversible bonds in the hydrogel’s crosslinked network, the self-healing and other key properties of the material can be significantly improved.

To achieve this objective, the research team synthesized four distinct precursor materials: catechol-functionalized chitosan (CHI-C), cholesterol hemisuccinate (CH), cholesteryl and aldehyde-modified dextran (Dex-ALD-CH), poly(3,4-ethylenedioxythiophene)-heparin (PEDOT:Hep), and TA-coated LM nanodroplets (LM-TA). These materials were blended to form conductive biopolymers/liquid metal hydrogels with dynamic self-healing properties, termed DECPLMH, which contain multiple self-healing mechanisms. Specifically, the hydrogel’s external self-healing mechanism stems from the encapsulated liquid metal microcapsules, while internal self-healing relies on a series of reversible bonds. The self-healing mechanisms within DECPLMH include reversible covalent bonds (e.g., imine bonds, Schiff base bonds) and various non-covalent interactions, such as hydrogen bonding, electrostatic interactions, anion/cation-π interactions, π-π stacking, hydrophobic interactions, and coordination interactions between the liquid metal and polyphenolic groups. These reversible bonds form an interconnected dynamic hydrogel network, making the material highly adhesive and cohesive strengths under external stress. The research team evaluated the self-healing properties of the hydrogel with strain-dependent oscillatory rheology. In cyclic testing with alternating strains from 1 % to 1000 %, changes in storage modulus (G') and loss modulus (G'') revealed that the hydrogel exhibits viscoelastic fluid characteristics under high strain and rapidly recovers its gel state under low strain, as shown in Fig. 5(p). The multi-cycle stability of the material demonstrates a highly robust self-healing process, further confirming its excellent self-healing capabilities. Additionally, in a real-time electrical monitoring system, DECPLMH exhibited a current drop to zero upon being cut, and electrical conductivity rapidly recovered when the severed interface was reconnected, and the hydrogel recovery process is shown in Fig. 5(q). Notably, the hydrogel fully self-healed within approximately one minute after cutting, the healing rate significantly superior to that of many conventional self-healing hydrogels, which fully demonstrates the role of multiple self-healing mechanisms and its cross-linked structure on the overall performance of the material.

4.2. *Liquid metal self-healing materials with external resource supporting*

Compared to self-healing materials that only rely on reversible chemical bonds and microstructures, those enhanced by external resources do not require complex internal chemical bond designs within the elastomer to achieve rapid healing. The addition of external fields or materials not only accelerates the self-healing efficiency but also enables the customization of self-healing materials for specific applications. In the field of self-healing materials, a wide variety of external resources can be employed, offering great flexibility and adaptability in material design.

For instance, Yang et al. used a one-pot two-step method with polyetheramine (PEA), adipic acid dihydrazide (ADH), terephthalaldehyde (TA), and benzene-1,3,5-tricarbaldehyde (TFB) as raw materials to develop a highly stretchable elastomer, PE0.5–0.2 (where 0.5 and 0.2 represent the molar ratios of ADH to PEA amine groups and TFB to acrolein aldehyde groups, respectively) [200]. Based on this elastomer, they prepared PVP@LM conductive ink using ethanol as the solvent, which was evenly coated onto the surface of the elastomer to create a flexible sensor. The sensor was then connected to a circuit containing a DC power supply and an LED, as shown in Fig. 6(a). When the material was cut, the LED turned off immediately, but it relight after self-healing. Fig. 6(b) presents SEM images of the fracture before and after healing, indicating that the crack becomes barely visible after healing. In the conductive layer above the elastomer, carbonyl groups of PVP form ion-dipole interactions with Ga_2O_3/Ga^{3+} on the surface of the liquid metal, which allows PVP to completely encapsulate the liquid metal droplets. There is a slight distance between droplets, requiring a poly-tetrafluoroethylene (PTFE) rod to be rolled over the damaged area to reactivate the conductive layer, as illustrated in Fig. 6(c). This externally applied force not only re-establishes conductive pathways by reconnecting broken liquid metal droplets but also promotes contact between the flexible layer’s broken sections. After healing, the elastomer was used to monitor finger joint motion, as shown in Fig. 6(d). The electrical signal output of the healed sensor showed minimal fluctuation compared to the original sensor, demonstrating the remarkable effectiveness of external field-assisted self-healing.

As previously mentioned, in cyclic testing with alternating strains of hydrogels, the self-healing performance is reflected in the transformation between viscoelastic liquid and gel states. Based on this property, Lopes et al. designed a steam exposure technique for self-healing, reversible polymer gels applicable in integrated circuits [201]. They prepared a styrene-isoprene block copolymer (SIS) substrate, using styrene and toluene in a 1:2 ratio. The Ag-EGaIN-SIS composite conductive ink was then printed onto this substrate, and surface-mounted device (SMD) resistors were placed on the conductive circuits. The circuit is placed in a sealed chamber as a whole, and toluene vapor is generated by the evaporation of the solvent contained in the fabric or paper soaked in toluene, thus realizing the automatic welding of the chip and sealing of the printed circuit, as shown in Fig. 6(e). In the presence of toluene vapor, both the conductive ink and the substrate underwent a sol-gel transition, with the SMD components sinking into the softened SIS substrate due to capillary forces, thus completing the encapsulation of components in the circuit without the need for heating. Simultaneously, the microstructure of the Ag-EGaIn conductive ink

changed, resulting in enhanced conductivity. Figs. 6(f) and 6(g) show a schematic of the steam-exposed, self-healing process for cut materials and an optical profilometer image. Exposure to toluene vapor accelerates the sol-gel transition during self-healing, reducing healing time. While the material is in the viscoelastic healing state, liquid metal mobility is further promoted, aiding the recovery of electrical and mechanical properties. Unlike other gels, low-density solvents have a higher evaporation rate, which can speed up the healing process. However, extended exposure to high-density vapor may alter the overall thickness of the device, potentially impacting performance.

To minimize the impact of external resources on the overall performance of the material, such resources should primarily target damaged areas rather than the material as a whole. Guo et al. designed a magnetically responsive liquid metal electronic component with this concept [202]. Since liquid metal itself has limited magnetic responsiveness, they mixed Fe particles with the liquid metal. The oxide layer formed on the liquid metal surface effectively encapsulates the Fe particles, resulting in Fe-EGaIn particles with magnetic responsiveness. These Fe-EGaIn particles exhibit good wettability with fructose but poor wettability with PVA. Take advantage of this property, the researchers printed a fructose layer onto a PVA substrate using a ball-point pen, then used a magnet to selectively and uniformly attract the magnetic Fe-EGaIn particles to the fructose layer, forming a conductive pathway. In practical applications, a magnet placed under the PVA substrate guides the movement of the particles without affecting the PVA substrate itself. When the material is damaged, moving the magnet laterally around the break causes additional Fe-EGaIn particles to be drawn to the damaged area, accelerating the self-healing rate, as shown in Fig. 6(h). The healing time for a single cut is approximately 3 s, while multiple cuts heal within 10 s. Fig. 6(i) provides a top-down view of the robot's damage and magnetic repair process. After being repaired by a magnet, the robot quickly continued to move along its original path. This remote repair method minimizes physical contact and, by controlling the fluidity of the liquid metal, enables self-healing without the internal particle breakage and material loss that can occur in liquid metal hydrogel composites.

However, the combination of iron and liquid metal also has some drawbacks. While the addition of iron imparts magnetic responsiveness to the liquid metal, it also reduces the overall fluidity of Fe-EGaIn. Consequently, the Fe content is thus a crucial parameter in experimentation: a low iron content may lead to insufficient magnetic responsiveness, while a high content can result in sharp, spiked structures during movement, leading to phase separation between Fe and the liquid metal and impairing self-healing performance. Nevertheless, the fluidity of the liquid metal reduces resistance to Fe movement within the matrix, preserving the electrical performance of the material.

In addition to surface printing or coating, self-healing liquid metal-based materials can also work in encapsulated forms within a polymer matrix. Due to its metallic properties, liquid metal has not only excellent electrical conductivity but also exceptional thermal conductivity. Lv et al. developed a thermally self-healing liquid metal foam composite (LMF composite) by encapsulating liquid metal within a polymer [203]. Unlike the sugar-template method mentioned previously, this approach uses a salt-template method, which does not caramelize at high temperatures. By mixing salt and water in a 37:1 ratio, drying it to form a salt template, and immersing it in molten styrene-ethylene-propylene-styrene (SEPS) fluid for cooling, a porous SEPS elastomer material was obtained after water washing. By vacuum technology, liquid metal was injected into this porous structure, forming the LMF composite. After cutting the surface of the material, the self-healing process was activated by applying a hot air gun at 130°C for 1 min, which melts and fuses the cut surfaces, as shown in Fig. 6(j). Aside from the thermoplasticity and excellent flowability of SEPS upon heating, combined with the flowing liquid metal filler, ensured that the material remained undamaged after being cut. This is a key factor in maintaining the overall mechanical and thermal stability of the material post-healing. The recovery rates for both mechanical and thermal performance after cutting were around 98 %. To further investigate the material's high thermal conductivity, the researchers attached heating wires to both the LMF composite and an SEPS substrate and applied a 300 mA current for 1 min before cutting off the power. Infrared imaging results, as shown in Fig. 6(k), indicate that the LMF composite dissipates heat more effectively than the SEPS substrate, showing the superior thermal conductivity characteristic of liquid metal. The excellent heat dissipation capability of the internal LMF composite does not occur when the external SEPS have healed, and the internal heat cannot be consumed quickly, helping to maintain stability during the application and self-healing process.

Liquid metal represents an extremely promising technology for electrical self-healing by leveraging its unique physicochemical properties combined with electrically driven mechanisms. Liu Jing's team developed a direct-printing method for liquid metal electrodes in DEAs, enabling self-healing solely through applied electric fields [46]. When both electrodes carry opposite charges, the entire device functions as a capacitor. At converging electrode boundaries (where gaps narrow and electrostatic attraction intensifies), the liquid metal ruptures its oxide skin and merges. Simultaneously, during DEA actuation, voltage-induced microflow drives liquid metal outward from the electrode center, with flow reversing upon voltage removal. These dual mechanisms—oxide rupture at tips and field-directed microflow—operate independently or synergistically throughout actuation cycles to achieve self-repair. This printing approach facilitates compatibility with diverse materials and surfaces while simplifying manufacturing and reducing costs. The resulting electrodes achieve 2D planar self-healing under operational electric fields, significantly enhancing fault tolerance and harsh-environment adaptability in DEA applications.

The application of thermal energy in self-healing materials is not limited to external sources; internally generated heat (such as Joule heating induced by electric fields) can also act as an effective heating method. Zhou et al. developed a novel electromagnetic interference (EMI) shielding material based on LM@Mxene particles embedded in a waterborne polyurethane (WPU) polymer matrix [204]. To enhance the stability and dispersion of liquid metal in WPU, they used a ball milling technique to evenly mix Mxene with liquid metal, producing homogeneous LM@Mxene composite particles, as shown in Fig. 6(l). The key to the realization of ball milling technology relies on the electrostatic interaction between liquid metal and Mxene, along with coordination reactions between Ga^{3+} ions in the oxidized layer of the liquid metal and oxygen groups on the Mxene surface, illustrated in Fig. 6(m). Through surface modification of Mxene, hydrogen bonding between LM@Mxene and WPU was enhanced, significantly improving the compatibility of liquid metal within the WPU matrix. Additionally, the polymer chain structure of WPU effectively suppressed LM leakage under tensile stress. The addition of solid particles can also limit the crack propagation in the WPU matrix, thus improving the mechanical properties of LMW films. The material system is labeled xLMW, with the x representing the addition ratio of LM@Mxene. Specifically, x values of 1, 2, 3, 4, 5, and 6 correspond to LM contents of 3 wt%, 6 wt%, 9 wt%, 12 wt%, 15 wt%, and 18 wt%, respectively.

The researchers evaluated the EMI and self-healing properties of the composite materials with different LM contents, with results displayed in Fig. 6(n) and (o). For xLMW samples with cut damage, applying a 5 V circuit induced conductive connections among LM@Mxene particles, generating Joule heat in the damaged area, as shown in Fig. 6(p). This internal heating mechanism accelerates molecular chain mobility and facilitates the reformation of reversible bonds, significantly enhancing self-healing efficiency. Among the composites, 3LMW exhibited the highest self-healing efficiency at 87 %, while 6LMW achieved 62 %. The lower efficiency of 6LMW is attributed to partial contamination at the interface caused by the high solid phase content after fracture, which affects the cross-linking of hydrogen bonds in the WPU matrix. Both of

Table 3
Performance comparison of liquid metals in flexible electronic device applications.

LM in materials	LM composition	Substrates	Synergistic mechanisms	Healing conditions	Initial performance	Performance after self-healing	Repair efficiency	Application	Ref.
Surface	EGaIn	TSPU/Diol–Upy/BT	Hydrogen bonds	100 ℃，36 h	Strain: ~2500 %	Strain: ~2400 %	94.60 %	Soft electronic device	[205]
Surface	EGaIn	PHEA-co-PEGDA	Hydrogen bonds	R.T., 5 min	Strain: ~1500 %	Strain: ~800 %	53.33 %	Self-healable electrodes	[178]
Surface	GaInSn	PE (PEA/ADH/TA/DMAc)	Imine bonds/Hydrogen bonds	Force field	GFs: 0.08 (response ranges: 0–100 %)	GFs: 0.07 (response ranges: 0–100 %)	87.50 %	Wearable electronics	[200]
Encapsulation	EGaIn	PVA	Hydrogen bonds	R.T., 24 h	Strain: ~339 %	Strain: ~150 %	44.25 %	Soft robotics	[206]
Encapsulation	EGaIn	PMI	Hydrogen bonds/Disulfide bonds	R.T., 72 h	Tensile strength: ~3.54 MPa Elongation at break: 995 %	Tensile strength: ~2.83 MPa Elongation at break: 933 %	~80 %	Wearable electronics	[207]
Encapsulation	EGaIn	α-TA-BA	Hydrogen bonds/Disulfide bonds	60 ℃，8 h	Strain: ~760 %	Strain: ~760 %	~100 %	Flexible electronics	[208]
Encapsulation	EGaIn	Styrene-ethylene-propylene-styrene	Substrate melting (Fluidity)	130 ℃, 1 min	Thermal conductivity: 8.9 $Wm^{-1}K^{-1}$	Thermal conductivity: 6.8 $Wm^{-1}K^{-1}$	~80 %	Flexible heat dissipation material	[203]
Encapsulation	EGaIn	PDMS-MDU-IU	Hydrogen bonds	Artificial sweat, 2 h	Resistance: 0.8 Ω	Resistance: 1.1 Ω	72.73 %	E-skin	[93]
Encapsulation	GaInSn	SHP	Imine bonds/Disulfide bonds	R.T., 8 h	Stress: ~173 kPa Strain: ~218 %	Stress: ~164 kPa Strain: ~214 %	Stress: 95 % Strain: 98 %	Wearable electronics	[209]
Encapsulation	GaInSn	PVP/Honey /H_2O	Substrate melting	80 % humidity 90 min	Strain: ~30 %	Strain: ~25 %	~ 80 %	Stretchable electronics	[210]
Encapsulation	GaInSn	OC-PU	Hydrogen bonds	65 ℃, 6 h	Sensitivity: 0.011 kPa^{-1} (Range: 0–50 kPa) Sensitivity: 0.003 kPa^{-1} (Range: 50–200 kPa)	Sensitivity: 0.011 kPa^{-1} (Range: 0–50 kPa) Sensitivity: 0.002 kPa^{-1} (Range: 50–200 kPa)	100 % (Range: 0–50 kPa) ~66.67 % (Range: 50–200 kPa)	Skin-attachable integrated devices	[211]
Mixture	Ga	PU	Diels–Alder (DA) reactions	120 ℃, 10 min, and 65 ℃, 72 h	Modulus: ~235 MPa Strength: ~18 MPa Strain: ~814 %	Modulus: ~216 MPa Strength: ~13 MPa Strain: ~553 %	Modulus: 92 % Strength: 71 % Strain: 68 %	Soft robotics/Transient devices	[212]
Mixture	Ga	PAA	Hydrogen bonds/Metal-ligand coordination	R.T., 24 h	Stress: ~136 kPa	Stress: ~125 kPa	Stress: 92 % Strain: 87 % Conductivity: 100 %	Flexible electronics	[213]
Mixture	Ga	PAA	Hydrogen bonds/Electrostatic interactions	R.T., 20 min	Stress: ~117 kPa	Stress: ~96 kPa	~82 %	Wearable electronics	[214]
Mixture	EGaIn	SPU	Disulfide bonds	120 ℃, 24 h	EMI SE: 36 db (LM40–300)	EMI SE: 32 db (LM40–300)	88.89 %	Electromagnetic interference shielding	[215]
Mixture	EGaIn	SBS	π–π stacking	80 ℃, 30 min	Conductivity: 12000 S/cm	Conductivity: 8500 S/cm	70.83 %	Flexible electronics	[216]
Mixture	EGaIn	PAA	Electrostatic interactions/Metal-ligand coordination/Hydrogen bonds	R.T., 2 h	Strain: ~2907 %	Strain: ~2712 %	~93.39 %	Wearable electronics	[217]
Mixture	EGaIn	PAA	Hydrogen bonds/Electrostatic interactions	R.T., 3 h	Strain: ~2270 %	Strain: ~1450 %	~65 %	Wearable electronics	[218]
Mixture	EGaIn	PAM	Metal-ligand coordination/Hydrogen bonds	R.T., 1 min	Strain: ~2080 kPa	Strain: ~318 kPa	~15.29 %	Wearable flexible electronics	[219]

(*continued on next page*)

Table 3 (*continued*)

Mixture	EGaIn	PDES	Hydrophobic interactions/ Hydrogen bonds	R.T., 24 h	Stress: ~137 kPa Strain: ~2700 %	Stress: ~130 kPa Strain: ~2650 %	Stress: ~ 95 % Strain: ~ 98 %	Sensing specific handwriting	[220]
Mixture	EGaIn	DECPLMH	Hydrogen bonds/ Imine bonds/ π–π stacking/ Electrostatic interaction/ Hydrophobic interaction/	R.T., 1 min	Current response: ~3.33 mA/cm^2	Current response: ~2.72 mA/cm^2	~81.68 %	Bioadhesive	[199]
Mixture	EGaIn	PVA/Borax	Hydrogen bonds	R.T., 5 min	Strain: ~445 % (Freezing 10 min)	Strain: ~430 % (Freezing 10 min)	0.964	Soft robotics	[221]
Mixture	EGaIn	Gelatin/ Ethylene glycol	Electrostatic interaction/ Hydrogen bonds	70 ℃ , 12 h	Strain: ~225 % (200 % LM contents)	Strain: ~225 % (200 % LM contents)	~100 %	Wearable electronics	[222]

LM in materials	LM composition	Substrates	Synergistic mechanisms	Healing conditions	Initial performance	Performance after self-healing	Repair efficiency	Application	Ref.
Mixture	EGaIn	PAM/SA	Metal-ligand coordination/ Hydrogen bonds	R.T., 6 s	Current: ~0.0193 mA	Current: ~0.0182 mA	~94.30 %	Wearable electronics	[223]
Mixture	EGaIn	PAM/SA	Hydrophobic interactions/ Hydrogen bonds	R.T., ≤ 10 s	Current: ~0.0725 mA	Current: ~0.0725 mA	~100 %	Health monitoring	[224]
Mixture	EGaIn	P(AAm-co-SMA)	Hydrophobic association/ Hydrogen bonds	R.T., 24 h	Stress: ~0.200 MPa Strain: ~1218 %	Stress: ~0.194 MPa Strain: ~1208 %	Stress: ~ 97 % Strain: ~ 100 %	Infrared camouflage	[197]
Mixture	EGaIn	PVA/TO-CNF	Hydrogen bonds/ Borate ester bonds	R.T., 30 min	Stress: ~560 kPa Strain: ~515 %	Stress: ~535 kPa Strain: ~515 %	Stress: ~ 96 % Strain: ~ 100 %	Electromagnetic interference shielding	[225]
Mixture	EGaIn	HEA/EDDT/ TMADA	Thiol-Michael reactions/ Hydrogen bonds/ Thioether bonds	90 ℃ , 24 h	Resistance: 40 Ω	Resistance: 48 Ω	0.8333	Modular soft robotics	[226]
Mixture	GaInSn	PU	Diels–Alder (DA) reactions/ Hydrogen bonds	120 ℃, 2 h, and 60 ℃, 48 h	R/R_0: 1	R/R_0: ~1.62	~61.73 %	Flexible transient electronics	[70]

LM in materials	LM composition	Substrates	Synergistic mechanisms	Healing conditions	Initial performance	Performance after self-healing	Repair efficiency	Application	Ref.
Mixture	GaInSn	WPU	Hydrogen bonds	5 V voltage, 15 min	Stress: 6 MPa (3LMW)	Stress: ~5.1 MPa (3LMW)	87 %	Electromagnetic interference shielding	[204]
Mixture	GaInSn	PUUE	Hydrogen bonds/ Metal-ligand coordination	60 ℃, 40 h	Elongation at break: 3485 %	Elongation at break: 3470 %	~100 %	Flexible electronics	[227]
Mixture	EGaInSn	TPU	Hydrogen bonds	160 ℃, 10 min	Resistance: ~6 Ω	Resistance: ~6 Ω	~100 %	Electromagnetic and ray shielding	[228]
Mixture	EGaInSn	PEG2000-b-P (TMC-co-MCC)n	Metal-ligand coordination/ Hydrogen bonds	808 nm near-infrared laser (1 W/cm^2), 7 min	Strain: ~120 %	Strain: ~108 %	90.30 %	Flexible sensors	[229]
Mixture/ Surface	EGaIn	WPU/FM	Hydrogen bonds	90 ℃, 24 h	Tensile strength: 22.19 MPa Elongation at break: 493.98 %	Tensile strength: 23.15 MPa Elongation at break: 360.04 %	104.32 %	Wearable electronics	[230]

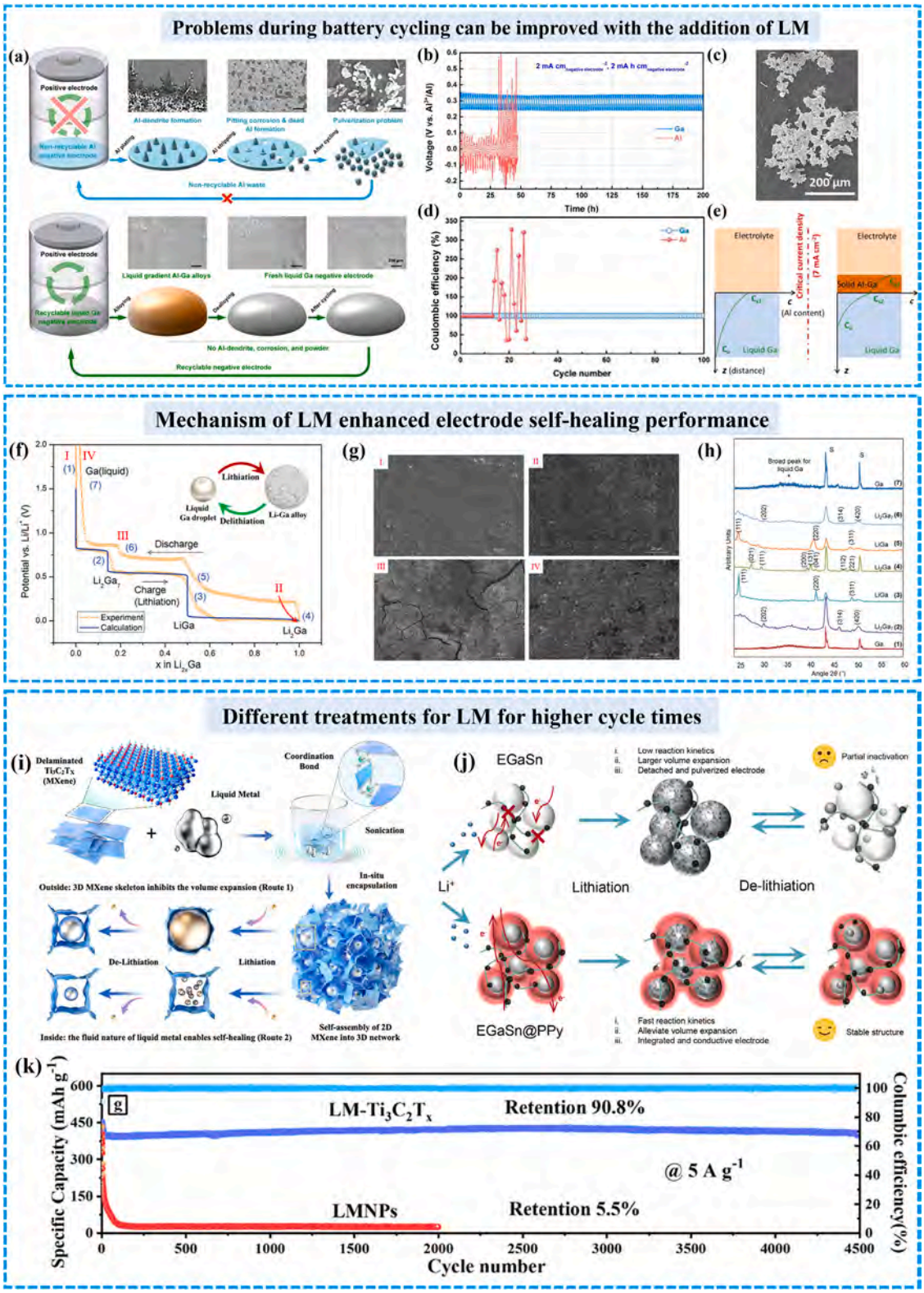

Fig. 7. Self-healing mechanism and application of LM in batteries. (a) Schematic and SEM images of the key problems in batteries using metal as the negative electrode, and the new liquid Ga negative electrode that improves the problems. (b and d) Comparison of the cycling performance and coulombic efficiency of symmetric cells with aluminum foil and liquid Ga. (c) SEM image of Al electrode after 28 cycles. (e) Schematic diagram of surface solidification evolution of liquid Ga anode during alloying at different current densities [234], Copyright 2019, Elsevier. (f) Different stages of LiGa electrodes in the cycling process and a schematic diagram of alloying. (g and h) Images and XRD patterns of electrode surface changes at different cycling stages (corresponds to Fig. 7(f) diagram) [44], Copyright 2011, The Electrochemical Society. (i) Schematic representation of the preparation process of LM-$Ti_3C_2T_x$ and lithiation and delithiation during the battery cycling process [236], Copyright 2022, The Royal Society of Chemistry. (j) Schematic representation of EGaSn as well as EGaSn@PPy during the cycling process [237], Copyright 2022, Elsevier. (k) Comparison of cycling performance of LM-$Ti_3C_2T_x$ and LMNPs anodes under the same conditions [236], Copyright 2022, The Royal Society of Chemistry.

these composites outperformed pure WPU, which had a self-healing efficiency of 21 %. More importantly, 6LMW still retains more than 96 % of the EMI performance after self-healing. The electromagnetic shielding performance is mainly supported by LM@Mxene particles. This self-healing strategy, which uses externally applied voltage to convert internal joule heat, gives the film excellent self-healing capabilities and ensures that the electromagnetic shielding performance remains at a high level even when the material is damaged, thus guaranteeing the stable use of the material in complex environments. This design offers an effective self-repair solution for liquid metal-based materials across various application domains.

Liquid metal, as a novel self-healing material, demonstrates unique advantages in autonomously restoring the electrical properties of materials. However, this "leakage" healing approach, while effective for electrical performance recovery, may adversely affect the mechanical properties of elastomers such as strength and toughness, potentially limiting its application in specific fields. When investigating the properties of liquid metal self-healing materials, comparative analysis of pre- and post-repair performance data reveals comprehensive insights into their restoration efficacy and limitations. As shown in Table 3, the conditions for external self-healing are specified under "Healing conditions", while other self-healing mechanisms synergizing with it are detailed in the "Synergistic mechanisms" section. Based on this observation, we can conclude that an increased number of synergistic self-healing mechanisms within a material correlates significantly with reduced self-healing duration. This phenomenon occurs because multiple complementary mechanisms—such as crack closure via liquid metal flow, dynamic bond reorganization, and reactive interface regeneration—operate concurrently through distinct pathways.

Specifically, increased internal self-healing chemical bonds create more dynamic reversible reaction sites within the material. These sites enable a rapid damage response through bond dissociation and reformation, accelerating the self-healing process of mechanical properties. The enhanced reversible chemical bond density consequently reduces repair time while improving overall efficiency. Furthermore, the coordinated operation of multiple healing mechanisms empowers materials with superior environmental adaptability, significantly expanding their potential applications. This trend holds substantial scientific significance, indicating that synergistic interactions between multiple self-healing mechanisms can dramatically enhance repair efficiency, thereby paving the way for new advancements in materials science.

In conclusion, while liquid metal self-healing materials show remarkable potential for electrical property restoration, their mechanical performance impacts require deeper investigation. Strategically increasing endogenous healing bonds and leveraging multi-mechanism synergy presents an effective pathway to enhance repair efficiency, representing a crucial development trend in advanced materials science. This integrated approach not only addresses current limitations but also opens new frontiers for functional material design.

4.3. Alloying and De-alloying Self-healing Electrodes Based on Liquid Metal

As summarized above, during the self-healing process of elastomers, liquid metal demonstrates its remarkable fluidity and metallic properties. Its excellent fluidity enables it to swiftly migrate toward cracks or fractures, effectively facilitating the reconnection of damaged surfaces. The metallic nature of liquid metal is reflected in its outstanding electrical and thermal conductivity. The conductivity allows the material to self-heal during electrification, and the current in the conductive path can also be converted into Joule heat to assist the internal cross-linking of the self-healing material. Meanwhile, the superior thermal conductivity ensures the stable dissipation of heat from the elastomer and its surroundings, further promoting the self-healing process.

In the application of self-healing electrodes, in addition to the above-mentioned use of liquid metal dispersion to reduce the impact of volume changes caused by cracks, the high chemical reactivity of the liquid metal surface also plays a crucial role. Specifically, the liquid metal can complete the self-healing of the electrode through alloying and de-alloying during the electrode working process.

Currently, rechargeable battery electrodes face three primary challenges. The first challenge is the formation of dendritic crystals, caused by the uneven deposition of active materials on the electrode surface during charge and discharge cycles [231]. The second challenge arises from behavior such as pitting corrosion at the electrodes, driven by factors like high overpotential differences, which negatively impact cycling efficiency [232]. The third challenge is the pulverization of electrode materials. During prolonged charge-discharge cycling, continuous phase transitions induce volume expansion and stress accumulation, which are the primary causes of material pulverization [233]. The introduction of liquid metal has partially mitigated these issues, as illustrated in Fig. 7(a).

Jiao and colleagues used liquid metal Ga as the anode material for rechargeable aluminum-ion batteries in the $AlCl_3$-[EMIm]Cl system [234]. At a current density of 2 mA cm^{-2} and a fixed area capacity of 2 mAh cm^{-2}, they conducted voltage hysteresis and cycling stability tests on Ga-Al batteries and Al-Al symmetric batteries, as shown in Fig. 7(b). The results demonstrated that using liquid metal Ga as the anode significantly enhanced the battery's cycling life and stability. In contrast, traditional Al anodes exhibited a high voltage hysteresis of about 200 mV after 14 cycles, and the battery failed after 28 cycles. The SEM image of the detached Al powder is shown in Fig. 7(c), corresponding to the red line in Fig. 7(d), which represents the 28th cycle of the Al anode. The redox electrochemical reaction of conventional Al electrodes is described by Eq. (2):

$$4Al_2Cl_{7^-} + 3e^- \leftrightharpoons Al + 7AlCl_{4^-} \quad (2)$$

The corrosion during the cycling process leads to the formation of "dead" Al, which reduces the battery's lifespan. However, when liquid metal Ga is used as the anode, underpotential deposition (UPD) of Al occurs on the Ga surface, resulting in the formation of $AlGa_x$ alloys, as described by Eq. (3):

$$4Al_2Cl_{7^-} + 3e^- + xGa \leftrightharpoons AlGa_x + 7AlCl_{4^-} \quad (3)$$

Based on this process, the researchers adjusted the current density to investigate its effect on the Ga alloying process. The experimental results revealed that the critical anodic current density required to maintain the Ga anode in a liquid state is 7 mA cm^{-2}. At this current density, the diffusion rate of Al into the liquid Ga anode slightly exceeds or closely matches the reduction rate of Al. This balance between alloying and de-alloying rates enhances the battery lifespan, as illustrated in Fig. 7(e). However, when the anodic current density exceeds this critical value, the electrochemical reduction rate of Al increases. This prevents the reduced Al from diffusing efficiently into the liquid Ga anode, leading to surface issues such as dendrite formation, similar to those observed with conventional Al electrodes. Thus, the introduction of liquid metal as the anode material effectively mitigates the corrosion problems associated with traditional electrodes, significantly improving the cycling lifespan and stability of rechargeable batteries.

In addition to rechargeable aluminum-ion batteries, liquid metals are also frequently incorporated into lithium-ion batteries. Deshpande et al. fabricated a coin cell using liquid metal Ga and 304 stainless steel foil as the working electrode, with lithium metal foil serving as the counter electrode [44]. Because the melting point of liquid Ga is 29.8°C, the electrochemical cycling experiments were conducted at 40°C to maintain Ga in its liquid state. Owing to the high chemical reactivity of liquid Ga, alloying and de-alloying reactions occur between Li and Ga during the electrochemical process. The relationship between the open-circuit voltage and the specific capacity of the liquid Ga electrode is shown in Fig. 7(f). The morphological changes of the Ga electrode at stages I, II, III, and IV are depicted in Fig. 7(g). The in-situ XRD analysis of the alloying and de-alloying processes is presented in Fig. 7(h),

Table 4
The addition of liquid metals in the field of battery performance comparison.

Battery type	LM Composition	Usage	Charge Storage Mechanism	Performance without LM	Cycle number	Performance with LM	Cycle number	Capacity retention	Ref.
Li-ion	GaSn	Anode	Intercalation/Insertion Reaction	~100 mAh·g^{-1} (2 A·g^{-1}) (LMNPs)	1500	552 mAh·g^{-1} (2 A·g^{-1}) (LMNPs@CS)	1500	LMNPs@CS: 91.30 % LMNPs: ~40 %	[239]
Li-ion	GaSn	Anode	Alloying reaction	—	—	413 mAh·g^{-1} (5 A·g^{-1})	5000	~100 %	[240]
Li-ion	GaIn	Anode	Metal electrodeposition	< 30 mAh·g^{-1} (0.5 C)	< 130	> 100 mAh·g^{-1} (0.5 C)	> 320	—	[241]
Li-ion	EGaIn	Anode	Alloying reaction	< 200 mAh·g^{-1} (1 A·g^{-1})	< 60	~160 mAh·g^{-1} (1 A·g^{-1})	800	~83 %	[242]
Li-ion	EGaIn	Anode	Alloying reaction	20 mAh·g^{-1} (5 A·g^{-1}) (LMNP)	2000	489 mAh·g^{-1} (5 A·g^{-1}) (LM-$Ti_3C_2T_x$)	4500	LMNP: 5.5 % LM-$Ti_3C_2T_x$:90.8 %	[236]
Li-ion	EGaSn	Anode	Alloying reaction	< 400 mAh·g^{-1} (0.2 A·g^{-1}) (EGaSn)	< 100	590.6 mAh·g^{-1} (0.2 A·g^{-1}) (EGaSn(PPy))	500	~100 %	[237]
Li-ion	GaInSn	Anode	Alloying reaction	~266.1 mAh·g^{-1} (0.5 A·g^{-1}) (NP-SiGe)	100	1141.3 mAh·g^{-1} (0.5 A·g^{-1}) (NP-SiGe/LM1:2)	100	NP-SiGe: 11.1 % NP-SiGe/LM1:2: ~60 %	[243]
Li-ion	GaInSn	Anode	Conversion reaction	~50 mAh·g^{-1} (1 A·g^{-1}) (LM_2@WSe_2)	500	224.5 mAh·g^{-1} (1 A·g^{-1}) (LM_5@WSe_2)	500	LM_2@WSe_2: 20.0 % LM_5@WSe_2: 51.6 %	[244]
Battery type	LM Composition	Usage	Charge Storage Mechanism	Performance without LM	Cycle number	Performance with LM	Cycle number	Capacity retention	Ref.
Li-ion	GaInSn	Anode	Intercalation/Insertion Reaction	243.3 mAh·g^{-1} (2.1 A·g^{-1})	100	806.7 mAh·g^{-1} (2.1 A·g^{-1}) (20 % GaInSn)	100	—	[245]
Li-ion	GaInSnZn	Anode	Alloying reaction	688 mAh·g^{-1} (2 A·g^{-1})	300	846 mAh·g^{-1} (2 A·g^{-1}) (80℃)	300	—	[246]
Zn-ion	Ga	Anode	Metal electrodeposition	~63.7 mAh·g^{-1} (1 A·g^{-1})	1000	~271.4 mAh·g^{-1} (1 A·g^{-1})	100	Zn@CP: ~36.73 %% Zn-Ga@CP: ~100 %	[247]
Zn-ion	GaIn	Anode	Metal electrodeposition /Alloying reaction	~100 mAh·cm^{-3} (2 A·cm^{-3})	600	~160 mAh·cm^{-3} (2 A·cm^{-3})	600	Zn: ~67.88 % Zn@LM: ~100 %	[248]
Zn-ion	GaInSn	Anode	Metal electrodeposition /Alloying reaction	~28 mAh·g^{-1} (2 A·g^{-1})	1000	~162 mAh·g^{-1} (2 A·g^{-1})	1000	Zn/AgT: ~19.51 % Zn@LM/AgT: ~89.29 %	[249]
Zn-ion	GaInSn	Anode	Metal electrodeposition	~30 mAh·g^{-1} (2 A·g^{-1})	~600	69 mAh·g^{-1} (2 A·g^{-1}) (80℃)	1000	Zn@CC: ~50 % Zn@LM@CC: ~95 %	[250]
Zn-ion	GaInZn	Anode	Metal electrodeposition	51.3 mAh·g^{-1} (5 A·g^{-1})	~2010	149.3 mAh·g^{-1} (5 A·g^{-1})	10000	Zn: ~49.02 % LM@Zn: ~127.82 %	[251]
Zn-ion	GaInSnZn	Anode	Metal electrodeposition	~25 mAh·g^{-1} (0.5 A·g^{-1})	500	~72 mAh·g^{-1} (0.5 A·g^{-1})	500	Zn: ~49.02 % SLC−2: ~72.52 %	[252]
Battery type	LM Composition	Usage	Charge Storage Mechanism	Performance without LM	Cycle number	Performance with LM	Cycle number	Capacity retention	Ref.
Na-ion	Ga	Anode	Alloying reaction	~30 mAh·g^{-1} (10 C)	~470	100 mAh·g^{-1} (10 C)	500	Na: ~39.45 % NGAL-Na: ~100 %	[253]
Na-ion	Ga	Anode	Alloying reaction	~78 mAh·g^{-1} (2 C)	200	~100 mAh·g^{-1} (2 C)	200	NVP-SSFNa: 69.4 % NVP-Ga-SSFNa: 92.6 %	[254]
Na-ion	GaIn	Anode	Alloying reaction	~50 mAh·g^{-1} (0.5 C)	78	~100 mAh·g^{-1} (0.5 C)	100	NZSP: 47.8 % LM@NZSP: 85.1 %	[255]
Na-ion	GaSb	Anode	Conversion reaction	193 mAh·cm^{-3} (50 mA·g^{-1})	300	773 mAh·cm^{-3} (50 mA·g^{-1})	300	Hard C: ~100 % GaSb/C: ~100 %	[256]
Na-ion	GaInSn	Anode	Conversion reaction	~50 mAh·g^{-1} (0.5 A·g^{-1})	300	~150 mAh·g^{-1} (0.5 A·g^{-1})	300	MoS_2-PVDF: ~17.8 % MoS_2-LM: ~90.5 %	[257]
Na-ion	GaInSn	Anode	Alloying reaction	~20 mAh·g^{-1} (5 C)	< 50	~90 mAh·g^{-1} (5 C)	250	Na-CF: < 20 % Na-GSIC: 80.4 %	[258]
Mg-ion	Ga	Anode	Alloying reaction	33 mAh·g^{-1} (0.1 A·g^{-1}) (ssm-Ga)	100	225.7 mAh·g^{-1} (0.1 A·g^{-1}) (ssm-$CuGa_2$-Ga)	100	ssm-Ga: ~90.28 % ssm-$CuGa_2$-Ga: ~13.20 %	[259]
Battery type	LM Composition	Usage	Charge Storage Mechanism	Performance without LM	Cycle number	Performance with LM	Cycle number	Capacity retention	Ref.
Mg-ion	Ga	Anode	Alloying reaction	—	—	~300 mAh·g^{-1} (3 C)	200	~156.85 %	[260]

(*continued on next page*)

Table 4 (*continued*)

Mg-ion	Ga	Anode	Metal electrodeposition /Alloying reaction	~227 mAh·g^{-1} (0.1 C)	30	~320 mAh·g^{-1} (0.1 C)	30	Mg/S: ~50.75 % Ga_5Mg_2-Mg/S: ~63.61 %	[261]
Mg-ion	EGaIn	Anode	Alloying reaction	—	—	~220 mAh·g^{-1} (0.2 C)	2000	—	[262]
Al-ion	Ga	Anode	Alloying reaction	—	—	76.73 mAh·g^{-1} (100 mA·g^{-1})	1000	~92.8 %	[234]
Al-ion	Ga	Anode	Alloying reaction	—	—	127 mAh g^{-1} (1 A·g^{-1})	1200	~94.1 %	[263]
Al-ion	EGaIn	Anode	Alloying reaction	~80 mAh·g^{-1} (2 A·g^{-1}) (Mo)	4935	82.8 mAh·g^{-1} (2 A·g^{-1}) (EGaIn@Mo)	6000	EGaIn@Mo: ~100 %	[264]

corresponding to stages (1) through (7) in Fig. 7(f). The results indicate that three intermetallic alloy phases—Li_2Ga_7, LiGa, and Li_2Ga—are formed during the electrochemical reactions between Ga and Li. The lithiation and delithiation processes are described by Eqs. (4 and 5):

Lithiation:

$$Ga(l) \rightarrow Li_2Ga_7 \rightarrow LiGa \rightarrow Li_2Ga \quad (4)$$

Delithiation:

$$Li_2Ga \rightarrow LiGa \rightarrow Li_2Ga_7 \rightarrow Ga(l) \quad (5)$$

Upon full lithiation of the Ga electrode, its state transitions from liquid to solid, leading to an increase in surface roughness due to the influence of surface tension. During the delithiation process, the electrode surface transitions back from solid to liquid, resulting in the formation of some penetrating cracks, as shown in stage III of Fig. 7(g). After complete delithiation, these cracks undergo self-healing, and the surface is restored to a relatively smooth state. The introduction of liquid metal changes the conventional solid-to-solid transformation mechanism in traditional batteries. Owing to the high surface tension of liquid metal in its molten state, the electrode exhibits self-healing behavior, effectively mitigating issues such as crack formation on the electrode surface.

Ga-based liquid metals readily form alloys with alkali metals. For non-metallic electrodes, such as Si electrodes, alloy formation does not occur during charge and discharge cycles. Instead, the liquid metal oxide layer fractures due to electrode cracking, allowing the internal liquid metal to flow into the cracks for self-healing. However, this approach has limitations: the supply of dispersible liquid metal is finite, and for large cracks, the flow of liquid metal has a limited effect. Although this mechanism extends battery cycling life to some extent, the long-term stability after multiple cycles cannot be maintained.

When the electrode is composed entirely of liquid metal, a liquid-to-solid phase transition occurs during lithiation. This process proceeds from the exterior to the interior, with the outer layer of the liquid metal solidifying first. The internal liquid then flows out through cracks, leading to phase separation within the liquid metal [235]. As a result, the alloyed liquid metal fragments into solid pieces. Although the liquid metal can regain its original liquid state after de-alloying, the detachment of solid fragments during this process causes the solid electrolyte interphase (SEI) layer to break. The repeated breaking of the SEI layer continuously consumes lithium ions from the battery and progressively reduces its capacity.

To address this issue, researchers have developed various strategies to immobilize liquid metals within the electrode, thereby enhancing the cycling life and stability of the battery. Numerous methods have been proposed for achieving this immobilization.

Zhang et al. used MXene ($Ti_3C_2T_x$) as a conductive framework to encapsulate liquid metal EGaIn [236]. The functional groups on the MXene surface (–F, –O, and –OH) form coordination bonds with the oxide layer on the surface of EGaIn, as illustrated in Fig. 7(i). In situ XRD measurements during electrochemical reactions revealed that Ga in EGaIn undergoes lithiation first, forming Li_2Ga. As the Ga content decreases, phase separation occurs between In and Ga, followed by alloying reactions to form Li_3In_2 and Li_2In. During subsequent delithiation, Li_2Ga and Li_2In dealloy to reform EGaIn. Throughout this process, EGaIn remains confined within the layered structure of MXene. Encapsulating EGaIn within MXene effectively prevents agglomeration and buffers the stress caused by external volume changes, thereby maintaining the stability of the internal EGaIn. Even if external impacts cause the liquid metal to fracture, its high surface tension enables self-healing.

Qi et al. introduced a polypyrrole (PPy) layer onto the surface of liquid metal EGaSn via electroless plating, as shown in Fig. 7(j) [237]. Experimental results demonstrated that pure EGaSn electrodes exhibited significant cracks and sub-liquid metal (sub-LM) particles on the surface

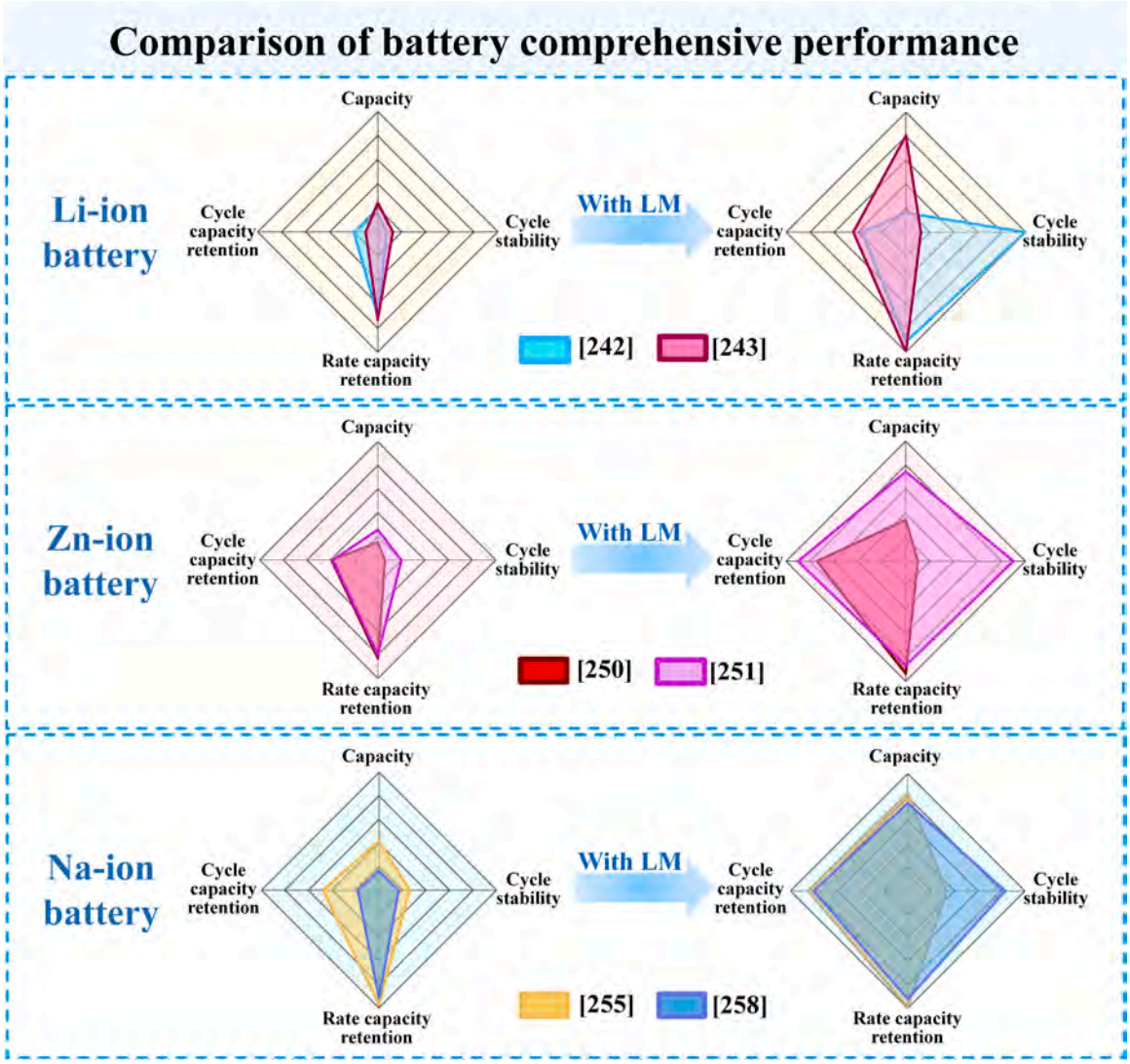

Fig. 8. Performance comparison of lithium-ion, zinc-ion, and sodium-ion batteries before and after incorporating liquid metal into the electrodes. (light blue: [242], pink: [243], red: [250], purple: [251], yellow: [255], deep blue: [258]).

during cycling, which are the primary causes of electrode degradation after repeated cycles. In contrast, the surface of EGaSn@PPy anodes showed no cracks, and the improved internal contact reduced impedance compared to pure EGaSn anodes. This approach is similar to the conductive core-shell material structure commonly used in hydrogels. The PPy outer layer buffers internal and external volume expansion and prevents the detachment of solidified products. Moreover, the excellent adhesion of PPy avoids leakage issues caused by liquid metal exposure. The core-shell structure enhances the surface reactivity and the reversibility of liquid metal, improves self-healing efficiency, and ensures the stability of the liquid metal during alloying and de-alloying processes.

Using liquid metal as an electrode effectively addresses issues such as pitting corrosion and pulverization commonly observed in traditional electrodes, thereby improving the cycling life and stability of batteries. Immobilizing liquid metal within the electrode further elevates its performance to a new level. As shown in Fig. 7(k), a comparison of the cycling performance between LM-$Ti_3C_2T_x$ (with an LM: MXene mass ratio of 2:1) and LMNP anodes at a current density of 5 A g^{-1} reveals significant differences. After 4500 cycles, the LM-$Ti_3C_2T_x$ anode retains 90.8 % of its capacity, whereas the LMNP anode fails after approximately 2000 cycles due to the agglomeration of liquid metal during lithiation and delithiation. These results demonstrate that immobilizing liquid metal can significantly enhance the electrochemical performance of electrodes, providing a substantial boost to their cycling life and stability.

As outlined above, the self-healing mechanisms of liquid metals can be broadly categorized into two types. The first mechanism leverages the fluidity and metallic properties of liquid metals to restore electrical and mechanical functionalities at fractured interfaces within elastomeric materials. When combined with external resources or multiple healing strategies, the self-healing speed and efficiency of the material can be significantly enhanced. The second mechanism relies on the high reactivity of metal ions within the liquid metal, primarily utilized for self-healing in battery electrodes. Through alloying and de-alloying reactions, surface cracks and defects on the electrodes are repaired. The introduction of liquid metal successfully mitigates issues such as dendrite formation, pitting corrosion, and pulverization, which are common in traditional metal electrodes. Self-healing electrodes incorporating liquid metals significantly improve the cycling life and stability of batteries. Building on these mechanisms, surface modification or immobilization of liquid metals can further enhance their compatibility with elastomers or improve their surface activity and reversibility. These advancements can further elevate the electrical, mechanical, and electrochemical performance of liquid metal-based materials.

We summarize recent applications and performance comparisons of liquid metals in various types of metal batteries, as shown in Table 3.

Overall, lithium-ion batteries dominate research in the field of metal batteries, with significantly more literature and studies than other battery types. This predominance is primarily attributed to their widespread applications in consumer electronics, electric vehicles, and other fields. Meanwhile, zinc-ion and sodium-ion batteries have gradually emerged as research hotspots, driven by their high operational safety [238]. The number of related studies has been steadily increasing, demonstrating promising application potential.

Compared to lithium-ion batteries, emerging metal-ion batteries such as aluminum-ion and magnesium-ion batteries remain in the early stages of research. However, they exhibit significant potential in the energy storage sector. Aluminum and magnesium, as anode materials, offer distinct advantages. Aluminum, due to its electron configuration, boasts a gravimetric capacity approximately four times higher than that of lithium-ion batteries, enabling greater energy storage per unit weight [265–268]. Magnesium, with its low reactivity and abundant natural reserves, shows potential to overcome technical challenges associated with high-activity anode materials [269,270]. Additionally, the abundant reserves and low cost of aluminum and magnesium provide economic advantages for large-scale energy storage applications [271]. With the growing global demand for novel energy storage technologies—particularly in renewable energy storage and electric vehicles—research on aluminum-ion and magnesium-ion batteries is attracting increasing attention. These technologies hold promise not only for performance breakthroughs but also for offering new solutions in cost efficiency and safety. In the future, aluminum-ion and magnesium-ion batteries may become critical directions for energy storage technology, supporting the global energy transition and sustainable development.

Other stress-free liquid metal electrodes, such as Na-K alloy liquid metals, are commonly used in battery applications. Ga-based liquid metal electrodes share the following similarities with Na-K liquid metal electrodes [272–278]: (1) High fluidity: This liquid characteristic enables excellent physical and electrochemical contact with electrolytes, significantly reducing interfacial impedance and facilitating charge transfer processes. Such liquid-liquid interfacial contact is more efficient than solid-solid interfaces. It also allows liquid metals to better adapt to complex electrode structures. (2) Self-healing capability: During cycling, both can dynamically repair electrode damage and maintain structural integrity. Even if minor dendrites form, their high reactivity redistributes metal ions to eliminate dendrites, preventing short-circuit risks. (3) Dendrite Suppression: Liquid, non-dendritic metals possess the potential ability to suppress dendrite formation when utilized as stress-free interlayers. This capability becomes particularly pronounced after optimizing wettability and electrolyte compatibility. For example, they can inhibit electrolyte decomposition and the uncontrolled growth of the SEI, thereby enhancing the battery's cycle life and performance.

However, Na-K alloys have certain drawbacks. Their high chemical reactivity may pose safety hazards, whereas Ga-based liquid metals naturally form an oxide layer that prevents self-discharge during cycling, enhancing battery safety. Furthermore, Na-K alloys require storage and encapsulation in kerosene or inert atmospheres with high-cost safety measures, while Ga-based liquid metals remain stable at room temperature without inert gas protection [279].

Pure liquid metals are rarely employed directly as standalone electrodes in battery systems, primarily due to the inherent challenges arising from their liquid property. First, the high density of liquid metals (compared with electrolyte) makes them prone to gravitational settling within the electrolyte [280]. This causes droplets of the active material to detach from the current collector and accumulate at the bottom of the cell, leading to structural collapse of the electrode and a complete loss of electrical contact. If there is no appropriate packaging or interface control structure, it will cause settlement and loss of electrical contact. Secondly, their extremely high surface tension drives thermodynamically spontaneous coalescence (agglomeration) [281]. This behavior not only drastically reduces the effective electrochemically active interface, diminishing specific capacity utilization, but also makes it exceedingly difficult for the resulting spherical droplets to maintain stable, intimate contact with either the current collector or a solid-state electrolyte. Consequently, interfacial contact resistance is significantly increased. Because of these critical bottlenecks, the application of liquid metals in battery anodes currently relies almost exclusively on composite electrode architectures. By encapsulating the liquid metal within conductive matrices, constructing core-shell structures, or dispersing it in polymer networks, the physical confinement provided by the host material effectively suppresses coalescence and migration, stabilizes interfaces, and synergistically enhances performance. This approach is essential to harness the advantageous properties of liquid metals, such as high capacity, intrinsic dendrite suppression, and self-healing capabilities.

To visually illustrate the impact of liquid metal on the performance of metal-ion batteries, we selected the experimental data of lithium-ion batteries, zinc-ion batteries and sodium-ion batteries before and after the addition of liquid metal from some literature and drew a comprehensive performance radar comparison chart, as shown in Fig. 8. This comparison clearly highlights the specific effects of liquid metals on battery performance across four dimensions: capacity, cycle stability, rate capability retention, and cycle capacity retention. These findings provide valuable insights into the application of liquid metals in metal-ion batteries and offer guidance for future research directions.

Conventional anode materials for lithium-ion batteries (LIBs) include graphite [282], silicon-based materials [283], lithium titanate (LTO) [284], and lithium metal [285]. During charge/discharge cycling,

Fig. 9. Schematic representation of current challenges and future research strategies for LM and self-healing composites.

detrimental phenomena, such as lithium dendrite growth, significant volume expansion, and decomposition or fracture of the SEI layer, may occur. These processes degrade the electrode material's structure, disrupt the integrity and capacity balance of the electrode, and lead to irreversible capacity loss [239,286]. Huang et al. (light blue area in Fig. 8) developed a composite electrode by coating a conventional copper foil current collector with a layer of EGaIn liquid metal [242]. The incorporation of LM significantly enhanced the battery's cycling capacity retention, rate capability, and overall cycling stability. This improvement is primarily attributed to the high specific surface area of the nano-sized LM particles, which increases the electrode-electrolyte contact area, shortens the lithium-ion diffusion distance, and accelerates reaction kinetics. Furthermore, the self-healing properties of the LM particles enable them to maintain structural integrity despite repeated volume changes during lithium insertion (expansion) and extraction (contraction/pulverization). Notably, the conductive carbon black and polyvinylidene fluoride (PVDF) binder within the composite electrode matrix help mitigate nanoparticle agglomeration, maintain structural stability, and reduce overall electrode volume expansion. In a distinct approach, Meng et al. (pink area in Fig. 8) utilized GaInSn LM to modify a nanoporous SiGe alloy anode [243]. This strategy also resulted in markedly improved cycling capacity retention, rate capability, and overall capacity. Unlike Huang et al.'s system, the key mechanism highlighted involves the difference in equilibrium lithiation/delithiation potentials between Si and Ge within the alloy. This potential difference helps alleviate instantaneous mechanical stress. The LM further enhances structural stability through physical buffering and its intrinsic self-healing capability. Additionally, the LM rapidly reacts with the electrolyte to form a stable SEI layer, suppressing detrimental side reactions and improving Coulomb efficiency. Collectively, these mechanisms - nanoparticle size reduces volume expansion stress, self-healing property maintains structural integrity, stabilized SEI formation via interface modification - synergistically contribute to the superior cycling performance of the lithium-ion batteries employing these LM-modified composite anodes.

The anode in zinc-ion batteries (ZIBs) is conventionally fabricated from materials such as metallic Zn [287], Zn alloys [288], carbon-based structures [289], and metal oxides [290]. ZIBs inherently exhibit high initial rate capacity retention, attributed to zinc's high redox potential, which enables the use of aqueous electrolytes possessing high ionic conductivity. However, the thermodynamic reaction between zinc and the aqueous electrolyte promotes detrimental phenomena such as zinc dendrite growth, hydrogen evolution corrosion, electrode volume expansion, and passivation layer thickening. These behaviors lead to structural degradation of the anode material, compromising electrode integrity and disrupting reaction kinetics, ultimately resulting in irreversible capacity loss [287,291–295]. Jiang et al. (red region in Fig. 8) reported a GaInSn-modified carbon cloth serving as the anode current collector for flexible ZIBs [250]. Following the incorporation of this liquid metal, significant enhancements in both cycling capacity retention and rate capacity retention were observed. The LM, acting as an intermediate layer, filled the porous structure of the carbon cloth, improving electrolyte wettability. Simultaneously, the liquid-liquid interface of the LM optimized the adsorption/desorption behavior of zinc ions, lowered the nucleation barrier, and promoted uniform zinc deposition. Crucially, the LM layer mitigated undesirable side reactions between zinc and the electrolyte (e.g., suppressing hydrogen evolution) through physical barrier effects and chemical inertness, thereby enhancing electrode stability. Complementary experimental results from Jia et al. (purple region in Fig. 8) demonstrated comprehensive improvements across four key performance metrics upon LM addition: capacity, cycling stability, cycling capacity retention, and rate capacity retention [251]. This superior performance enhancement is intrinsically linked to the specific LM alloy GaInZn. Beyond functionalities shared with other LMs, GaInZn, containing zinc within its composition, provides an additional zinc source to replenish the active material. During cycling, GaInZn exhibits a lower deposition overpotential, superior volume adaptability, and a more stable interfacial layer compared to alternatives like GaInSn, collectively optimizing the overall performance of ZIBs. In summary, the introduction of liquid metals, particularly zinc-containing variants like GaInZn, significantly contributes to the development of high-performance aqueous zinc metal batteries.

Sodium-ion batteries (SIBs) commonly utilize carbon-based materials [296], alloy compounds [297], or transition metal oxides/sulfides [298] as anodes, leveraging sodium's abundance and cost efficiency while benefiting from their relatively low and safe sodium insertion/extraction potentials. Although metallic sodium offers a high theoretical capacity of 1165 mAh g^{-1}. However, as shown in Table 3, its actual capacity is not particularly high. Many researchers attribute this difference to uneven deposition, severe dendrite growth, and the continuous growth of unstable SEI that consumes active sodium ions and electrolytes. These issues collectively cause structural collapse, electrode pulverization, interfacial degradation, and sluggish kinetics, resulting in irreversible capacity loss and poor cycling stability [299–303]. To address these challenges, Gu et al. (yellow region in Fig. 8) employed a liquid GaIn interlayer between the Na anode and $Na_3Zr_2Si_2PO_{12}$ (NZSP) solid electrolyte, where GaIn filled surface voids on NZSP to enhance interfacial contact while spontaneously forming Ga_4Na/NaIn alloys that established continuous Na^+ pathways and homogenized electric fields, thereby suppressing dendritic growth [255]. Similarly, Fu et al. (deep blue region in Fig. 8) engineered a GaSnIn (64:27:9 w/w/w)-coated copper current collector (GSIC), which improved electrolyte wettability, buffered volume changes during cycling, and reduced local current density via alloying reactions to inhibit dendrite initiation [258]. Notably, the composition of Na-Ga alloys (e.g., $Na_{22}Ga_{39}$) varies with synthesis conditions [253]. Collectively, liquid metal-modified electrodes demonstrate enhanced corrosion resistance, interfacial stability, and electrolyte compatibility, effectively mitigating dendrite formation and significantly improving overall electrochemical performance.

In summary, the introduction of liquid metal offers an effective strategy for optimizing the performance of metal-ion batteries such as lithium-ion, zinc-ion, and sodium-ion batteries. Notably, it provides significant advantages in inhibiting dendrite growth, enhancing cycling stability, and improving interfacial reactivity. The incorporation of liquid metal delivers both theoretical and practical support for the advancement of high-performance metal batteries, and facilitates their application in areas such as all-solid-state batteries, high-energy-density energy storage and beyond.

5. Conclusion and perspectives

As a next-generation functional material, liquid metal has become a research hotspot at the forefront of emerging technologies. Its outstanding electrical properties enable the introduction of conductivity into otherwise insulating elastomers. Unlike traditional metals, the excellent fluidity of liquid metal allows it to integrate seamlessly with self-healing materials, significantly enhancing their healing efficiency. Self-healing materials can autonomously restore structural integrity after damage, thereby extending their service life. This capability reduces the frequency of material replacement, lowers waste generation, and improves product cost-effectiveness. The synergy between liquid metals and self-healing materials is expected to drive breakthroughs in advanced manufacturing, next-generation batteries, flexible wearable devices, electronic information technology, phase-change materials, and other future-oriented industries. Despite these promising prospects, several challenges and unresolved issues remain. Addressing these will be critical to fully unlocking the potential of this innovative material

system. The challenges and solutions of liquid metal self-healing are briefly described in Fig. 9.

5.1. Challenges and solutions for liquid metals

(1) Further research on the cost, composition, and oxide layer of liquid metals.

The price issue of liquid metal is the primary consideration when discussing gallium-based liquid metals. The high cost of Ga and In restricts the application of liquid metals to some extent. To reduce the overall price of liquid metals, improvements can be made in the following aspects. Firstly, incorporating other metals or adjusting the composition content of the liquid metal. As argued previously, adding the Zn element to form GaInZn alloy not only reduces the Ga content in the alloy but also significantly enhances the performance of zinc-ion batteries. Therefore, beyond well-known Ga-based liquid metals like Ga, Ga_xIn_y, Ga_xSn_y, and $Ga_xIn_ySn_z$, further exploration of their compositions and variants is essential. Adjusting the composition content of the liquid metal is also one of the main methods to reduce the Ga element content. The metal ratios in multi-component liquid metals significantly affect key properties, including melting point and fluidity, and can be tailored to meet specific application requirements. For example, the aforementioned GaSnIn (64:27:9 w/w/w) reduces the content of precious metals while improving wettability with the solid electrolyte by altering its own fluidity, thereby enhancing battery performance. Secondly, designing structures for liquid metal circulation and reuse within the material system, which is fully demonstrated in the alloying reaction within self-healing batteries utilizing liquid metal. For flexible and stretchable electronic devices, specific liquid metal recycling mechanisms should be established, such as selecting degradable matrix materials to facilitate the separation of liquid metal from other substances during recycling. This method achieves high recovery rates and high purity, enabling the recycled liquid metal to be reused for its original purpose or for cascaded utilization.

Research on the surface oxide of liquid metal is also crucial. Since gallium-based liquid metals rapidly form an oxide film upon exposure to air, this film alters their chemical properties, wettability, and rheological characteristics. Studying the oxide film allows for a better understanding of these changes in the liquid metal's properties, enabling precise control of its performance. The liquid metal oxide film is a double-edged sword; it is both a functional enabler and a performance limiter. Surface modification of liquid metal largely relies on this surface oxide layer. For instance, introducing functional groups like hydrogen bonds enables better integration with polymer substrates for applications in flexible electronics. The oxide layer interacts with functional groups (e.g., -F, -O, -OH) on MXene to enhance battery performance. Furthermore, the oxide layer serves as a critical "skeleton" providing structural support for the liquid metal and can form composite oxide layers with other oxides like Fe_3O_4, thereby enhancing the magnetism of the liquid metal. The above are the beneficial aspects of the liquid metal oxide layer. In the future, further research can focus on surface modification of the oxide layer or the development of composite oxide layers.

However, we must also be mindful of the impacts caused by the oxide layer. Firstly, when the oxide film grows uncontrollably or interferes with core functions, it becomes a performance bottleneck, requiring targeted removal or inhibition. In the field of flexible and stretchable electronics, liquid metals rely on their self-healing properties for fracture-healing to fill cracks generated in the matrix. However, during repeated stretching, the liquid metal continuously oxidizes, and this process is irreversible. Consequently, the material interior accumulates oxides overall. This is detrimental for applications relying solely on liquid metal conductivity within the material. Future research goals can focus on slowing the oxidation rate of the liquid metal by controlling the properties of its carrier medium (e.g., acidic environments) or designing internal channels within the material structure to reduce the contact area between the fractured liquid metal and oxygen, thereby suppressing the formation rate of the oxide layer. In battery applications, preformed oxide films also affect electrochemical behavior at the interface, acting as one of the obstacles to performance enhancement. This issue can be addressed by optimizing the battery manufacturing process, specifically by performing all steps from liquid metal preparation to battery encapsulation under oxygen-free conditions to minimize oxide formation and improve overall battery performance. Building on the points mentioned above, the primary method for oxide removal remains acid washing. However, this method affects the liquid metal surface and requires immediate post-treatment to enhance corrosion resistance and prevent secondary oxidation. In the future, specific catalysts could be developed to achieve non-destructive in-situ decomposition of the oxides, minimizing damage to the liquid metal itself. Future material design may benefit from strategies capable of selectively removing or recovering oxides, contributing to more sustainable and effective self-healing systems and waste conversion technologies. Simultaneously, the requirements for the liquid metal oxide film vary significantly across different application scenarios, yet current research often lacks specificity towards these particular needs. Future work can focus on modifying the surface functional groups of the oxide while concentrating on modifying the oxide layer itself to impart better mechanical, electrical, or other properties, thereby achieving efficient utilization of the oxides.

(2) The particle size uniformity of liquid metal droplets affects the properties.

The size variability of liquid metal particles can significantly affect their mass, thereby influencing their distribution within a substrate. This variation also affects how the LM disperses in uncured elastomers. During the curing process of flexible materials, particles of different sizes undergo sedimentation: larger particles settle while smaller particles rise, leading to the formation of a layered structure within the LM-based elastomer. This stratification has both advantages and disadvantages. On the positive side, it can induce anisotropic electrical behavior, enabling the material to respond differently to stimuli from different directions—an advantage for motion-responsive applications. However, this structure may compromise the material's mechanical integrity, subsequently affecting the mechanical properties of the flexible material. Different particle size ranges find application in different fields; larger LM particles are commonly used in flexible conductive applications and self-healing, while smaller LM particles, due to their larger specific surface area, are more often used in battery technology and biomedical targeted carrier applications, among others. Therefore, controlling the particle size of LM is one of the essential prerequisites for achieving high performance. Currently, using ultrasonication to reduce LM particle size is the most common method. However, factors such as ultrasonication time, ultrasonic power, dispersant type, and concentration require significant time to explore the optimal process parameters. More critically, if the ultrasonication time is too long, the solution temperature increases significantly, accelerating the recombination rate of smaller LM particles and consequently increasing the LM particle size. Microfluidic methods are also commonly used for sorting LM sizes. Although this method allows for precise control of LM particle size, its cost is relatively high, and the LM may adhere to the channel walls, leading to channel blockage. Building upon existing technologies, future efforts should focus on in-depth research into the interrelationships of various parameters in current separation methods and developing fully automated intelligent control systems to further improve the uniformity and controllability of particle size. Furthermore, innovating LM

preparation techniques by developing novel methods that incorporate high-energy control means (such as lasers, high voltage, etc.) during the preparation process to induce the generation of specific sizes will enhance the quality of LM produced in a single batch.

(3) Insufficient research on the impact of morphological changes on performance

The lack of research on the dynamic changes in the surface morphology of liquid metals represents a significant gap in this field. In practical applications, the surface morphology of liquid metals is influenced by a range of external factors, such as temperature, pressure, electric fields, magnetic fields, and chemical interactions with other substances. These influences cause the surface to maintain a state of constant flux, which profoundly affects the performance and application potential of liquid metals. This gap fundamentally stems from insufficient research on the surface oxide layer of liquid metals. Liquid metal oxide films often exhibit amorphous, discontinuous, or self-healing characteristics, yet systematic studies are lacking on their compositional gradients, thickness control mechanisms, and evolution behavior under stress, flow, and temperature fluctuations. Currently, there is limited knowledge about the thermodynamic stability of the initial oxide growth on liquid metal surfaces, and the specific conditions and processes of its formation remain unclear. Furthermore, liquid metals exist in a molten state at high or even room temperatures, meaning their oxidation processes fundamentally differ from those of solid metals. In practical applications, the oxide film of liquid metals is subject to dynamic changes in its surface morphology and properties due to external influences like temperature, pressure, electric fields, and magnetic fields. Current research rarely delves deeply into these dynamic surface changes, particularly under real-time, in-situ conditions. The absence of such research makes it difficult to accurately capture the true behavior and change patterns of liquid metals in working environments, thereby hindering material optimization and limiting innovation in application development. To address this challenge, incorporating in situ observation techniques into future research is imperative. Developing novel in-situ observation methods coupled with multi-scale computational models is essential to deepen the understanding of these critical issues at the dynamic interface. These techniques allow for real-time monitoring of surface morphology without disrupting operating conditions, providing valuable dynamic information. This approach not only enhances our fundamental understanding of the physical and chemical properties of liquid metals but also provides crucial technical support and theoretical insights for their applications in electronic devices, energy storage and conversion, biomedicine, and other emerging fields.

5.2. Challenges and solutions for self-healing materials

(1) Limited research on external encapsulation materials for self-healing devices

In practical applications, self-healing materials rarely function independently; they typically require external encapsulation as the primary physical protection. Effectively integrating self-healing materials with external encapsulation materials presents a significant challenge. The interface between the encapsulation material and the internal self-healing layer or functional core is a critical weak point. It is essential to ensure strong interfacial bonding to prevent delamination, while simultaneously ensuring that this interface does not hinder the propagation of cracks towards the self-healing region or the flow of healing agents when damage occurs. These sealants must not only accommodate the flexibility of the internal self-healing materials but also, in certain cases, ensure strong adhesion to rigid components.

However, excellent barrier materials typically difficult to allow the effective permeation and reaction of healing agents. Conversely, materials that allow permeation often exhibit poor barrier properties. Modern devices often demand that the encapsulation possess additional functionalities beyond protection, such as transparency, electrical conductivity, thermal conductivity, and biocompatibility. Integrating these functionalities with the requirement to "allow controlled damage to trigger self-healing" makes the design extremely complex.

The ideal self-healing encapsulation material should be capable of recovering from substantial damage while also creating favorable self-healing conditions, such as locally controlling and regulating the temperature of the internal system. A promising strategy involves integrating the design principles of shape-memory polymers (SMPs) into the encapsulation layer. SMPs can impart self-healing functionality to the shell while maintaining electrical connectivity for the internal self-healing device and reducing external interference. This approach enhances the overall stability and performance of the system while minimizing the need for manual intervention. Additionally, a gradient design can be applied to the material encapsulation structure. For example, the outermost layer utilizes high-hardness, high-wear-resistant, high-barrier materials to resist environmental erosion. The middle layer is designed with controlled fracture behavior, allowing damage to penetrate controllably to the inner layer. The innermost layer is designed to be tough and compatible with healing agents, promoting healing initiation. This inner layer can also integrate specific functionalities. Overcoming these challenges will further expand the application of self-healing technologies in key fields such as electronic devices, biomedicine, and energy.

(2) Studies on the interaction between synergistic mechanisms are insufficient

Current research has confirmed that the synergistic effect of multiple self-healing mechanisms can significantly shorten healing time. However, studies on the interactions among these different mechanisms remain limited. When various self-healing mechanisms operate concurrently, they may either complement or interfere with each other. For example, the formation of certain chemical bonds might hinder the effectiveness of other repair pathways, or discrepancies in the kinetics of distinct mechanisms lead to mismatches, ultimately resulting in suboptimal healing performance. This research gap has led to a lack of theoretical guidance for the design and optimization of multifunctional self-healing materials, thereby impeding the full utilization of synergistic advantages. To address this issue, future studies should focus on comprehensive simulation modeling of chemical bonding interactions and self-healing systems. Molecular dynamics (MD) simulations, for instance, can be used to explore the dynamic behavior and energy evolution of various bonds during the healing process, offering insights into their influence on healing efficiency and material performance. Moreover, the establishment of multi-physics coupling models for self-healing devices would enable the simulation of the healing process under realistic operational conditions. These models can assess the impacts of external factors such as temperature, mechanical stress, and electric fields on the interplay between different healing mechanisms. Such analyses would provide valuable guidance for optimizing device architecture and enhancing overall self-healing performance. Through simulation-based approaches, a deeper understanding of the interaction dynamics between diverse self-healing mechanisms can be achieved, facilitating the prediction of key performance metrics such as healing time and recovery efficiency. This will lay a solid theoretical foundation for the design and advancement of next-generation high-performance self-healing materials.

(3) No unified evaluation system for the healing efficiency of the self-healing system

Currently, there is no unified standard for evaluating the efficiency of self-healing systems. Instead, evaluations are often based on fragmented metrics such as healing time, stress-strain recovery, and specific capacity retention in batteries. This lack of consistency and standardization

hampers effective cross-study comparisons and comprehensive assessments, thereby hindering the further development and practical deployment of self-healing materials. Each of the existing evaluation methods presents certain limitations.

Firstly, using healing time as the sole indicator of self-healing efficiency is inherently reductive. While it offers an intuitive measure, healing time alone does not fully reflect the recovery of mechanical properties or the reconstruction of chemical structures during the healing process. For instance, some materials may exhibit rapid surface repair, yet their internal molecular bonds remain partially damaged, resulting in compromised performance. Moreover, healing time is highly sensitive to experimental conditions such as temperature, humidity, and pressure, reducing its reliability and comparability across different studies.

Secondly, stress-strain recovery provides useful insights into the restoration of mechanical properties but fails to capture the underlying chemical reactions or microstructural evolution during the healing process. Given the diverse mechanical behaviors of different materials under varying testing conditions, relying solely on stress-strain data is insufficient as a universal evaluation criterion.

Thirdly, metrics such as the retention ratio of battery-specific capacity are primarily relevant to energy storage applications and do not extend to other functional domains. This approach also neglects other key performance indicators like electrical conductivity and operational stability, limiting its generalizability as a comprehensive evaluation metric for self-healing systems.

To address these challenges, future research should prioritize the development of more comprehensive and rational evaluation models, particularly those based on multi-parameter weighted averages. By integrating metrics such as healing time, mechanical recovery, and functional performance (e.g., specific capacity), and assigning appropriate weights based on their relevance to different application contexts, a more robust and scientifically grounded evaluation framework can be established. Such a multi-dimensional evaluation approach would more accurately reflect the true performance restoration of self-healing materials under real-world conditions. It would also enable standardized comparisons across different material systems and application scenarios.

By advancing the development of multi-parameter evaluation formulas and working toward a unified standard in the self-healing field, researchers can better benchmark progress, facilitate material optimization, and accelerate the translation of self-healing technologies into practical applications.

5.3. Challenges and solutions for liquid metal-based self-healing materials

(1) Balancing self-healing and mechanical performance in liquid metal composites

The incorporation of liquid metal into self-healing materials imparts unique self-healing capabilities but can also lead to a reduction in mechanical properties. The primary reason for this phenomenon lies in the differences in fluidity and compliance between liquid metals and traditional rigid materials. The distribution and interaction of the LM within the material significantly influence its overall mechanical performance. For instance, the addition of LM can lower the material's modulus and strength, making it more prone to deformation and failure under external forces. Furthermore, the interfacial bonding strength between the LM and the matrix material also affects the mechanical properties. If the interfacial bonding is weak, delamination or interfacial slip may occur under stress, further compromising the material's mechanical integrity.

To mitigate the mechanical performance loss caused by LM incorporation, subsequent material design processes must carefully address this issue. Firstly, optimizing the content and distribution of the LM helps balance self-healing ability and mechanical properties. Research indicates that an appropriate amount of LM can provide effective self-healing, while excess amounts lead to significant mechanical degradation. Therefore, determining the optimal quantity of LM is crucial. Secondly, selecting a suitable matrix material for compounding with the LM is equally important. Matrix materials with high mechanical strength and good compatibility can help reduce the negative impact of LM on mechanical performance. Additionally, designing specialized micro- or nanostructures to confine the flow of LM can enhance the overall mechanical properties of the material. For example, constructing multilayer or microcapsule structures can confine the LM to specific regions, preventing its uncontrolled flow within the material. During the self-healing process of the LM, the continuous formation of the oxide layer severely affects their long-term stability and durability, limiting their broad application across various fields.

In summary, although the introduction of liquid metals endows self-healing materials with unique dynamic repair capabilities, the accompanying mechanical performance loss and the long-term stability issues associated with the oxide film remain key bottlenecks hindering the widespread application of this material system. Looking forward, research efforts should focus on: 1) deeply exploring the synergistic mechanism between the micro-nano scale flow behavior of LMs and the microstructure of the matrix to provide theoretical support for precise regulation of their distribution and confinement; 2) developing novel interfacial engineering strategies, particularly targeting the weak interfacial bonding between the LM oxide layer and the matrix, to significantly enhance the overall mechanical performance of the composite; 3) concurrently, there is an urgent need to innovate material design concepts (such as constructing hierarchical structures or introducing dynamically responsive units) to fundamentally solve the problems of uncontrolled thickening and performance degradation of the oxide film during cyclic service, ultimately achieving high performance and long service life for LM-based self-healing materials while maintaining their efficient healing characteristics.

(2) Interfacial compatibility challenges of liquid metals in self-healing battery applications

Although the application of liquid metals in self-healing batteries can significantly enhance the stability of the electrode/electrolyte interface through dynamic crack filling, it still faces several distinct challenges. Firstly, the high reactivity of LMs, while endowing the battery with reversible alloying-based self-healing capability, also exacerbates side reactions at the electrolyte interface. This leads to uncontrollable growth of interfacial impedance and continuous consumption of active materials. The frequent occurrence of side reactions destabilizes the SEI, relying solely on the fluidity of unreacted LM to ensure stable interfacial contact. This not only affects the battery's cycle life but may also lead to safety concerns. Secondly, the problem of oxide accumulation prevalent in flexible and stretchable electronics also occurs in batteries. The Ga element in LMs continuously participates in reversible alloying reactions while simultaneously generating an oxide layer. Gallium oxide does not participate in reversible alloying reactions; instead, it consumes active materials through interfacial side reactions and weakens ion transport. Finally, and more critically, LMs within the battery primarily undergo alloying/dealloying reactions. The LM experiences a process of transitioning from liquid to solid and back to liquid. The high density of LMs (compared to the electrolyte) may cause them to detach and precipitate to the bottom of the battery, potentially leading to short circuits and other phenomena. Therefore, based on the above challenges, future application directions for LMs in self-healing batteries should focus on the following points: 1) Regulating LM composition ratio or introducing other self-healing materials: Adjusting the composition ratio of the LM can optimize its performance and reduce the occurrence of side reactions. Additionally, introducing self-healing materials, such as polymer electrolytes, can effectively suppress LM dendrite growth by leveraging their self-healing function, thereby improving the overall battery performance. 2) Specific electrode structure design: Developing

porous matrix skeletons or cage-like carriers can physically confine the flow area of the LM, optimizing both the healing function and the mechanical/electrochemical performance. Simultaneously, structural design can be utilized to regulate ion transport pathways and block electrolyte erosion, further enhancing battery stability and safety. 3) Strengthening encapsulation of LMs within the electrode: Improving encapsulation technology reduces the possibility of LM detachment, thereby enhancing the comprehensive performance of the battery. For example, employing self-healing polymer materials as the encapsulation layer can effectively protect electrode materials, enabling automatic repair upon damage and extending battery lifespan. These multi-dimensional synergistic strategies establish a dynamic balance between suppressing side reactions and maintaining structural stability through a cascade of "composition optimization-structural confinement-interface encapsulation" regulation. This provides an engineerable pathway for LM-based self-healing batteries that combine high repair efficiency with long cycle life.

(3) The multifunctional integration of liquid metal self-healing materials needs further research

The development of liquid metal self-healing materials for multifunctional integrated devices faces several key challenges:

The most important is the material compatibility and performance balance. Liquid metal self-healing materials need to coexist with other functional materials (such as conductive or optical materials) in multifunctional integrated devices. However, differences in the physical and chemical properties of these materials may lead to poor interactions or performance conflicts, affecting overall device performance. For instance, the fluidity and softness of liquid metals may be incompatible with high-hardness, high-strength materials, potentially causing delamination or interfacial failure when the device is under stress.

Next, the complexity in manufacturing processes also needs to be deserves attention. The processing and fabrication of liquid metal self-healing materials require specialized techniques and equipment, increasing production costs and complexity.

To address these challenges, the following solutions can be implemented: By integrating artificial intelligence (AI) design systems, the selection and structural optimization of multifunctional integrated materials can be achieved. AI-driven design can help identify compatible material combinations and optimize their performance balance, ensuring seamless integration of liquid metals with other functional components. Next, combining multiple advanced manufacturing techniques, such as 3D printing, microencapsulation, and precision coating, can enhance the design freedom and manufacturing precision of multifunctional integrated devices. These technologies enable the precise placement and structuring of liquid metals within complex device architectures, minimizing compatibility issues and improving overall performance.

More importantly, it is crucial to strengthen interdisciplinary research. Integrating theories and methods from materials science, chemical engineering, physics, biology, and other disciplines will enable an in-depth exploration of the physicochemical properties of gallium-based liquid metals, the microscopic mechanisms involved in their preparation processes, and their intrinsic connections to application scenarios. This will provide a solid theoretical foundation for developing high-performance gallium-based liquid metal materials and preparation technologies, thereby driving innovative applications in more fields.

By implementing these solutions, the challenges associated with liquid metal self-healing materials in multifunctional integrated devices can be effectively overcome. This will pave the way for their widespread application in fields such as flexible electronics, wearable devices, and intelligent robotics, driving innovation and expanding their practical utility.

CRediT authorship contribution statement

Chao Yang: Writing – review & editing, Investigation, Funding acquisition, Conceptualization. **Zicheng Sa:** Validation, Investigation, Formal analysis. **Kaizheng Gao:** Validation, Software, Investigation, Formal analysis. **Changming Cao:** Resources, Formal analysis. **Paul K. Chu:** Writing – review & editing, Investigation, Funding acquisition, Conceptualization. **Jiayun Feng:** Writing – review & editing, Visualization, Resources, Investigation. **Xiaoqin Zeng:** Writing – review & editing, Software, Investigation, Data curation. **Chen Zhang:** Visualization, Validation, Methodology. **Rui Yin:** Software, Investigation, Formal analysis. **Yuxin Sun:** Supervision, Resources, Methodology. **Yaming Liu:** Visualization, Formal analysis, Data curation. **Minghan Yu:** Writing – original draft, Supervision, Methodology, Investigation, Formal analysis, Conceptualization. **Youyou Chen:** Visualization, Software, Methodology. **Jianchao Liang:** Software, Investigation, Formal analysis. **Xinyang Ma:** Investigation, Formal analysis, Data curation. **Yanhong Tian:** Writing – review & editing, Supervision, Project administration, Funding acquisition, Data curation, Conceptualization. **Qing Sun:** Visualization, Resources, Investigation.

Declaration of Competing Interest

The authors declare that they have no known competing financial interests or personal relationships that could have appeared to influence the work reported in this paper.

Acknowledgments

This work was supported by the National Natural Science Foundation of China (Grant Nos. 52175300 and 52401101) and Heilongjiang Province Key Research and Development Program. Grant Number: 2022XJ03C07, the Postdoctoral Fellowship Program of CPSF under Grant Number GZC20231545, China Postdoctoral Science Foundation (2024T170557 and 2023M742224), Shanghai Post-doctoral Excellence Program (No. 2023440), and City University of Hong Kong Donation Research Grants (DON-RMG Nos. 9229021 and 9220061).

Data availability

Data will be made available on request.

References

[1] Y. Wu, Z.W. Li, Digital transformation, entrepreneurship, and disruptive innovation: evidence of corporate digitalization in China from 2010 to 2021, Humanit. Soc. Sci. Commun. 11 (2024) 16.
[2] Y. Wang, C. Xu, X. Yu, H. Zhang, M. Han, Multilayer flexible electronics: manufacturing approaches and applications, Mater. Today Phys. 23 (2022) 100647.
[3] Y. Jung, M. Kim, S. Jeong, S. Hong, S.H. Ko, Strain-insensitive outdoor wearable electronics by thermally robust nanofibrous radiative cooler, ACS Nano 18 (2024) 2312–2324.
[4] X.Y. Zhang, Y.H. Zhang, J.H. Zhang, J. Shang, L.P. Lin, Q. Liu, Q. An, Acoustoelectric materials & devices in biomedicine, Chem. Eng. J. 483 (2024) 149314.
[5] J. Liang, W. Wu, A new frontier of flexible energy devices: aqueous proton supercapacitors, Appl. Phys. Rev. 11 (2024) 011301.
[6] J.X. Ma, Z.C. Sa, H. Zhang, J.Y. Feng, J.Y. Wen, S. Wang, Y.H. Tian, Microconfined assembly of high-resolution and mechanically robust EGaIn liquid metal stretchable electrodes for wearable electronic systems, Adv. Mater. 11 (2024) 2402818.
[7] Y.H. He, J. You, M.D. Dickey, X.L. Wang, Controllable flow and manipulation of liquid metals, Adv. Funct. Mater. 34 (2024) 2309614.
[8] K.H. Kim, E. Kabir, S.A. Jahan, A review on the distribution of Hg in the environment and its human health impacts, J. Hazard. Mater. 306 (2016) 376–385.
[9] K.G. Pearce, H.Y. Liu, S.E. Neale, H.M. Goff, M.F. Mahon, C.L. McMullin, M. S. Hill, Alkali metal reduction of alkali metal cations, Nat. Commun. 14 (2023) 8147.

[10] D.C. Seoane, M.D. Saint-Hubert, S. Ahenkorah, C.S. Vargas, M. Ooms, L. Struelens, M. Koole, Gamma counting protocols for the accurate quantification of 225Ac and 213Bi without the need for a secular equilibrium between parent and gamma-emitting daughter, EJNMMI Radiopharm. Chem. 7 (2022) 28.
[11] Y.M. Liu, R. Yin, Y.Y. Chen, C. Zhang, P. He, W.W. Zhao, Fully elastic and high-sensitivity liquid metal sensor based on concave–convex structured microchannel for human activity monitoring and object recognition sensor array, ACS Appl. Electron. Mater. 5 (2023) 6157–6164.
[12] Y.M. Liu, C. Zhang, Y.Y. Chen, R. Yin, P. He, W.W. Zhao, Rational design of conductive pathways in flexible tactile sensors via indirect 3D-printing of liquid metal for high-precision monitoring and recognition, ACS Appl. Mater. Interfaces 15 (2023) 38572–38580.
[13] M.A.H. Khondoker, D. Sameoto, Fabrication methods and applications of microstructured gallium based liquid metal alloys, Smart Mater. Struct. 25 (2016) 093001.
[14] Y.L. Lin, J. Genzer, M.D. Dickey, Attributes, fabrication, and applications of gallium-based liquid metal particles, Adv. Sci. 7 (2020) 2000192.
[15] H. Bark, P.S. Lee, Surface modification of liquid metal as an effective approach for deformable electronics and energy devices, Chem. Sci. 12 (2021) 2760–2777.
[16] N.L. Yang, F. Gong, Y.K. Zhou, Q. Yu, L. Cheng, Liquid metals: preparation, surface engineering, and biomedical applications, Coord. Chem. Rev. 471 (2022) 214731.
[17] S.Y. Tang, C. Tabor, K.K. Zadeh, M.D. Dickey, Gallium liquid metal: the devil's elixir, Ann. Rev. Mater. Res. 51 (2021) 381–408.
[18] M.K. Akbari, F. Verpoort, S. Zhuiykov, State-of-the-art surface oxide semiconductors of liquid metals: an emerging platform for development of multifunctional two-dimensional materials, J. Mater. Chem. A. 9 (2021) 34–73.
[19] Y. Peng, H.Z. Liu, H. Peng, J.Y. Zhang, Biological self-healing strategies from mechanically robust heterophasic liquid metals, Matter 6 (2023) 226–238.
[20] S.U. Barrios, R. Verdejo, M.A. López-Manchado, M.H. Santana, Evolution of self-healing elastomers, from extrinsic to combined intrinsic mechanisms: a review, Mater. Horiz. 7 (2020) 2882–2902.
[21] L. Mezzomo, C. Ferrara, G. Brugnetti, D. Callegari, E. Quartarone, P. Mustarelli, R. Ruffo, Exploiting self-healing in lithium batteries: strategies for next-generation energy storage devices, Adv. Energy Mater. 10 (2020) 2002815.
[22] W.Z. Zu, H.E. Carranza, M.D. Bartlett, Enhancing electrical conductivity of stretchable liquid metal–silver composites through direct ink writing, ACS Appl. Mater. Interfaces 16 (2024) 23895–23903.
[23] T. Qian, Reconfigurable metasurface antenna based on the liquid metal for flexible scattering fields manipulation, Micromachines 12 (2021) 243.
[24] Z.P. Ye, S.Y. Li, S.Y. Zhao, L.D. Deng, J.H. Zhang, A.J. Dong, Textile coatings configured by double-nanoparticles to optimally couple superhydrophobic and antibacterial properties, Chem. Eng. J. 420 (2021) 127680.
[25] Z.Q. Ye, Y. Jiang, L. Li, F. Wu, R.J. Chen, Rational design of MOF-based materials for next-generation rechargeable batteries, NanoMicro Lett. 13 (2021) 203.
[26] S.Y. Zheng, J.H. Zhou, S.B. Wang, Y.J. Wang, S.Q. Liu, G.Y. Du, D. Zhang, J.M. Fu, J. Lin, Z.L. Wu, Q. Zheng, J.T. Yang, Water-triggered spontaneously solidified adhesive: From instant and strong underwater adhesion to in situ signal transmission, Adv. Funct. Mater. 32 (2022) 2205597.
[27] S. Chen, M.Z. Jiang, B. Wang, X.Y. Zhu, X.H. Shan, J. Liu, In situ fabricated liquid metal capacitors for plant sensing, Biosensors 13 (2023) 603.
[28] C.B. Liang, Z.J. Gu, Y.L. Zhang, Z.L. Ma, H. Qiu, J.W. Gu, Structural design strategies of polymer matrix composites for electromagnetic interference shielding: a review, NanoMicro Lett. 13 (2021) 181.
[29] Y.C. Lai, S. Ginnaram, S.P. Lin, F.C. Hsu, T.C. Lu, M.H. Lu, Breathable and stretchable multifunctional triboelectric liquid-metal E-skin for recovering electromagnetic pollution, extracting biomechanical energy, and as whole-body epidermal self-powered sensors, Adv. Funct. Mater. 34 (2024) 2312443.
[30] S.S. Swayamprabha, D.K. Dubey, R.A.K. Shahnawaz, M.R. Yadav, A. Nagar, F. C. Sharma, J.H. Tung, Jou. Approaches for long lifetime organic light emitting diodes, Adv. Sci. 8 (2021) 2002254.
[31] Y.Y. Chen, C. Zhang, R. Yin, M.H. Yu, Y.J. Liu, Y.M. Liu, H.R. Wang, F.H. Liu, F. Cao, G.Q. Chen, W.W. Zhao, Ultra-robust, high-adhesive, self-healing, and photothermal zwitterionic hydrogels for multi-sensory applications and solar-driven evaporation, Mater. Horiz. 10 (2023) 3807–3820.
[32] M.D. Bartlett, N. Kazem, M.J. Powell-Palm, X.N. Huang, W.H. Sun, J.A. Malen, C. Majidi, High thermal conductivity in soft elastomers with elongated liquid metal inclusions, Proc. Natl. Acad. Sci. U. S. A. 114 (2017) 2143–2148.
[33] C.W. Li, M.W. Qiao, H.M. Zhang, Y.X. Zhou, J. Liu, L. Wang, Z.S. Deng, Thermopneumatic liquid metal radiofrequency switch actuated by low-boiling-point fluid, Adv. Eng. Mater. 36 (2024) 2400090.
[34] D.H. Ho, Y.M. Kim, U.J. Kim, K.S. Yu, J.H. Kwon, H.C. Moon, J.H. Cho, Zwitterionic polymer gel-based fully self-healable ionic thermoelectric generators with pressure-activated electrodes, Adv. Energy Mater. 13 (2023) 2301133.
[35] C. Yeh, F.C. Kao, P.H. Wei, A. Pal, K. Kaswan, Y.T. Huang, P. Parashar, H.Y. Yeh, T.W. Wang, N. Tiwari, T.T. Tsai, Y.F. Huang, Z.H. Lin, Bioinspired shark skin-based liquid metal triboelectric nanogenerator for self-powered gait analysis and long-term rehabilitation monitoring, Nano Energy 104 (2022) 107852.
[36] L.C. Jia, Y.F. Jin, J.W. Ren, L.H. Zhao, D.X. Yan, Z.M. Li, Highly thermally conductive liquid metal-based composites with superior thermostability for thermal management, J. Mater. Chem. C. 9 (2021) 2904–2911.
[37] D. Pradhan, S. Panda, L.B. Sukla, Recent advances in indium metallurgy: A review, Miner. Process Extr. Metall. Rev. 39 (2018) 167–180.
[38] S.H. Wang, T. Gancarz, S. Uporov, T. Wang, E. Gao, F.J. Stadler, X.C. Zhou, A short history of fusible metals and alloys – towards room temperature liquid metals, Eur. J. Inorg. Chem. 2022 (2022) e202200313.
[39] P.S. Dorozhkin, S.V. Tovstonog, D. Golberg, J.H. Zhan, Y.J. Ishikawa, M. Shiozawa, H. Nakanishi, K. Nakata, Y. Bando, A liquid-Ga-filled carbon nanotube: a miniaturized temperature sensor and electrical switch, Small 1 (2005) 1088–1093.
[40] X.X. Chen, M.A. Dam, K. Ono, A. Mal, H.B. Shen, S.R. Nutt, K. Sheran, F. Wudl, A thermally re-mendable cross-linked polymeric material, Science 295 (2002) 1698–1702.
[41] R.S. Trask, I.P. Bond, Biomimetic self-healing of advanced composite structures using hollow glass fibres, Smart Mater. Struct. 15 (2006) 704–710.
[42] K.S. Toohey, N.R. Sottos, S.R. White, Characterization of microvascular-based self-healing coatings, Exp. Mech. 49 (2009) 707–717.
[43] J.H. So, J. Thelen, A. Qusba, G.J. Hayes, G. Lazzi, M.D. Dickey, Reversibly deformable and mechanically tunable fluidic antennas, Adv. Funct. Mater. 19 (2009) 3632–3637.
[44] R.D. Deshpande, J.C. Li, Y.T. Cheng, M.W. Verbrugge, Liquid metal alloys as self-healing negative electrodes for lithium ion batteries, J. Electrochem. Soc. 158 (2011) A845–A849.
[45] B.J. Blaiszik, S.L.B. Kramer, M.E. Grady, D.A. McIlroy, J.S. Moore, N.R. Sottos, S. R. White, Autonomic restoration of electrical conductivity, Adv. Mater. 24 (2012) 398–401.
[46] Y. Liu, M. Gao, S.F. Mei, Y.T. Han, J. Liu, Ultra-compliant liquid metal electrodes with in-plane self-healing capability for dielectric elastomer actuators, Appl. Phys. Lett. 103 (2013) 064101.
[47] G.Y. Li, X. Wua, D.W. Lee, A galinstan-based inkjet printing system for highly stretchable electronics with self-healing capability, Lab Chip 16 (2016) 1366–1373.
[48] Y.Z. Yu, F.J. Liu, R.C. Zhang, J. Liu, Suspension 3D printing of liquid metal into self-healing hydrogel, Adv. Mater. Technol. 2 (2017) 1700173.
[49] K. Chu, B.G. Song, H.I. Yang, D.M. Kim, C.S. Lee, M. Park, C.M. Chung, Smart passivation materials with a liquid metal microcapsule as self-healing conductors for sustainable and flexible perovskite solar cells, Adv. Funct. Mater. 28 (2018) 1800110.
[50] S. Park, G. Thangavel, K. Parida, S.H. Li, P.S. Lee, A stretchable and self-healing energy storage device based on mechanically and electrically restorative liquid-metal particles and carboxylated polyurethane composites, Adv. Mater. 31 (2019) 1805536.
[51] Z.X. Zhou, C.H. Qian, W.Z. Yuan, Self-healing, anti-freezing, adhesive and remoldable hydrogel sensor with ion-liquid metal dual conductivity for biomimetic skin, Compos. Sci. Technol. 203 (2021) 108608.
[52] B.L. He, Y.X. Du, B.W. Wang, X.Y. Zhao, S.J. Liu, Q. Ye, F. Zhou, Self-healing polydimethylsiloxane antifouling coatings based on zwitterionic poly-ethylenimine-functionalized gallium nanodroplets, Chem. Eng. J. 427 (2022) 131019.
[53] L. Yang, Z.H. Wang, H. Wang, B.Q. Jin, C.Z. Meng, X. Chen, R.Z. Li, H. Wang, M. Y. Xin, Z.S. Zhao, S.J. Guo, J.R. Wu, H.Y. Cheng, Self-healing, reconfigurable, thermal-switching, transformative electronics for health monitoring, Adv. Mater. 35 (2023) 2207742.
[54] M.C. Freitas, A.L. Sanati, P.A. Lopes, A.F. Silva, M. Tavakoli, 3D printed gallium battery with outstanding energy storage: toward fully printed battery-on-the-board soft electronics, Small 20 (2024) 2304716.
[55] T. Yamanaka, Surfactant-mediated growth of an ordered flat film of an intrinsic liquid metal on a semiconductor surface: Ga on Si(111) -4 ×1-In, Phys. Rev. B. 66 (2002) 153309.
[56] J.M. Makela, L.B. King. Progress on re-generable field emission cathodes for low-power electric propulsion. 30th International Electric Propulsion Conference. (2007) 17-20.
[57] W.D. Miller, The self-healing capacity of the human dental pulp, Int Dent. J. (Philos.) 24 (1903) 649–652.
[58] Y.J. Tan, G.J. Susanto, H.P.A. Ali, B.C.K. Tee, Progress and roadmap for intelligent self-healing materials in autonomous robotics, Adv. Mater. 33 (2021) 2002800.
[59] N.D. Jones, Self-healing fuse development, IEEE Power Process. Electron. Spec. Conf. (1972) 140–145.
[60] D. Jung, A. Hegeman, N.R. Sottos, P.H. Geubelle, S.R. White, Self-healing composites using embedded microspheres, Int. Mech. Eng. Congr. Expo. (1997) 265–275.
[61] K. Aramaki, Improvement in the self-healing ability of a protective film consisting of hydrated cerium(III) oxide and sodium phosphate layers on zinc, Corros. Sci. 45 (2003) 451–464.
[62] E. Palleau, S. Reece, S.C. Desai, M.E. Smith, M.D. Dickey, Self-healing stretchable wires for reconfigurable circuit wiring and 3D microfluidics, Adv. Mater. 25 (2013) 1589–1592.
[63] F. Krisnadi, L.L. Nguyen, J. Ankit, M.R. Ma, N. Kulkarni, M.D. Mathews, Dickey. Directed assembly of liquid metal-elastomer conductors for stretchable and self-healing electronics, Adv. Mater. 32 (2020) 2001642.

[64] J.Y. Xie, L. Han, Z. Luo, Q. Li, J.L. He, Microcapsule-based autonomous self-healing of electrical damage in dielectric polymers induced by in situ generated radicals, ACS Appl. Mater. Interfaces 15 (2023) 11185–11192.
[65] S.R. White, N.R. Sottos, P.H. Geubelle, J.S. Moore, M.R. Kessler, S.R. Sriram, E. N. Brown, S. Viswanathan, Autonomic healing of polymer composites, Nature 415 (2002) 817.
[66] M.M. Zhu, J.Y. Yu, Z.L. Li, B. Ding, Self-healing fibrous membranes, Angew. Chem. Int. Ed. 61 (2022) e202208949.
[67] Y.J. Chang, X.X. Yan, Z.H. Wu, Application and prospect of self-healing microcapsules in surface coating of wood, Colloid Interface Sci. Commun. 56 (2023) 100736.
[68] W. Du, Q.T. Li, R.S. Lin, X. Su, Preparation and characterization of microcrystalline wax/epoxy resin microcapsules for self-healing of cementitious materials, Materials 14 (2021) 1725.
[69] S.H. Cho, S.R. White, P.V. Braun, Self-healing polymer coatings, Adv. Mater. 21 (2009) 645–649.
[70] G.K. Chen, X.B. Deng, L.F. Zhu, S.H. Wang, T.S. Gan, B. Wang, Q.X. Wu, H. Fang, N.L. Ren, X.C. Zhou, Recyclable, weldable, mechanically durable, and programmable liquid metal-elastomer composites, J. Mater. Chem. A. 9 (2021) 10953–10965.
[71] M. Qi, R.Q. Yang, Z. Wang, Y.T. Liu, Q.C. Zhang, B. He, K.W. Li, Q. Yang, L. Wei, C.F. Pan, M.X. Chen, Bioinspired self-healing soft electronics, Adv. Funct. Mater. 33 (2023) 2214479.
[72] Y.Z. He, K. Xiong, J.P. Zhang, F.C. Guo, Y. Li, Q.S. Hu, A state-of-the-art review and prospectives on the self-healing repair technology for asphalt materials, Constr. Build. Mater. 421 (2024) 135660.
[73] I.P. Bon, R.S. Trask, H.R. Williams, G.J. Williams, Self healing fibre-reinforced polymer composites: An overview, in: Dordrecht. Springer Series in Materials Science, 100, Springer, Dordrecht, 2007, pp. 115–138.
[74] Y.D. Guo, X.M. Xie, J.F. Su, R. Mu, X.F. Wang, H.P. Jin, Y. Fang, Z. Ding, L.Y. Lv, N.X. Han, Mechanical experiment evaluation of the microvascular self-healing capability of bitumen using hollow fibers containing oily rejuvenator, Constr. Build. Mater. 225 (2019) 1026–1035.
[75] G. Williams, R. Trask, I. Bond, A self-healing carbon fibre reinforced polymer for aerospace applications, Compos. Pt. AAppl. Sci. Manuf. 38 (2007) 1525–1532.
[76] C. Dry, Procedures developed for self-repair of polymer matrix composite materials, Compos. Struct. 35 (1996) 263–269.
[77] Z. Wang, Y. Li, H.Y. Tu, The mode II interlaminar fracture toughness and healing efficiency of repeatable self-healing composite, Compos. Pt. AAppl. Sci. Manuf. 161 (2022) 107096.
[78] Q. Sun, X. Gao, S. Wang, R.Y. Shao, X.Y. Wang, J.F. Su, Microstructure and self-healing capability of artificial skin composites using biomimetic fibers containing a healing agent, Polymers 15 (2023) 190.
[79] K.S. Toohey, N.R. Sottos, J.A. Lewis, J.S. Moore, S.R. White, Self-healing materials with microvascular networks, Nat. Mater. 6 (2007) 581–585.
[80] A.P. Esser-Kahn, P.R. Thakre, H.F. Dong, J.F. Patrick, V.K. Vlasko-Vlasov, N. R. Sottos, J.S. Moore, S.R. White, Three-dimensional microvascular fiber-reinforced composites, Adv. Mater. 23 (2011) 3654–3658.
[81] C.D. Nardi, B.L. Freeman, D. Gardner, T. Jefferson, Mechanical response and predictive modelling of vascular self-healing cementitious materials using novel healing agents, Cem. Concr. Compos 142 (2023) 105143.
[82] C.J. Norris, G.J. Meadway, M.J.O. Sullivan, I.P. Bond, R.S. Trask, Self-healing fibre reinforced composites via a bioinspired vasculature, Adv. Funct. Mater. 21 (2011) 3624–3633.
[83] A.R. Hamilton, N.R. Sottos, S.R. White, Local strain Concentrations in a microvascular network, Exp. Mech. 50 (2010) 255–263.
[84] C. De Nardi, D. Gardner, A.D. Jefferson, Development of 3D printed networks in self-healing concrete, Materials 13 (2020) 1328.
[85] X.X. Zhang, G.P. Chen, L.Y. Sun, F.F. Ye, X. Shen, Y.J. Zhao, Claw-inspired microneedle patches with liquid metal encapsulation for accelerating incisional wound healing, Chem. Eng. J. 406 (2021) 126741.
[86] J. Kolosnjaj-Tabi, L. Gibot, I. Fourquaux, M. Golzio, M.P. Rols, Electric field-responsive nanoparticles and electric fields: physical, chemical, biological mechanisms and therapeutic prospects, Adv. Drug Deliv. Rev. 138 (2019) 56–67.
[87] R. Guo, J.B. Tang, S.J. Dong, J. Lin, H.Z. Wang, J. Liu, W. Rao, One-step liquid metal transfer printing: Toward fabrication of flexible electronics on wide range of substrates, Adv. Mater. Technol. 3 (2018) 1800265.
[88] J.R. Huang, Z. Gong, Y.K. Chen, A stretchable elastomer with recyclability and shape memory assisted self-healing capabilities based on dynamic disulfide bonds, Polymer 242 (2022) 124569.
[89] C. Russo, J.L. Ramírez, X. Fernández-Francos, S.D.L. Flor, Electro-responsive shape-memory composites obtained via dual-curing processing, Polym. Adv. Technol. 33 (2022) 1715–1726.
[90] C. Chluba, W.W. Ge, R.L.D. Miranda, J. Strobel, L. Kienle, E. Quandt, M. Wuttig, Ultralow-fatigue shape memory alloy films, Science 348 (2015) 1004–1007.
[91] C.C. Wang, Z. Ding, H. Purnawali, W.M. Huang, H. Fan, L. Sun, Repeated instant self-healing shape memory composites, J. Mater. Eng. Perform. 21 (2012) 2663–2669.
[92] Q. Wang, Y.T. Li, J.B. Xiao, L. Xia, Intelligent Eucommia ulmoides rubber/ionomer blends with thermally activated shape memory and self-healing properties, Polymers 15 (2023) 1182.
[93] J. Kang, D.H. Son, G.N. Wang, Y.X. Liu, J. Lopez, Y. Kim, J.Y. Oh, T. Katsumata, J. Mun, Y. Lee, L.H. Jin, J.B.H. Tok, Z.N. Bao, Tough and water-insensitive self-healing elastomer for robust electronic skin, Adv. Mater. 30 (2018) 1706846.
[94] P. Ravindra, X.R. Advincula, C. Schran, A. Michaelides, V. Kapil, Quasi-one-dimensional hydrogen bonding in nanoconfined ice, Nat. Commun. 15 (2024) 7301.
[95] X.M. Liu, G.L. Liu, T. Fu, K.R. Ding, J.R. Guo, Z.R. Wang, W. Xia, H.Y. Shangguan, Structural design and energy and environmental applications of hydrogen-bonded organic frameworks: A systematic review, Adv. Sci. 11 (2024) 2400101.
[96] P. Cordier, F. Tournilhac, C. Soulié-Ziakovic, L. Leibler, Self-healing and thermoreversible rubber from supramolecular assembly, Nature 451 (2008) 977–980.
[97] L.L. Yang, X.X. Tan, Z.Q. Wang, X. Zhang, Supramolecular polymers: historical development, preparation, characterization, and functions, Chem. Rev. 115 (2015) 7196–7239.
[98] J. Tellers, S. Canossa, R. Pinalli, M. Soliman, J. Vachon, E. Dalcanale, Dynamic cross-linking of polyethylene via sextuple hydrogen bonding array, Macromolecules 51 (2018) 7680–7691.
[99] S.Y. Wang, M.W. Urban, Self-healable fluorinated copolymers governed by dipolar interactions, Adv. Sci. 8 (2021) 2101399.
[100] L. Tan, Y.Q. Zhang, W.M. Liu, Quantum phase transitions for two coupled cavities with dipole-interaction atoms, Phys. Rev. A. 84 (2011) 063816.
[101] Y.Q. Fan, J. He, S.Z. Guo, H. Jiang, Host-guest chemistry in binary and ternary complexes utilizing π-conjugated carbon nanorings, ChemPlusChem 89 (2024) e202300536.
[102] M.M. Zhang, X.Z. Yan, F.H. Huang, Z.B. Niu, H.W. Gibson, Stimuli-responsive host-guest systems based on the recognition of cryptands by organic guests, Acc. Chem. Res. 47 (2014) 1995–2005.
[103] D.Y. Xia, P. Wang, X.F. Ji, N.M. Khashab, J.L. Sessler, F.H. Huang, Functional supramolecular polymeric networks: The marriage of covalent polymers and macrocycle-based host–guest interactions, Chem. Rev. 120 (2020) 6070–6123.
[104] J. Li, D. Yim, W.D. Jang, J. Yoon, Recent progress in the design and applications of fluorescence probes containing crown ethers, Chem. Soc. Rev. 46 (2017) 2437–2458.
[105] J. Park, J. Park, J. Lee, C. Lim, D.W. Lee, Size compatibility and concentration dependent supramolecular host–guest interactions at interfaces, Nat. Commun. 13 (2022) 112.
[106] J.Y.W. Yeung, F.K.W. Kong, F.K.W. Hau, M.H.Y. Chan, M. Ng, M.Y. Leung, V.W. W. Yam, Solvent-dependent supramolecular host-guest assemblies of platinum(II) tweezers and a guest system: From discrete molecules to high-ordered oligomers, Angew. Chem. Int. Ed. 61 (2022) e202207313.
[107] Z.Y. Wang, C. Sun, K.K. Yang, X.Y. Chen, R.B. Wang, Cucurbituril-based supramolecular polymers for biomedical applications, Angew. Chem. Int. Ed. 61 (2022) e202206763.
[108] S. Burattini, B.W. Greenland, D.H. Merino, W.G. Weng, J. Seppala, H. M. Colquhoun, W. Hayes, M.E. Mackay, I.W. Hamley, S.J. Rowan, A healable supramolecular polymer blend based on aromatic π-π stacking and hydrogen-bonding interactions, J. Am. Chem. Soc. 132 (2010) 12051–12058.
[109] W.R. Zhuang, Y. Wang, P.F. Cui, L. Xing, J. Lee, D. Kim, H.L. Jiang, Y.K. Oh, Applications of π-π stacking interactions in the design of drug-delivery systems, J. Control. Release 294 (2019) 311–326.
[110] J.F. Mei, X.Y. Jia, J.C. Lai, Y. Sun, C.H. Li, J.H. Wu, Y. Cao, X.Z. You, Z.N. Bao, A highly stretchable and autonomous self-healing polymer based on combination of Pt···Pt and π-π interactions, Macromol. Rapid Commun. 37 (2016) 1667–1675.
[111] S. Jun, J.W. Lee, S.C. Kim, S.J. Oh, S.H. Jeong, Unveiling the ligand-mediated phase engineering mechanism in two-dimensional transition metal chalcogenides through coordination geometry control, J. Mater. Chem. A. 12 (2024) 7522–7527.
[112] Q.B. Lv, J. Lin, H. Huang, B.X. Ma, W.J. Li, J.W. Chen, M.H. Wang, X.Y. Wang, G. S. Fu, Y. Xiao, Nanosponge for iron chelation and efflux: A ferroptosis-inhibiting approach for myocardial infarction therapy, Adv. Sci. 11 (2024) 2305895.
[113] I. Hussain, S.M. Sayed, S.L. Liu, F. Yao, O. Oderinde, G.D. Fu, Hydroxyethyl cellulose-based self-healing hydrogels with enhanced mechanical properties via metal-ligand bond interactions, Eur. Polym. J. 100 (2018) 219–227.
[114] M.H. Yu, J.Y. Feng, S.P. Xie, Y.P. Wang, Y.S. Li, R.Z. Wang, G.F. Lu, K. Li, R. Wu, W.W. Zhao, Y.H. Tian, Synthesis of thick-shell Cu@Ag particles with nanorod-shape surface morphology for printed electronics, J. Alloy. Compd. 1024 (2025) 179870.
[115] L.J. Zhang, H. Xiong, Q. Wu, Y. Peng, Y. Zhu, H. Wang, Y. Yang, X.K. Liu, G. S. Huang, J.R. Wu, Constructing hydrophobic protection for ionic interactions toward water, acid, and base-resistant self-healing elastomers and electronic devices, Sci. China Mater. 64 (2021) 1780–1790.
[116] M. Nichifor, Role of hydrophobic associations in self-healing hydrogels based on amphiphilic polysaccharides, Polymers 15 (2023) 1065.
[117] H. Ren, X.L. He, Y. Long, Q.Q. Li, S.S. Li, X.P. Zhou, Polyionic liquid ionogels formed via hydrophobic association for flexible strain sensors, J. Mater. Chem. C. 12 (2024) 4737–4750.
[118] S. Nevejans, N. Ballard, J.I. Miranda, B. Reckc, J.M. Asua, The underlying mechanisms for self-healing of poly(disulfide)s, Phys. Chem. Chem. Phys. 18 (2016) 27577–27583.
[119] J.M. Matxain, J.M. Asua, F. Ruipérez, Design of new disulfide-based organic compounds for the improvement of self-healing materials, Phys. Chem. Chem. Phys. 18 (2016) 1758–1770.
[120] A. Oluwasanmi, C. Hoskins, Potential use of the Diels-Alder reaction in biomedical and nanomedicine applications, Int. J. Pharm. 604 (2021) 120727.

[121] K. Pojnar, B. Pilch-Pitera, S. Ataei, P. Gazdowicz, B. Mossety-Leszczak, A. Bobrowski, Self-healing thermal-reversible low-temperature polyurethane powder coating based on Diels–Alder reaction, Materials 17 (2024) 3555.
[122] L. Fabbrizzi, Beauty in chemistry: Making artistic molecules with Schiff bases, J. Org. Chem. 85 (2020) 12212–12226.
[123] C.W. Lou, Y. Wang, Y.X. Wang, X.F. Zhang, Y.T. Wang, X.M. Wang, H.T. Ren, T. T. Li, J.H. Lin, B.C. Shiu, Ultrahigh tough, self-healing copolymer elastomer crosslinked by reversible imine system, Prog. Org. Coat. 185 (2023) 107948.
[124] A. Pettignano, S. Grijalvo, M. Häring, R. Eritja, N. Tanchoux, F. Quignard, D. D. Díaz, Boronic acid-modified alginate enables direct formation of injectable, self-healing and multistimuli-responsive hydrogels, Chem. Commun. 53 (2017) 3350–3353.
[125] C.X. Zhang, H.Y. Lu, X. Wang, Transient polymer hydrogels based on dynamic covalent borate ester bonds, Chin. J. Chem. 40 (2022) 2794–2800.
[126] M. Capelot, M.M. Unterlass, F. Tournilhac, L. Leibler, Catalytic control of the vitrimer glass transition, ACS Macro Lett. 1 (2012) 789–792.
[127] F.Y. Fu, M.Q. Huang, W.L. Zhang, Y. Zhao, X.D. Liu, Thermally assisted self-healing behavior of anhydride modified polybenzoxazines based on transesterification, Sci. Rep. 8 (2018) 10325.
[128] V.I. Anikeev, D.A. Stepanov, A. Ermakova, Calculating the thermodynamic characteristics of the stepwise transesterification of simple triglycerides, Russ. J. Phys. Chem. A. 85 (2011) 2082–2087.
[129] D. Ramimoghadam, D.J. Eyckens, R.A. Evans, G. Moad, S. Holmes, R. Simons, Towards sustainable materials: A review of acylhydrazone chemistry for reversible polymers, Chem. Eur. J. 30 (2024) e202401728.
[130] G.H. Deng, C.M. Tang, F.Y. Li, H.F. Jiang, Y.M. Chen, Covalent cross-linked polymer gels with reversible sol−gel transition and self-healing properties, Macromolecules 43 (2010) 1191–1194.
[131] C.J. Zhang, X.L. Luo, T.F. Wei, Y.F. Hu, G.K. Li, Z.M. Zhang, Acylhydrazone bond dynamic covalent polymer gel monolithic column online coupling to high-performance liquid chromatography for analysis of sulfonamides and fluorescent whitening agents in food, J. Chromatogr. A. 1519 (2017) 28–37.
[132] C. Yang, Z.G. Guo, Biomimetic Xanthium strumarium inspired superhydrophobic anti-/de-icing films with near-infrared light-induced self-healing, Small (2025) 2500016.
[133] S. Aiswarya, S.S. Banerjee, Construction and characterization of multi-stimuli responsive shape memory assisted self-healing thermoplastic elastomeric materials based on TPU/ENR/Fe_3O_4 blends, Macromol. Chem. Phys. (2025) 2400346.
[134] M.D. Bartlett, M.D. Dickey, C. Majidi, Self-healing materials for soft-matter machines and electronics, NPG Asia Mater. 11 (2019) 21.
[135] P. Chakma, L.H.R. Possarle, Z.A. Digby, B.R. Zhang, J.L. Sparks, D. Konkolewicz, Dual stimuli responsive self-healing and malleable materials based on dynamic thiol-Michael chemistry, Polym. Chem. 8 (2017) 6534–6543.
[136] C.F.H. Allen, The thermal reversibility of the Michael reaction:v.The effect of the structure of certain thiol adducts on cleavage, Can. J. Chem. 44 (1966) 2315–2321.
[137] K. Akyildiz, J.H. Kim, J.H. So, H.J. Koo, Recent progress on micro- and nanoparticles of gallium-based liquid metals: From preparation to applications, J. Ind. Eng. Chem. 116 (2022) 120–141.
[138] S. Eristoff, A.M. Nasab, X.N. Huang, R. Kramer-Bottiglio, Liquid Metal + x: A review of multiphase composites containing liquid metal and other (x) fillers, Adv. Funct. Mater. 34 (2024) 2309529.
[139] M. Kim, H.J. Lim, S.H. Ko, Liquid metal patterning and unique properties for next-generation soft electronics, Adv. Sci. 10 (2023) 2205795.
[140] N. Ochirkhuyag, R. Matsuda, Z.H. Song, F. Nakamura, T. Endoa, H. Ota, Liquid metal-based nanocomposite materials: Fabrication technology and applications, Nanoscale 13 (2021) 2113–2135.
[141] M.K. Zhang, S.Y. Yao, W. Rao, J. Liu, Transformable soft liquid metal micro/nanomaterials, Mater. Sci. Eng. R. Rep. 138 (2019) 1–35.
[142] M. Wang, Y.L. Lin, Gallium-based liquid metals as reaction media for nanomaterials synthesis, Nanoscale 16 (2024) 6915–6933.
[143] D.K. Yu, Z.M. Xue, T.C. Mu, Eutectics: formation, properties, and applications, Chem. Soc. Rev. 50 (2021) 8596–8638.
[144] T. Daeneke, K. Khoshmanesh, N. Mahmood, I.A. de Castro, D. Esrafilzadeh, S. J. Barrow, M.D. Dickeyb, K. Kalantar-zadeh, Liquid metals: fundamentals and applications in chemistry, Chem. Soc. Rev. 47 (2018) 4073–4111.
[145] L. Ren, J.C. Zhuang, G. Casillas, H.F. Feng, Y.Q. Liu, X. Xu, Y.D. Liu, J. Chen, Y. Du, L. Jiang, S.X. Dou, Nanodroplets for stretchable superconducting circuits, Adv. Funct. Mater. 26 (2016) 8111–8118.
[146] J.J. Yan, Y. Lu, G.J. Chen, M. Yang, Z. Gu, Advances in liquid metals for biomedical applications, Chem. Soc. Rev. 47 (2018) 2518–2533.
[147] G. Ryu, I. Park, H. Kim, Liquid metal micro- and nanodroplets: characteristics, fabrication techniques, and applications, ACS Omega 8 (2023) 15819–15830.
[148] S.S. Zhao, J.Q. Zhang, L. Fu, Liquid Metals: A novel possibility of fabricating 2D metal oxides, Adv. Mater. 33 (2021) 2005544.
[149] M.D. Dickey, Stretchable and soft electronics using liquid metals, Adv. Mater. 29 (2017) 1606425.
[150] J.Y. Yang, P. Nithyanandam, S. Kanetkar, K.Y. Kwon, J. Ma, S. Im, J.H. Oh, M. Shamsi, M. Wilkins, M. Daniele, T. Kim, H.N. Nguyen, V.K. Truong, M. D. Dickey, Liquid metal coated textiles with autonomous electrical healing and antibacterial properties, Adv. Mater. Technol. 8 (2023) 2202183.
[151] J.H. Kim, S.J. Kim, J.H. So, K. Kim, H.J. Koo, Cytotoxicity of gallium–indium liquid metal in an aqueous environment, ACS Appl. Mater. Interfaces 10 (2018) 17448–17454.
[152] S. Chen, R.Q. Zhao, X.Y. Sun, H.Z. Wang, L. Li, J. Liu, Toxicity and biocompatibility of liquid metals, Adv. Healthc. Mater. 12 (2023) 2201924.
[153] Y. Lu, Y.L. Lin, Z.W. Chen, Q.Y. Hu, Y. Liu, S.Y. Yu, W. Gao, M.D. Dickey, Z. Gu, Enhanced endosomal escape by light-fueled liquid-metal transformer, Nano Lett. 17 (2017) 2138–2145.
[154] S.A. Chechetka, Y. Yu, X. Zhen, M. Pramanik, K.Y. Pu, E. Miyako, Light-driven liquid metal nanotransformers for biomedical theranostics, Nat. Commun. 8 (2017) 15432.
[155] C.C. Qu, Y.T. Liang, X.Q. Wang, S. Gao, Z.Z. He, X.Y. Sun, Gallium-based liquid metal materials for antimicrobial applications, Bioengineering 9 (2022) 416.
[156] M. Chen, J.D. Wu, T. Ye, J.Y. Ye, C. Zhao, S. Bi, J.W. Yan, B.W. Mao, G. Feng, Adding salt to expand voltage window of humid ionic liquids, Nat. Commun. 11 (2020) 5809.
[157] L. Ren, X. Xu, Y. Du, K. Kalantar-Zadeh, S.X. Dou, Liquid metals and their hybrids as stimulus-responsive smart materials, Mater. Today 34 (2020) 92–114.
[158] H.Z. Wang, Y.Y. Yao, Z.Z. He, W. Rao, L. Hu, S. Chen, J. Lin, J.Y. Gao, P.J. Zhang, X.Y. Sun, X.J. Wang, Y.T. Cui, Q. Wang, S.J. Dong, G.Z. Chen, J. Liu, A highly stretchable liquid metal polymer as reversible transitional insulator and conductor, Adv. Mater. 31 (2019) 1901337.
[159] E.J. Markvicka, M.D. Bartlett, X.N. Huang, C. Majidi, An autonomously electrically self-healing liquid metal–elastomer composite for robust soft-matter robotics and electronics, Nat. Mater. 17 (2018) 618–624.
[160] C. Jiang, R. Guo, Liquid metal-based paper electronics: Materials, methods, and applications, Sci. China Technol. Sci. 66 (2023) 1595–1616.
[161] J.X. Wang, G.F. Cai, S.H. Li, D.C. Gao, J.Q. Xiong, P.S. Lee, Printable superelastic conductors with extreme stretchability and robust cycling endurance enabled by liquid-metal particles, Adv. Mater. 30 (2018) 1706157.
[162] M.D. Bartlett, A. Fassler, N. Kazem, E.J. Markvicka, P. Mandal, C. Majidi, Stretchable, high-k dielectric elastomers through liquid-metal inclusions, Adv. Mater. 28 (2016) 3726–3731.
[163] Y.F. Shen, D.D. Jin, T.F. Li, X.X. Yang, X. Ma, Magnetically responsive gallium-based liquid metal: preparation, property and application, ACS Nano 18 (2024) 20027–20054.
[164] L.X. Cao, D.H. Yu, Z.S. Xia, H.Y. Wan, C.K. Liu, T. Yin, Z.Z. He, Ferromagnetic liquid metal putty-like material with transformed shape and reconfigurable polarity, Adv. Mater. 32 (2020) 2000827.
[165] D. Kim, J.B. Lee, Magnetic-field-induced liquid metal droplet manipulation, J. Korean Phys. Soc. 66 (2015) 282–286.
[166] J. Zhang, R. Guo, J. Liu, Self-propelled liquid metal motors steered by a magnetic or electrical field for drug delivery, J. Mater. Chem. B. 4 (2016) 5349–5357.
[167] X. Wan, L. Luo, Y.J. Liu, J.S. Leng, Direct ink writing based 4D printing of materials and their applications, Adv. Sci. 7 (2020) 2001000.
[168] R. Guo, T.Y. Li, Z.Y. Wu, C.X. Wan, J. Niu, W.X. Huo, H.X. Yu, X. Huang, Thermal transfer-enabled rapid printing of liquid metal circuits on multiple substrates, ACS Appl. Mater. Interfaces 14 (2022) 37028–37038.
[169] Q. Zhang, Y. Gao, J. Liu, Atomized spraying of liquid metal droplets on desired substrate surfaces as a generalized way for ubiquitous printed electronics, Appl. Phys. A. 116 (2014) 1091–1097.
[170] G.H. Lee, Y.R. Lee, H. Kim, D.A. Kwon, H. Kim, C.Q. Yang, S.Q. Choi, S. Park, J. W. Jeong, S. Park, Rapid meniscus-guided printing of stable semi-solid-state liquid metal microgranular-particle for soft electronics, Nat. Commun. 13 (2022) 2643.
[171] G. Li, S. Wang, Z.W. Zhang, Y.X. Sun, J.Y. Wen, J.Y. Feng, S.J. Wang, Q. Sun, Y. H. Tian, Precision control of aerosol jet printing for conformal electronics fabrication with ultra-fine and wide-range resolution, Adv. Mater. Technol. 10 (2025) 2402114.
[172] R. Guo, X.L. Wang, H. Chang, W.Z. Yu, S.T. Liang, W. Rao, J. Liu, Ni-GaIn amalgams enabled rapid and customizable fabrication of wearable and wireless healthcare electronics, Adv. Eng. Mater. 20 (2018) 1800054.
[173] U. Daalkhaijav, O.D. Yirmibesoglu, S. Walker, Y. Mengüç, Rheological modification of liquid metal for additive manufacturing of stretchable electronics, Adv. Mater. Technol. 3 (2018) 1700351.
[174] X.M. Yuan, P.C. Wu, Q. Gao, J. Xu, B. Guo, Y. He, Multifunctionally wearable monitoring with gelatin hydrogel electronics of liquid metals, Mater. Horiz. 9 (2022) 961–972.
[175] S.L. Wang, Y.Y. Nie, H.Y. Zhu, Y.R. Xu, S.T. Cao, J.X. Zhang, Y.Y. Li, J.H. Wang, X. H. Ning, D.S. Kong, Intrinsically stretchable electronics with ultrahigh deformability to monitor dynamically moving organs, Sci. Adv. 8 (2022) eabl5511.
[176] D.H. Yu, Y. Liao, Y.C. Song, S.L. Wang, H.Y. Wan, Y.H. Zeng, T. Yin, W.H. Yang, Z. Z. He, A super-stretchable liquid metal foamed elastomer for tunable control of electromagnetic waves and thermal transport, Adv. Sci. 7 (2020) 2000177.
[177] S. Chen, W.K. Xing, H. Wang, W.Z. Cheng, Z.H. Lei, F.Y. Zheng, P. Tao, W. Shang, B.W. Fu, C.Y. Song, M.D. Dickey, T. Deng, A bottom-up approach to generate isotropic liquid metal network in polymer-enabled 3D thermal management, Chem. Eng. J. 439 (2022) 135674.
[178] Jung-Eun Park, Han Sol Kang, Min Koo, Cheolmin Park, Autonomous surface reconciliation of a liquid-metal conductor micropatterned on a deformable hydrogel, Adv. Mater. 32 (2020) 2002178.

[179] X.L. Chen, P. Sun, H.M. Tian, X.M. Li, C.H. Wang, J.K. Duan, Y.S. Luo, S. Li, X. M. Chen, J.Y. Shao, Self-healing and stretchable conductor based on embedded liquid metal patterns within imprintable dynamic covalent elastomer, J. Mater. Chem. C. 10 (2022) 1039–1047.
[180] J. Zhou, Y. Liu, F.L. Zhuo, H. Chen, H. Cao, Y.Q. Fu, Jianfei Xie, Huigao Duan, Superior compressive and tensile bi-directional strain sensing capabilities achieved using liquid metal hybrid-hydrogels empowered by machine learning algorithms, Chem. Eng. J. 479 (2024) 147790.
[181] C. Hua, J.Y. Gao, J. Liu, Room temperature self-healing liquid metals: capabilities, applications and challenges, Int. J. Smart Nano Mater. 15 (2024) 469–501.
[182] J.Y. Du, X. Wang, Y.Z. Li, Q. Min, How an oxide layer influences the impact dynamics of galinstan droplets on a superhydrophobic surface, Langmuir 38 (2022) 5645–5655.
[183] K.Y. Kwon, V.K. Truong, F. Krisnadi, S. Im, J. Ma, N. Mehrabian, T. Kim, M. D. Dickey, Surface modification of gallium-based liquid metals: mechanisms and applications in biomedical sensors and soft sctuators, Adv. Intell. Syst. 3 (2021) 2000159.
[184] J.H. Kim, S. Kim, M.D. Dickey, J.H. So, H.J. Koo, Interface of gallium-based liquid metals: oxide skin, wetting, and applications, Nanoscale Horiz. 9 (2024) 1099–1119.
[185] J.S. Benas, F.C. Liang, M. Venkatesan, Z.L. Yan, W.C. Chen, S.T. Han, Y. Zhou, C. C. Kuo, Recent development of sustainable self-healable electronic skin applications, a review with insight, Chem. Eng. J. 466 (2023) 142945.
[186] J. Shaikh, N.D. Patil, A. Sharma, R. Bhardwaj, Numerical simulations and experiments on droplet coalescence dynamics over a liquid-air interface: mechanism and effect of droplet-size/surface-tension, SN Appl. Sci. 3 (2021) 292.
[187] J.R. Castrejón-Pita, E.S. Betton, K.J. Kubiak, M.C.T. Wilson, I.M. Hutchings, The dynamics of the impact and coalescence of droplets on a solid surface, Biomicrofluidics 5 (2011) 14112.
[188] H.Z. Wang, S. Chen, X.Y. Zhu, B. Yuan, X.Y. Sun, J. Zhang, X.H. Yang, Y. Wei, J. Liu, Phase transition science and engineering of gallium-based liquid metal, Matter 5 (2022) 2054–2085.
[189] E. Arzt, H.C. Quan, R.M. McMeeking, R. Hensel, Functional surface microstructures inspired by nature - from adhesion and wetting principles to sustainable new devices, Prog. Mater. Sci. 120 (2021) 100823.
[190] J.Y. Wen, S. Wang, J.Y. Feng, J.X. Ma, H. Zhang, P. Wu, G. Li, Z.H. Wu, F.Z. Meng, L.Q. Li, Y.H. Tian, Recent progress in polyaniline-based chemiresistive flexible gas sensors: design, nanostructures, and composite materials, J. Mater. Chem. A. 12 (2024) 6190.
[191] Y.X. Chen, Q. Wang, L.F. Hou, H. Huang, Z.Q. Gao, Y.H. Wei, Self-warning and self-repairing mechanisms in functional coatings: a review, Exploration (2025) e20240066.
[192] R. Tutika, A.B.M.T. Haque, M.D. Bartlett, Self-healing liquid metal composite for reconfigurable and recyclable soft electronics, Commun. Mater. 2 (2021) 64.
[193] R.M. Zheng, Z.F. Peng, Y. Fu, Z.F. Deng, S.Q. Liu, S.T. Xing, Y.Y. Wu, J.Y. Li, L. Liu, A novel conductive core-shell particle based on liquid metal for fabricating real-time self-repairing flexible circuits, Adv. Funct. Mater. 30 (2020) 1910524.
[194] Y. Lin, T. Fang, C. Bai, Y.P. Sun, C. Yang, G.H. Hu, H.R. Guo, W.J. Qiu, W. X. Huang, L. Wang, Z.H. Tao, Y.Q. Lu, D.S. Kong, Ultrastretchable electrically self-healing conductors based on silver nanowire/liquid metal microcapsule nanocomposites, Nano Lett. 23 (2023) 11174–11183.
[195] B. Han, Y. Yang, X.B. Shi, G.Z. Zhang, L. Gong, D.W. Xu, H.B. Zeng, C.Y. Wang, M. Gu, Y.H. Deng, Spontaneous repairing liquid metal/Si nanocomposite as a smart conductive-additive-free anode for lithium-ion battery, Nano Energy 50 (2018) 359–366.
[196] Y.M. Xin, H. Peng, J. Xu, J.Y. Zhang, Ultrauniform embedded liquid metal in sulfur polymers for recyclable, conductive, and self-healable materials, Adv. Funct. Mater. 29 (2019) 1808989.
[197] X.F. Li, M. Jiang, Y.M. Du, X. Ding, C. Xiao, Y.Y. Wang, Y.Y. Yang, Y.Z. Zhuo, K. Zheng, X.L. Liu, L. Chen, Y. Gong, X.Y. Tian, X. Zhang, Self-healing liquid metal hydrogel for human-computer interaction and infrared camouflage, Mater. Horiz. 10 (2023) 2945–2957.
[198] P.L. Fang, X.L. Ji, X. Zhao, R.Y. Do, Y.Y. Wan, Y. Wang, Y.T. Zhang, P. Shi, Self-healing electronics for prognostic monitoring of methylated mirculating tumor DNAs, Adv. Mater. 35 (2023) 2207282.
[199] Y. Xu, R. Rothe, D. Voigt, S. Hauser, M.Y. Cui, T. Miyagawa, M.P. Gaillez, T. Kurth, M. Bornhäuser, J. Pietzsch, Y.X. Zhang, Convergent synthesis of diversified reversible network leads to liquid metal-containing conductive hydrogel adhesives, Nat. Commun. 12 (2021) 2407.
[200] P. Yang, H.Q. Li, X.Y. Mou, Z.P. Chen, X.J. Lai, J.P. Ding, X.R. Zeng, Functional and environmental friendly polyimine elastomer based on the dynamic covalent network for a flexible strain sensor, Macromolecules 56 (2023) 9766–9777.
[201] P.A. Lopes, B.C. Santos, A.T. de Almeida, M. Tavakoli, Reversible polymer-gel transition for ultra-stretchable chip-integrated circuits through self-soldering and self-coating and self-healing, Nat. Commun. 12 (2021) 4666.
[202] R. Guo, X.Y. Sun, B. Yuan, H.Z. Wang, J. Liu, Magnetic liquid metal (Fe-EGaIn) based multifunctional electronics for remote self-healing materials, degradable electronics, and thermal transfer printing, Adv. Sci. 6 (2019) 1901478.
[203] X.Z. Lü, H.Y. Tang, H. Wang, X.Y. Meng, F. Li, Ultra-soft thermal self-healing liquid-metal-foamed composite with high thermal conductivity, Compos. Sci. Technol. 226 (2022) 109523.
[204] M. Zhou, W.Q. Liu, H.Q. Fu, Construction of ultrathin self-healing films with highly efficient electromagnetic interference shielding and Joule heating capability by MXene decorating liquid metal, J. Alloy. Compd. 968 (2023) 171931.
[205] P. Wang, C.H. Fu, Z.H. Wu, H. Lan, S.W. Cui, T. Qi, A dynamic nanoconfinement strategy towards self-healing soft electronics with super stretchability, ultrahigh strength and reliably high conductivity, J. Mater. Chem. A. 10 (2022) 21093–21101.
[206] C.T. Xu, B. Ma, S. Yuan, C. Zhao, H. Liu, High-resolution patterning of liquid metal on hydrogel for flexible, stretchable, and self-healing electronics, Adv. Electron. Mater. 6 (2020) 1900721.
[207] C.P. Li, Y.T. Shi, H.X. Su, Y.F. Yang, W. Li, T. Zhang, W.Y. Chen, R.J. Lin, Y.Z. Li, L.S. Liao, Mechanically robust and recyclable siloxane elastomers enabled by adjustable dynamic polymer networks for electronic skin, Eur. Polym. J. 189 (2023) 111984.
[208] X.Y. Wang, M.Y. Zhao, L. Zhang, K. Li, D. Wang, L. Zhang, A.M. Zhang, Y. Xu, Liquid metal bionic instant self-healing flexible electronics with full recyclability and high reliability, Chem. Eng. J. 431 (2022) 133965.
[209] Y. Zhou, Y.Y. Zhu, Z. Hu, X.Y. Yang, P.K. Yang, L. Huang, Y.P. Wu, Liquid metal-based self-healable and elastic conductive fiber in complex operating conditions, Energy Environ. Mater. 6 (2023) e12448.
[210] H.S. Chen, T.F. Hou, M.H. Zhang, J.K. Du, L.C. Hua, X. Chen, A.B. Zhang, Y. Jin, L. W. Zhou, G.Y. Li, Fully recyclable liquid metal-based ultra-stretchable electronics enabled by water-modulation-fegradation-reconstruction polymer-gel, Energy Environ. Mater. 7 (2024) e12706.
[211] S. Kim, J.W. Kim, Y.H. Lee, Y.R. Jeong, K. Keum, D.S. Kim, H. Lee, J.S. Ha, Tough, self-healing polyurethane with novel functionality for fully recoverable layered sensor arrays, Chem. Eng. J. 464 (2023) 142700.
[212] X.B. Deng, G.K. Chen, Y.F. Liao, X. Lu, S.Y. Hu, T.S. Gan, S.H. Wang, X.L. Zhang, Self-healable and recyclable dual-shape memory liquid metal–elastomer composites, Polymers 14 (2022) 2259.
[213] Z.X. Zhang, L. Tang, C. Chen, H.T. Yu, H.H. Bai, L. Wang, M.M. Qin, Y.Y. Feng, W. Feng, Liquid metal-created macroporous composite hydrogels with self-healing ability and multiple sensations as artificial flexible sensors, J. Mater. Chem. A. 9 (2021) 875–883.
[214] S.H. Wu, B.Y. Wang, D. Chen, X.N. Liu, H.L. Wang, Z.P. Song, D.H. Yu, G.D. Li, S. H. Ge, W.X. Liu, Highly sensitive and self-healing conductive hydrogels fabricated from cationic cellulose nanofiber-dispersed liquid metal for strain sensors, Sci. China Mater. 66 (2023) 1923–1933.
[215] D. Mani, M.C. Vu, S. Anand, J.B. Kim, T.H. Jeong, I.H. Kim, B.K. Seo, M.A. Islam, S.R. Kim, Elongated liquid metal based self-healing polyurethane composites for tunable thermal conductivity and electromagnetic interference shielding, Compos. Commun. 44 (2023) 101735.
[216] L. Mou, J. Qi, L.X. Tang, R.H. Dong, Y. Xia, Y. Gao, X.Y. Jiang, Highly stretchable and biocompatible liquid metal-elastomer conductors for self-healing electronics, Small 16 (2020) 2005336.
[217] M. Wang, X. Feng, X.J. Wang, S.N. Hu, C.Z. Zhang, H.S. Qi, Facile gelation of a fully polymeric conductive hydrogel activated by liquid metal nanoparticles, J. Mater. Chem. A. 9 (2021) 24539–24547.
[218] Y.H. Ye, F. Jiang, Highly stretchable, durable, and transient conductive hydrogel for multi-functional sensor and signal transmission applications, Nano Energy 99 (2022) 107374.
[219] B. Chen, G.L. Liu, M.Y. Wu, Y.D. Cao, H.B. Zhong, J.F. Shen, M.X. Ye, Liquid metal-based organohydrogels for wearable flexible electronics, Adv. Mater. Technol. 8 (2023) 2201919.
[220] M. Wang, Z.B. Lai, X.L. Jin, T.L. Sun, H.C. Liu, H.S. Qi, Multifunctional liquid-free ionic conductive elastomer fabricated by liquid metal induced polymerization, Adv. Funct. Mater. 31 (2021) 2101957.
[221] Y.Y. Zhao, Y. Ohm, J.H. Liao, Y.C. Luo, H.Y. Cheng, P. Won, P. Roberts, M. R. Carneiro, M.F. Islam, J.H. Ahn, L.M. Walker, C. Majidi, A self-healing electrically conductive organogel composite, Nat. Electron 6 (2023) 206–215.
[222] S. Xu, Y. Zong, J.Z. Ma, L.P. Liu, A multifunctional skin-like sensor based on liquid metal activated gelatin organohydrogel, Adv. Mater. Interfaces 9 (2022) 2201212.
[223] Y.J. Hu, H. Zhuo, Y. Zhang, H.H. Lai, J.W. Yi, Z.H. Chen, X.W. Peng, X.H. Wang, C.F. Liu, R.C. Sun, L.X. Zhong, Graphene oxide encapsulating liquid metal to toughen hydrogel, Adv. Funct. Mater. 31 (2021) 2106761.
[224] M.M. Sun, P.Y. Li, H.Y. Qin, N. Liu, H.D. Ma, Z.L. Zhang, J.Y. Li, B.Y. Lu, X.F. Pan, L.D. Wu, Liquid metal/CNTs hydrogel-based transparent strain sensor for wireless health monitoring of aquatic animals, Chem. Eng. J. 454 (2023) 140459.
[225] X.Z. Feng, C. Wang, S.B. Shang, H. Liu, X.J. Huang, J.X. Jiang, Z.Q. Song, H. B. Zhang, Self-healing, EMI shielding, and antibacterial properties of recyclable cellulose liquid metal hydrogel sensor, Carbohydr. Polym. 311 (2023) 120786.
[226] E.F. Gomez, S.V. Wanasinghe, A.E. Flynn, O.J. Dodo, J.L. Sparks, L.A. Baldwin, C. E. Tabor, M.F. Durstock, D. Konkolewicz, C.J. Thrasher, 3D-printed self-healing elastomers for modular soft robotics, ACS Appl. Mater. Interfaces 13 (2021) 28870–28877.
[227] D. Wang, D.Y. Liu, J.H. Xu, J.J. Fu, K. Wu, Highly thermoconductive yet ultraflexible polymer composites with superior mechanical properties and autonomous self-healing functionality via a binary filler strategy, Mater. Horiz. 9 (2022) 640–652.

[228] J.L. Wu, J. Hu, Y.J. Feng, H.T. Fan, K.Z. Wang, Z.S. Deng, Mechanical sintering-induced conductive flexible self-healing eGaInSn@PDA NDs/TPU composite based on structural design to against liquid metal leakage, Chem. Eng. J. 458 (2023) 141400.
[229] S.Y. Han, S.W. Chen, Z. Hu, Y. Liu, W.H. Zhang, B. Wang, J.S. Hu, L.Q. Yang, A near-infrared light-promoted self-healing photothermally conductive polycarbonate elastomer based on Prussian blue and liquid metal for sensors, J. Colloid Interface Sci. 654 (2024) 955–966.
[230] E.D. Zhang, X.H. Liu, Y.C. Liu, J. Shi, X.B. Li, X.Y. Xiong, C.A. Xu, K. Wu, M.G. Lu, Highly stretchable, bionic self-healing waterborne polyurethane elastic film enabled by multiple hydrogen bonds for flexible strain sensors, J. Mater. Chem. A. 9 (2021) 23055–23071.
[231] A.K. Mishra, J. Parmar, I. Mukhopadhyay, Comprehensive review on nucleation, growth, and suppression of lithium dendrites in lithium anode batteries, J. Energy Storage 87 (2024) 111421.
[232] H.R. Zhang, M. Ulusel, F.F. Shi, Nucleation of pitting and evolution of stripping on lithium-metal anodes, ACS Appl. Mater. Interfaces 16 (2024) 66971–66980.
[233] Z.H. Li, H. Wang, Z.Z. Sun, J. Su, Z.Y. Wang, L.J. Wang, Self-activated continuous pulverization film: an insight into the mechanism of the extraordinary long-life cyclability of hexagonal $H_{4.5}Mo_{5.25}O_{18}\cdot(H_2O)_{1.36}$ microrods, J. Mater. Chem. A. 4 (2016) 303–313.
[234] H.D. Jiao, S.Q. Jiao, S.J. Li, W.L. Song, H.S. Chen, J.G. Tu, M.Y. Wang, D.H. Tian, D.N. Fang, Liquid gallium as long cycle life and recyclable negative electrode for Al-ion batteries, Chem. Eng. J. 391 (2020) 123594.
[235] W.T. Liang, L. Hong, H. Yang, F.F. Fan, Y. Liu, H. Li, J. Li, J.Y. Huang, L.Q. Chen, T. Zhu, S.L. Zhang, Nanovoid formation and annihilation in gallium nanodroplets under lithiation-delithiation cycling, Nano Lett. 13 (2013) 5212–5217.
[236] H.N. Zhang, P.Y. Chen, H. Xia, G. Xu, Y.P. Wang, T.F. Zhang, W.W. Sun, M. Turgunov, W. Zhang, Z.M. Sun, An integrated self-healing anode assembled via dynamic encapsulation of liquid metal with a 3D $Ti_3C_2T_x$ network for enhanced lithium storage, Energy Environ. Sci. 15 (2022) 5240–5250.
[237] Y.Q. Qi, C. Shen, Q. Hou, Z.Y. Ren, T. Jin, K.Y. Xie, A self-healing liquid metal anode for lithium-ion batteries, J. Energy Chem. 72 (2022) 522–531.
[238] P.Y. Dong, F. Peng, Q.M. Zhang, H. Wang, Y.Q. Chu, C.D. Chen, C.H. Yang, High entropy boosts the low temperature Na^+-storage performance of $Na_4Fe_3(PO_4)_2P_2O_7$, Angew. Chem. Int. Ed. (2025) e202502693.
[239] J.H. Zhu, Y.P. Wu, X.K. Huang, L. Huang, M.Y. Cao, G.Q. Song, X.R. Guo, X.Y. Sui, R. Ren, J.H. Chen, Self-healing liquid metal nanoparticles encapsulated in hollow carbon fibers as a free-standing anode for lithium-ion batteries, Nano Energy 62 (2019) 883–889.
[240] X.R. Lin, A. Chen, C.Y. Yang, K. Mu, T.L. Han, T. Si, J.J. Li, J.Y. Liu, A room-temperature self-healing liquid metal-infilled microcapsule driven by coaxial flow focusing for high-performance lithium-ion battery anode, Small 20 (2024) 2307071.
[241] P.B. Zhai, L.X. Liu, Y. Wei, J.H. Zuo, Z.L. Yang, Q. Chen, F.F. Zhao, X.K. Zhang, Y. J. Gong, Self-healing nucleation seeds induced long-term dendrite-free lithium metal anode, Nano Lett. 21 (2021) 7715–7723.
[242] C.H. Huang, X.D. Wang, Q.P. Cao, D.X. Zhang, J.Z. Jiang, A self-healing anode for Li-ion batteries by rational interface modification of room-temperature liquid metal, ACS Appl. Energy Mater. 4 (11) (2021) 12224–12231.
[243] F.R. Meng, F.Q. Wang, H.H. Yu, Z.J. Zhao, Y. Lv, C. Ma, D. Zhang, X.Z. Liu, Liquid metal-modified nanoporous SiGe alloy as an anode for Li-ion batteries and its self-healing performance, ACS Appl. Energy Mater. 4 (2021) 14575–14581.
[244] X. Zheng, L. Guo, C.H. Zhu, T. Hu, X.H. Gong, C.G. Wu, G.J. Wang, Y.J. Hou, Preparation and electrochemical performance study of a self-healing electrode composite material with WSe_2/liquid metal Galinstan for lithium-ion batteries, J. Alloy. Compd. 969 (2023) 172304.
[245] J. Yang, J.F. Li, Z.Y. Yang, J.R. Liu, Y. Xiang, F. Wu, Self-healing silicon anode via the addition of GaInSn-encapsulated microcapsules, ACS Appl. Energy Mater. 5 (2022) 12945–12952.
[246] Y.C. Zhang, L.W. Tan, Y. Wu, Y.L. An, Y.P. Liu, Y.S. Wang, C.L. Wei, B.J. Xi, S. L. Xiong, J.K. Feng, Self-healing and ultrastable anode based on room temperature liquid metal reinforced two-dimensional siloxene for high-performance lithium-ion batteries, Appl. Mater. Today 26 (2022) 101300.
[247] Q.Y. Luo, K.Z. Wang, D.T. Chen, K.J. Wang, Z.W. Sun, W.Y. Xu, J.K. Li, Y.F. Wang, Q.P. Guo, J.J. Liao, Z.S. Deng, J. Hu, S.Z. Xiong, Regulation of zinc deposition by in situ formed liquid metal interface for dendrite-free zinc metal anodes, Adv. Energy Mater. 15 (2025) 2405169.
[248] J. Pu, Q.H. Cao, Y. Gao, Q.Z. Wang, Z.Y. Geng, L.Q. Cao, F. Bu, N.T. Yang, C. Guan, Liquid metal-based stable and stretchable Zn-ion battery for electronic textiles, Adv. Mater. 36 (2024) 2305812.
[249] H.G. Chen, Z.C. Guo, H.S. Wang, W.Y. Huang, F. Pan, Z.Q. Wang, A liquid metal interlayer for boosted charge transfer and dendrite-free deposition toward high-performance Zn anodes, Energy Storage Mater. 54 (2023) 563–569.
[250] X.W. Jiang, Y. Lam, W.F. Li, S.X. Jiang, H. Jia, Self-healing composite anode induced by liquid-metal interlayer for flexible Zn ion storage application, Compos. Commun. 45 (2024) 101796.
[251] H. Jia, Z.Q. Wang, M. Dirican, S. Qiu, C.Y. Chan, S.H. Fu, B. Fei, X.W. Zhang, A liquid metal assisted dendrite-free anode for high-performance Zn-ion batteries, J. Mater. Chem. A. 9 (2021) 5597–5605.
[252] W. Wang, P.J. Zuo, G.P. Yin, C.Y. Du, H. Huo, Y.L. Ma, Y.Z. Gao, A dendrite-free Ga-In-Sn-Zn solid-liquid composite anode for rechargeable zinc batteries, Energy Storage Mater. 58 (2023) 195–203.
[253] X. Lv, F. Tang, Y. Yao, C. Xu, D. Chen, L. Liu, Y.Z. Feng, X.H. Rui, Y. Yu, Sodium-gallium alloy layer for fast and reversible sodium deposition, SusMat 2 (2022) 699–707.
[254] C.L. Wei, L.W. Tan, Y.C. Zhang, H.Y. Jiang, B.J. Xi, S.L. Xiong, J.K. Feng, Room-temperature liquid metal engineered iron current collector enables stable and dendrite-free sodium metal batteries in carbonate electrolytes, J. Mater. Sci. Technol. 115 (2022) 156–165.
[255] Y.F. Gu, H.C. Tao, X.L. Yang, Liquid metal interlayer for ultrastable solid-state sodium metal battery, Small 20 (2024) 2403864.
[256] I.S. Hwang, Y.H. Lee, J.M. Yoon, Y. Hwa, C.M. Park, GaSb nanocomposite: New high-performance anode material for Na- and K-ion batteries, Compos. Pt. BEng. 243 (2022) 110142.
[257] X.B. Zheng, X.W. Guan, X. Cheng, X.N. Li, Y. Fu, Y.T. Li, Z. Zheng, W.K. Pang, X. Xu, P. Li, T.Y. Ma, Liquid metal in prohibiting polysulfides shuttling in metal sulfides anode for sodium-ion batteries, J. Energy Chem. 96 (2024) 559–567.
[258] M.N. Fu, X.L. Zhang, W.J. Dong, B.C. Li, R.N. Tian, Q. Guo, J.J. Chen, D.J. Wang, C.L. Dong, Z.Y. Mao, Optimizing Na plating/stripping by a liquid sodiophilic Ga-Sn-In alloy towards dendrite-poor sodium metal anodes, Energy Storage Mater. 63 (2023) 103020.
[259] M.J. Song, J.Z. Niu, W.R. Cui, Q.G. Bai, Z.H. Zhang, Self-healing liquid Ga-based anodes with regulated wetting and working temperatures for advanced Mg ion batteries, J. Mater. Chem. A. 9 (2021) 17019–17029.
[260] L. Wang, J.N. Weker, R. Family, J.X. Liu, Morphology evolution in self-healing liquid-gallium-based Mg-ion battery anode, ACS Energy Lett. 8 (2023) 4932–4940.
[261] C.L. Wei, L.W. Tan, Y.C. Zhang, B.J. Xi, S.L. Xiong, J.K. Feng, Y.T. Qian, Highly reversible Mg metal anodes enabled by interfacial liquid metal engineering for high-energy Mg-S batteries, Energy Storage Mater. 48 (2022) 447–457.
[262] L. Wang, A. Ng, R. Family, E. Detsi, J. Pikul, Liquid eutectic gallium-indium as a magnesium-ion battery anode with ultralong cycle life enabled by liquid–solid phase transformation during (de)magnesiation at room temperature, J. Mater. Chem. A. 12 (2024) 27435–27442.
[263] J.X. Wang, H.D. Jiao, W.L. Song, M.Y. Wang, J.G. Tu, Z.F. Tang, H.M. Zhu, Stable interface between a NaCl-$AlCl_3$ Melt and a liquid Ga negative electrode for a long-life stationary Al-ion energy storage battery, ACS Appl. Mater. Interfaces 12 (2020) 15063–15070.
[264] T. Xu, L. Yao, G.L. Xia, X.B. Yu, Self-healing liquid metal layer as high-capacity and long cycle life anode for Al-ion batteries, Energy Storage Mater. 63 (2023) 103057.
[265] G.A. Elia, K. Marquardt, K. Hoeppner, S. Fantini, R.Y. Lin, E. Knipping, W. Peters, J.F. Drillet, S. Passerini, R. Hahn, An overview and future perspectives of aluminum batteries, Adv. Mater. 28 (2016) 7564–7579.
[266] A.H. Huang, C. Yang, X.Z. Liu, H. Zhang, F.W. Guo, B.N. Qian, J. Lu, X.F. Zhao, P. K. Chu, Oxidation behavior and failure mechanism of NiCoCrAl eutectic multi-principal element alloys co-doped with Y and Hf at 1100 ℃ and 1200 ℃, Corros. Sci. 253 (2025) 112944.
[267] C. Yang, Z.M. Sun, C.Y. Wang, A.H. Huang, Z.S. Ye, T. Ying, L.P. Zhou, S. Xiao, P. K. Chu, X.Q. Zeng, A self-sealing and self-healing MAO corrosion-resistant coating on aluminum alloy by in situ growth of $CePO_4/Al_2O_3$, Corros. Sci. 245 (2025) 112706.
[268] C. Yang, T. Ying, A.H. Huang, J. Huang, P.H. Chen, P.K. Chu, X.Q. Zeng, Enhancing corrosion resistance of MAO coatings on Al alloy LY12 through in situ co-doping with zinc phosphate and cerium phosphate, Corros. Commun. 17 (2025) 35–43.
[269] F. Bertasi, F. Sepehr, G. Pagot, S.J. Paddison, V.D. Noto, Toward a magnesium-iodine battery, Adv. Funct. Mater. 26 (2016) 4860–4865.
[270] C. Yang, C.Y. Wang, Z. Shen, L.P. Zhou, L.Y. Sheng, D.K. Xu, Y.F. Zheng, P.K. Chu, S. Xiao, T. Ying, X.Q. Zeng, Simultaneous improvement of wear and corrosion resistance of microarc oxidation coatings on ZK61 Mg alloy by doping with ZrO2 nanoparticles, J. Mater. Sci. Technol. 224 (2025) 312–327.
[271] K. Shahzad, I.I. Cheema, Aluminum batteries: Unique potentials and addressing key challenges in energy storage, J. Energy Storage 90 (2024) 111795.
[272] L.Y. Zhang, S.S. Peng, Y. Ding, X.L. Guo, Y.M. Qian, H.G. Celio, G.H. He, G.H. Yu, A graphite intercalation compound associated with liquid Na-K towards ultra-stable and high-capacity alkali metal anodes, Energy Environ. Sci. 12 (2019) 1989–1998.
[273] M. Shao, N.X. Wu, T.M. Chen, X. Han, Y. Shen, W.N. Zhang, B. Zheng, S. Li, F. W. Huo, Amorphous hollow carbon film as a flexible host for liquid Na-K alloy anode, Chin. Chem. Lett. 34 (2023) 107767.
[274] J.W. Wu, Z. Xue, L.X. Yuan, J.L. Ye, Q.H. Huang, L.J. Fu, Y.P. Wu, Advances on Na-K liquid alloy-based batteries, J. Energy Chem. 71 (2022) 313–323.
[275] C.L. Wei, L.W. Tan, Y.C. Zhang, Z.R. Wang, B.J. Xi, S.L. Xiong a, J.K. Feng, Y. T. Qian, Review of room-temperature liquid metals for advanced metal anodes in rechargeable batteries, Energy Storage Mater. 50 (2022) 473–494.
[276] Y.Y. Xie, J.X. Hu, Z.A. Zhang, A stable carbon host engineering surface defects for room-temperature liquid Na-K anode, J. Electroanal. Chem. 856 (2020) 113676.

[277] L.F. Zhao, Y. Tao, W.H. Lai, Z. Hu, J. Peng, Y.J. Lei, Y.L. Cao, S.L. Chou, Y. X. Wang, H.K. Liu, S.X. Dou, Enthalpy-driven room-temperature superwetting of liquid Na-K alloy as flexible and dendrite-free anodes, Adv. Funct. Mater. 34 (2024) 2302026.
[278] M. Huang, B.J. Xi, Z.Y. Feng, F.F. Wu, D.H. Wei, J. Liu, J.K. Feng, Y.T. Qian, S. L. Xiong, New insights into the electrochemistry superiority of liquid Na K alloy in metal batteries, Small 15 (2019) 1804916.
[279] X.R. Lia, J.H. Liu, C. Chena, J. Yang, Z.Q. Xua, Me.Q. Wu, Y.S. Wang, Z. Karim, Na-K liquid alloy: A review on wettability enhancement and ionic carrier selection mechanism, Chin. Chem. Lett. 32 (2021) 983–989.
[280] Q.L. Zeng, Z.P. Lv, S.L. Li, B. Yang, J.L. He, J.X. Song, Electrolytes for liquid metal batteries, Mater. Res. Bull. 170 (2024) 112586.
[281] B. Yuan, Z.Z. He, W.Q. Fang, X. Bao, J. Liu, Liquid metal spring: Oscillating coalescence and ejection of contacting liquid metal droplets, Sci. Bull. 60 (2015) 648–653.
[282] Y. Wang, B.M. Su, C. Yuan, An integrated simulation and experimental study of calendering process in water-based manufacturing of lithium-ion battery graphite electrode, J. Manuf. Process. 131 (2024) 861–865.
[283] J. Li, G.F. Zeng, S. Horta, P.R. Martínez-Alanis, J.J. Biendicho, M. Ibáñez, B.G. Xu, L.J. Ci, A. Cabot, Q. Sun, Crystallographic engineering in micron-sized SiOx anode material toward stable high-energy-density lithium-ion batteries, ACS Nano 19 (2025) 16096–16109.
[284] C.P. Sandhya, B. John, C. Gouri, Lithium titanate as anode material for lithium-ion cells: a review, Ionics 20 (2014) 601–620.
[285] Y.C. Jiang, H.T. Zhao, L.C. Yue, J. Liang, T.S. Li, Q. Liu, Y.L. Luo, X.Z. Kong, S. Y. Lu, X.F. Shi, K. Zhou, X.P. Sun, Recent advances in lithium-based batteries using metal organic frameworks as electrode materials, Electrochem. Commun. 122 (2021) 106881.
[286] Y.Q. Yao, S. Wang, X.Y. Ma, Y.H. Han, Z.R. Tong, G. Li, J.Y. Feng, M.D. Khan, N. Revaprasadu, Q. Sun, Y.H. Tian, Iridium cluster decoration on amorphous cobalt oxide-coated carbon nanotubes for high-performance lithium-oxygen battery cathodes, Small (2025) 2503521.
[287] J. Ming, J. Guo, C. Xia, W.X. Wang, H.N. Alshareef, Zinc-ion batteries: Materials, mechanisms, and applications, Mater. Sci. Eng. R. Rep. 135 (2019) 58–84.
[288] H.J. Tian, G.X. Feng, Q. Wang, Z. Li, W. Zhang, M. Lucero, Z.X. Feng, Z.L. Wang, Y.N. Zhang, C. Zhen, M. Gu, X.N. Shan, Y. Yang, Three-dimensional Zn-based alloys for dendrite-free aqueous Zn battery in dual-cation electrolytes, Nat. Commun. 13 (2022) 7922.
[289] L.T. Liang, J.,X. Meng, H. Shen, R.T. Chen, Y.Y. Wang, J.H. Cao, J.N. Yao, L.D. Li, H. Liu, G.Z. Zhang, C. Guo, F. Yu, W.Z. Bao, J.F. Li, Beyond conventional stabilization: Carbon materials for next-generation aqueous zinc-ion batteries, J. Power Sources 646 (2025) 237250.
[290] S.S. Shiam, J. Rath, A. Kiani, Advances in transition metal oxide cathodes for zinc-ion batteries - A review focusing on safety and toxicity, Int. J. Electrochem. Sci. 19 (2024) 100804.
[291] G.F. Zeng, Q. Sun, S. Horta, S. Wang, X. Lu, C.Y. Zhang, J. Li, J.S. Li, L.J. Ci, Y. H. Tian, M. Ibáñez, A. Cabot, A layered Bi_2Te_3@PPy cathode for aqueous zinc-ion batteries: mechanism and application in printed flexible batteries, Adv. Mater. 36 (2024) 2305128.
[292] H.D. Zhang, X.T. Gan, Y.J. Gao, H. Wu, Z.P. Song, J.P. Zhou, Carboxylic acid-functionalized cellulose hydrogel electrolyte for dual-interface stabilization in aqueous zinc-organic batteries, Adv. Mater. 37 (2025) 2411997.
[293] G.F. Zeng, Q. Sun, S. Horta, P.R. Martínez-Alanis, P. Wu, J. Li, S. Wang, M. Ibáñez, Y.H. Tian, L.J. Ci, A. Cabot, Modulating the solvation structure to enhance amorphous solid electrolyte interface formation for ultra-stable aqueous zinc anode, Energy Environ. Sci. 18 (2025) 1683–1695.
[294] S. Wang, G.F. Zeng, Q. Sun, Y. Feng, X.X. Wang, X.Y. Ma, J. Li, H. Zhang, J. Y. Wen, J.Y. Feng, L.J. Ci, A. Cabot, Y.H. Tian, Flexible electronic systems via electrohydrodynamic jet printing: a MnSe@rGO cathode for aqueous zinc-ion batteries, ACS Nano 17 (2023) 13256–13268.
[295] Y. Feng, Y.Q. Yao, S. Wang, X.Y. Ma, Y.H. Han, J.Y. Feng, J.Y. Wen, R.Y. Tian, Q. Sun, Y.H. Tian, Role of hetero-doped reduced graphene oxide in suppressing elemental dissolution in manganese selenide cathode for aqueous zinc-ion batteries, ChemSusChem 18 (2025) e202402101.
[296] T.F. Zhang, C. Li, F. Wang, A. Noori, M.F. Mousavi, X.H. Xia, Y.Q. Zhang, Recent advances in carbon anodes for sodium-ion batteries, J. Power Sources 615 (2024) 235116.
[297] J. Zhang, T.Y. Zheng, Group IVA alloy anodes for sodium-ion rechargeable batteries: electrochemistry, mechanics, and kinetics, Batt. Supercaps (2025) e202400823.
[298] J.J. Wang, X.Y. Yue, Z.K. Xie, A. Abudula, G.Q. Guan, MOFs-derived transition metal sulfide composites for advanced sodium ion batteries, Energy Storage Mater. 41 (2021) 404–426.
[299] V. Palomares, M. Casas-Cabanas, E. Castillo-Martínez, M.H. Han, T. Rojo, Update on Na-based battery materials. A growing research path, Energy Environ. Sci. 6 (2013) 2312–2337.
[300] H.Y. Kang, Y.C. Liu, K.Z. Cao, Y. Zhao, L.F. Jiao, Y.J. Wang, H.T. Yuan, Update on anode materials for Na-ion batteries, J. Mater. Chem. A. 3 (2015) 17899–17913.
[301] H. Su, H.J. Yu, Composite-structure materials for Na-ion batteries, Small Methods 3 (2019) 1800205.
[302] Y. Sun, P.C. Shi, H.F. Xiang, X. Liang, Y. Yu, High-safety nonaqueous electrolytes and interphases for sodium-ion batteries, Small 15 (2019) 1805479.
[303] M.I. Jamesh, A.S. Prakash, Advancement of technology towards developing Na-ion batteries, J. Power Sources 378 (2018) 268–300.

Dr. Minghan Yu is a Ph. D candidate at the School of Materials Science and Engineering, Harbin Institute of Technology. He received his master degree in Materials and Chemical Engineering from Harbin Institute of Technology (Shenzhen) in 2024. He has published 9 papers in internationally renowned journals. His research focuses on flexible electronic packaging technologies, including liquid metal-based packaging materials development, micro-joining and nano-joining. Yu's work aims to promote the practical application of packaging materials in the field of flexible electronic devices.

Dr. Chen Zhang served as an assistant researcher at the School of Materials Science and Engineering at Harbin Institute of Technology (Shenzhen). In the past 7 years, she has been mainly engaged in the application research of new materials such as hydrogels in flexible sensors. At present, the applicant has published more than 20 papers in Advanced Functional Materials, Chemical Engineering Journal and other journals, of which 12 are the first author and corresponding author. Two cover papers, 1 paper has been selected as ESI highly cited and cited more than 1000 times.

Dr. Jiayun Feng, is currently an associate research fellow at Harbin Institute of Technology. He received his Ph.D. degree from the School of Materials Science and Engineering at Harbin Institute of Technology in 2022. He was a visiting Ph.D student at University of Waterloo from 2018 to 2021. His research interests are flexible electronics and advanced electronic packaging technologies, and has published over 50 papers in renowned academic journals. His work has elucidated several key scientific questions in electronic packaging reliability and flexible sensors, driving progress in these fields.

Dr. Qing Sun obtained his B.S. from Harbin Institute of Technology in 2014 and his Ph.D. from Shandong University in 2022. He subsequently conducted research at the Shenzhen campus of Harbin Institute of Technology and the Catalonia Institute for Energy Research. His research focuses on the development of energy storage materials and devices. He is currently a senior researcher at the Catalonia Institute for Energy Research.

Dr. Chao Yang is an associate research fellow at the School of Materials Science and Engineering at Shanghai Jiao Tong University. He obtained his Ph.D. in Materials Physics and Chemistry from Peking University in 2023. Dr. Yang has been recognized with the China National Postdoctoral Research Program and the Shanghai Super Postdoctoral Incentive Program. He has published over 40 paper and has been granted more than 20 patents. His research focuses on self-healing metal and coating design, including biodegradable magnesium alloys and implantable microelectronic devices.

Prof. Xiaoqin Zeng is Chair professor at the School of Materials Science and Engineering at Shanghai Jiao Tong University. He received his Ph.D. in materials processing engineering from Shanghai Jiao Tong University in 2001. He has published over 400 paper and has been granted more than 140 patents and his papers have been cited more than 11,379 times (h-index ~60). He has been honored with national and provincial-level scientific and technological awards 11 times, talent program rewards 3 times, and international academic awards once. His accolades include the China National Technical Invention Award, the National Science and Technology Progress Award and the Shanghai Natural Science Award, etc. His primary research focuses on AI for materials and advanced magnesium alloy design and processing. He has developed theories and technical systems for advanced magnesium alloy designs, such as flame-retardant magnesium alloys, rare earth magnesium alloys, and stainless magnesium alloys.

Prof. Paul K. Chu is Chair Professor of Materials Engineering in the Department of Physics, Department of Materials Science & Engineering, and Department of Biomedical Engineering at City University of Hong Kong. He received his BS in mathematics (cum laude) from The Ohio State University in 1977 and his MS and PhD in chemistry from Cornell University in 1979 and 1982, respectively. In addition to being a Fellow and Council Member of the Hong Kong Academy of Engineering, he is a Fellow of the American Physical Society (APS), American Vacuum Society (AVS), Institute of Electrical and Electronics Engineers (IEEE), Materials Research Society (MRS), and Hong Kong Institution of Engineers (HKIE). He has received more than 30 research/technical awards, including the IEEE NPSS Merit Award and two first-class natural science awards from Shanghai (China) and the Chinese Ministry of Education. He has been granted more than 30 patents and his papers have been cited more than 120,000 times (h-index ~150). He is a highly cited researcher in materials science/cross-field (Web of Science, 2016 to present).

Prof. Yanhong Tian is a tenured professor of the School of Materials Science and Engineering at Harbin Institute of Technology. She mainly engaged in electronic packaging technology and flexible electronics. She is responsible for key projects of National Natural Science Foundation of China and Ministry of Science and Technology, as well as multiple industry cooperation projects. The research achievements have been applied to key devices in the fields of aerospace electronics, power electronics, and flexible electronics. She served as the chair of the Emerging Technologies of Microjoining and Nanojoining Session of the International Institute of Welding (IIW), co-chair of the Technical Committee of the International Conference on Electronic Packaging Technology (IEEE-ICEPT), and editorial board member of multiple academic journals such as Electron. She has published over 300 papers in renowned academic journals and top-level academic conferences, and she is the editor or co-editor of 6 books, and won 4 provincial and ministerial-level science and technology prizes.